Universidade do Porto
Faculdade de Engenharia
FEUP

Fluorinated peptides and functionalized liposomes to target amyloid deposits in Alzheimer's disease

Dissertation presented for obtaining the degree of:

Doctor of Philosophy in Chemical and Biological Engineering

by

University of Porto

By

Joana Angélica de Sousa Loureiro

Supervisor:
Maria do Carmo da Silva Pereira
Co-Supervisor:
Sandra Cristina Pinto da Rocha

Porto, 2013

Lepae Laboratory for Process, Environmental and Energy Engineering

UNIÃO EUROPEIA
Fundo Social Europeu

GOVERNO DE PORTUGAL

FCT Fundação para a Ciência e a Tecnologia
MINISTÉRIO DA EDUCAÇÃO E CIÊNCIA

COMPETE
PROGRAMA OPERACIONAL FACTORES DE COMPETITIVIDADE

POPH
PROGRAMA OPERACIONAL POTENCIAL HUMANO

QREN QUADRO DE REFERÊNCIA ESTRATÉGICO NACIONAL
PORTUGAL 2007.2013

To my family (specially my father),
friends and teachers…

"The mind that opens
to a new idea never
returns to its original size"
Albert Einstein (1879-1955)

Acknowledgments

I wish to acknowledge the many people that contributed to this dissertation and I am grateful to all of them.

My special thanks go to my supervisor Prof. Drª. Maria do Carmo Pereira for welcomed me as her PhD student. Other distinct thanks goes to my co-supervisor Drª. Sandra Rocha. Their scientific guidance and support were fundamental during the course of this work.

I also would like to thank Prof. Dr. Manuel Coelho for him enriching scientific discussions.

I express my reverence for the work group of my laboratory (no one mentioned, no one forgotten!). They were always helpful and friendly which made easier to overcome the difficult and frustrations of being a PhD student. I really appreciate the brain storming and scientific discussions. To LEPABE members and staff a special thank for their help and contribution.

I would like to thank Prof. Dr. Gert Fricker for the opportunity that he gave me to perform some experiments in their laboratory (in the Institute of Pharmacy and Molecular Biotechnology, University of Heidelberg, Heidelberg, Germany) and for his support in the *in vitro* and *in vivo* experiments.

Thanks to Drª. Isabel Cardoso from Institute for Molecular and Cell Biology (Porto, Portugal) for the help with the cellular assays.

I express my gratitude to all co-authors in this work, in special to the Prof. Dr[a]. Salette Reis and Dr[a]. Claudia Pinho, who help me in the liposomes experiments.

I thank Rui Fernandes for his training and support in transmission electron microscopy experiments and in the cryosections preparation, but also for his helpful suggestions.

Many thank to my family, in singular to my grandmother Laureta, and my friends, in special to my great friend Guilherme for all the time that he spent gave me incentive, my gratefully acknowledgement.

Finally, I offer my regards to my parents, for their always present support and I also recognize all the efforts they made for me and for proportionate everything that I have ever done till this present day.

This research work was supported by FCT research project PTDC/QUI-BIQ/102827/2008 and I am grateful.

Resumo

O péptido beta-amilóide (Aβ) é o principal constituinte das placas senis que caracterizam a doença de Alzheimer (DA). O péptido com a sequência de 42 aminoácidos é depositado no cérebro extracelularmente, o que resulta em morte neuronal. Apesar dos esforços para compreender a origem da DA e para encontrar tratamentos eficazes, ainda não existe uma cura para esta doença tão debilitante.

A transição da conformação do péptido Aβ de α-hélice para folhas-β leva à sua agregação e parece ser um passo crucial na formação de placas senis. A conformação do péptido determina se os agregados tóxicos serão formados. Por outro lado, a estrutura do péptido depende do ambiente e de interacções entre moléculas. Para compreender as alterações e o processo de agregação do péptido é importante realizar estudos de interacções do Aβ com diferentes moléculas de tensioactivos.

O presente trabalho descreve o efeito dos tensioactivos carregados e não carregados na fibrilogénese do $A\beta_{(1-42)}$. As interacções péptido–tensioativo foram caracterizadas através da análise ultra-estrutural, por ensaios de tioflavina T e pela análise da estrutura secundária. Estes estudos sugerem que os tensioactivos carregados interagem com o $A\beta_{(1-42)}$ através de interacções electrostáticas. No caso das micelas carregadas, estas tornam o processo de agregação mais lento e estabilizam o péptido no estado oligomérico. Por outro lado, os tensioactivos não carregados promovem a fibrilogénese do $A\beta_{(1-42)}$. Este estudo contribui para

compreender a agregação de péptidos e selecionar moléculas que sejam potenciais inibidores da agregação do péptido $A\beta_{(1-42)}$.

Três novos péptidos foram concebidos e testados como inibidores da agregação do $A\beta_{(1-42)}$. As sequências são baseadas nos resíduos hidrofóbicos do $A\beta_{(1-42)}$ (resíduos de 17-21) e no péptido inibidor LPFFD (iAβ5). Devido às vantagens que as moléculas fluoradas têm em medicina, foram adicionados átomos de flúor às sequências. Com o objetivo de aumentar a biodisponibilidade e a solubilidade destes péptidos, uma molécula de poli(etileno-glicol) (PEG) foi ligada covalentemente no terminal-C de cada péptido. Os péptidos fluorados conjugados foram caracterizados por ionização e dessorção a laser assistida por matriz e a cinética de agregação do Aβ(1-42) na sua presença foi analisada através do ensaio de tioflavina T. Para além disso, a morfologia dos agregados foi observada por microscopia electrónica de transmissão. Os estudos demonstram que duas sequências de péptidos fluorados conjugados (LVF_fFD-PEG e LV_fFFD-PEG) inibem a agregação do péptido $A\beta_{(1-42)}$ a baixas concentrações.

Fármacos promissores para o tratamento da DA podem nunca vir a ser utilizados devido à sua inaptidão em chegar ao cérebro em concentrações desejadas dado à existência da barreira hemato-encefálica. Para contornar este problema, foram concebidos e testados lipossomas peguilados funcionalizados com dois tipos de anticorpos: um que reconhece o receptor de transferrina (OX -26) e outro que reconhece o péptido beta amilóide (19B8). Estudos *in vivo* em ratos demonstraram que a concentração dos imunolipossomas é substancialmente mais elevada nos tecidos cerebrais do que a dos lipossomas não-funcionalizados. Este sistema foi utilizado para encapsular o inibidor LPFFD, demonstrando assim a sua aplicação como transportador de fármacos para o tratamento da DA.

Abstract

Amyloid-beta peptide (Aβ) is the major constituent of Alzheimer's disease (AD) plaques. The peptide, with a sequence of 42 amino acids, deposits in the brain extracellularly, which results in neuronal loss. Despite the efforts to understand the etiology of AD and to find effective treatments, there is still no cure for such debilitating disease.

The α-helix to β-sheet transition of Aβ peptide conformation leads to its aggregation and seems to be the crucial step of the formation of neuritic plaques. The peptide conformation determines if toxic aggregates will be formed. On the other hand, the peptide structure depends on the environment and molecule–molecule interactions. In order to understand the alterations and the aggregation process of the peptide, it is important to perform studies of Aβ interactions with different surfactant molecules.

The present work describes the effect of charged and non-charged surfactants on $A\beta_{(1-42)}$ fibrillization. The characterization of the peptide-surfactant interactions by ultra-structural analysis, thioflavin T (ThT) assay and secondary structure analysis suggests that charged surfactants interact with $A\beta_{(1-42)}$ through electrostatic interactions. Charged micelles slow down the aggregation process and stabilize the peptide in the oligomeric state, whereas non-charged surfactants promote the $A\beta_{(1-42)}$ fibril formation. This study contributes to better understand the peptide aggregation and screen for molecules that can inhibit amyloid fibril formation.

Three new peptides were designed and tested as inhibitors of Aβ aggregation. The sequences are based on the hydrophobic central residues of $A\beta_{(1-42)}$ (17-21) and on the beta-sheet breaker peptide LPFFD ($iA\beta_5$). Due to the benefits of fluorine in medicine, fluorine atoms were added to the sequences. For the purpose of increasing the bioavailability and solubility of these peptides, poly(ethylene glycol) (PEG) was covalently linked at their C-terminal. The fluorinated peptide conjugates were characterized by MALDI-TOF and the aggregation kinetic of $A\beta_{(1-42)}$ in their presence was monitored by ThT assay. Furthermore, the morphology of the aggregates was analysed by transmission electron microscopy. The studies demonstrate that two sequences conjugated to PEG (LVF_fFD-PEG and LV_fFFD-PEG) inhibit the aggregation of $A\beta_{(1-42)}$ peptide, at low molar ratios.

Potential drugs for the treatment of AD may not be able to access the brain at desired concentrations due to the blood brain barrier. To circumvent this problem, a novel carrier-based on pegylated liposomes functionalized with transferrin receptor antibody (OX-26) and anti-Aβ peptide (19B8) was prepared. *In vivo* studies in rats showed that the uptake of the immunoliposomes was substantially higher when compared to non-functionalized liposomes. This system was used to encapsulate a beta-sheet breaker peptide, demonstrating its application as a drug carrier for the treatment of AD.

Contents

Preface

Most of the research presented was done at the Faculty of Engineering, University of Porto (Porto, Portugal) and it was developed from 2010 to 2013, resulting in the following publications that are published or submitted for publication.

- *Chapters in books*

  J. A. Loureiro, S. Rocha, M. C. Pereira, "Interaction studies of amyloid-β peptide with ionic fluorinated amphiphiles", accepted for publication in Amyloid and Amyloidosis

- *Papers in international scientific periodicals with referees*

  S. Rocha, **J. A. Loureiro**, G. Brezesinski, M. C. Pereira, "Peptide-surfactant interactions: Consequences for the amyloid-beta structure", Biochemical and Biophysical Research Communications, Vol. 420, Pages 136–140, 2012

  J. A. Loureiro, S. Rocha, M. C. Pereira, "Charged micelles induce a non-fibrillar aggregation pathway of amyloid-beta peptide" , Journal of Peptides Science, Vol. 19, Pages 581-587, 2013

J. A. Loureiro, R. Crespo, H. Börner, P. M. Martins, F. A. Rocha, M. Coelho, M. C. Pereira**,** S. Rocha, **"**Fluorinated amino acids in amyloid-inhibitor peptides" (submitted to Journal of Materials Chemistry B)

J. A. Loureiro, B Gomes, M. Coelho, M. C. Pereira**,** S. Rocha, "Targeting nanoparticles across the blood brain barrier with monoclonal antibodies" (submitted to Nanomedicine)

CHAPTER 1

Introduction

Alzheimer's disease (AD) is characterized by an alteration of the structure of the proteins amyloid-beta and Tau protein and their subsequent aggregation. The aggregates deposit in the brain, extracellularly (amyloid-beta) or appear inside the cells (aggregates of hyperphosphorylated Tau protein) resulting in neuronal loss (Hardy, 2002). Several evidences from genetic and animal models have established a causative role of the amyloid beta-peptide (Aβ) in the onset of the disease (Hardy, 1992). The most abundant forms of Aβ peptide have 40 (~90%) and 42 (~10%) amino acids (a.a.) (Barrow, 1991). The shorter peptide, with 40 a.a., is found mainly in cerebrovascular amyloid deposits and the sequence of 42 residues is the major component of the amyloid plaque core.

Physiological Aβ in monomeric form is benign, but by an unknown mechanism it aggregates and becomes neurotoxic (Lorenzo, 1994). Initially, Aβ monomers are converted into soluble aggregates called oligomers that have a β-sheet structure. Oligomers will then aggregate further and form protofibrils. The aggregation of these protofibrils originates insoluble fibrils. The conversion of oligomers into fibrils may result from a transition of antiparallel to parallel β-sheet. In the brains of AD patients, the peptide is found in a fibrillar form organized in a β-sheet structure (Sarroukh, 2011).

The formation of Aβ soluble oligomers may be the critical factor in the development of AD rather than the insoluble fibrils. It was suggested that

these oligomeric structures induce toxicity through a mechanism related to the folded structure rather than their sequence (Bucciantini, 2002). Further evidence of toxic structures was obtained when antibodies specific to Aβ oligomers were shown to inhibit the toxicity not only of Aβ oligomers but also of several other protein oligomers (Kayed, 2003).

The steady state levels of Aβ in the brain are controlled by 3 factors (i) production; (ii) degradation and (iii) aggregation, which is a concentration dependent process. A plausible therapeutic strategy is to inhibit and reverse the peptide aggregation, because this appears to be the first step in the AD pathogenic process not associated with natural biological functions.

As several findings suggest that a conformational transition from random coil/α-helix structure to β-sheets is responsible for Aβ aggregation (Yang, 2008), a strategy to prevent this process could be the reconversion of Aβ conformation. This reconversion can be promoted by the addition of a compound that is able to remove the beta conformation out of the equilibrium (Levine, 2007). Until now, a range of small molecules was found to inhibit and reduce the aggregation of Aβ (Mason, 2003).

Fluoroorganic compounds are molecules with a lot of interest for medical applications due to the unique properties of the fluorine atom (Bohm, 2004). Fluorine is quite often introduced to improve the metabolic stability and to modulate the physicochemical properties such as lipophilicity or basicity of molecules. Few fluorinated compounds have been studied in regard to protein misfolding (Giacomelli, 2005). Organofluorine compounds were proven to be effective inhibitors of $A\beta_{(1-40)}$ fibrillogenesis (Torok, 2006). Also, complexes made of polyampholyte and the sodium salt of perfluorododecanoic acid induce α-helix rich structures in Aβ and prevent fibril formation, whereas the hydrogenated

analogues were not efficient, leading to β-sheet formation and aggregation (Saraiva, 2010).

Despite the knowledge already obtained about AD, most clinical trials of promising drugs for the treatment of this disease have failed. Most of these failures are due to the inability of drugs to cross the blood-brain barrier (BBB). Aproximately 100% of large-molecule drugs and 98% of small-molecule drugs do not cross the BBB (Pardridge, 2003). Only small molecules with high lipid solubility and low molecular mass of < 400–500 Daltons can effectively cross the BBB (Pardridge, 2003). However there are only a few brain diseases that consistently respond to this category of small molecules (Ajay, 1999).

The main objectives with the work presented in this thesis are:

- to better understand the interaction of Aβ peptide with charged and nonionic amphiphiles/micelles;

- to develop fluorinated peptides and conjugates as inhibitors of Aβ assembly;

- to design liposomal carriers as effective vehicles of fluorinated peptides and conjugates able to cross the BBB.

This thesis is organised into six chapters. This chapter, "Introduction", covers the objectives and scope of the research work. Chapter 2, "State of the art", contains an overview of the Aβ peptide and AD, the beta-sheet breaker peptides already developed, including their efficiency in inhibiting the peptide aggregation, the function of the BBB and drug delivery systems that target Aβ. Chapter 3, "Interaction of Aβ peptide with charged and nonionic surfactants", presents and discusses the interaction study of $A\beta_{(1-40)}$ and $A\beta_{(1-42)}$ with ionic and nonionic surfactants. Chapter 4, "Effect of fluorinated peptides on Aβ assembly", is dedicated to the design and characterization of sequences of five a.a.

including a fluorinated residue with the aim of inhibiting the Aβ aggregation. The chapter 5, "Design of liposomes coupled to monoclonal antibodies to cross the blood-brain barrier", describes the methodology involved in the preparation and characterization of the liposomes and their study *in vitro* and *in vivo*. Chapter 6, "Concluding remarks", summarizes the main findings of this research work.

References

Ajay; Bemis, G. W.; Murcko, M. A. **1999.** Designing libraries with CNS activity. *J Med Chem*. Vol. 42. n.º 24. p. 4942-51.

Barrow, C. J.; Zagorski, M. G. **1991.** Solution structures of beta peptide and its constituent fragments: relation to amyloid deposition. *Science*. Vol. 253. n.º 5016. p. 179-82.

Bohm, H. J.; Banner, D.; Bendels, S.; Kansy, M.; Kuhn, B.; Muller, K.; Obst-Sander, U.; Stahl, M. **2004.** Fluorine in medicinal chemistry. *Chembiochem*. Vol. 5. n.º 5. p. 637-43.

Bucciantini, M.; Giannoni, E.; Chiti, F.; Baroni, F.; Formigli, L.; Zurdo, J.; Taddei, N.; Ramponi, G.; Dobson, C. M.; Stefani, M. **2002.** Inherent toxicity of aggregates implies a common mechanism for protein misfolding diseases. *Nature*. Vol. 416. n.º 6880. p. 507-11.

Giacomelli, C. E.; Norde, W. **2005.** Conformational changes of the amyloid beta-peptide (1-40) adsorbed on solid surfaces. *Macromol Biosci*. Vol. 5. n.º 5. p. 401-7.

Hardy, J. A.; Higgins, G. A. **1992.** Alzheimer's disease: the amyloid cascade hypothesis. *Science*. Vol. 256. n.º 5054. p. 184-5.

Hardy, J.; Selkoe, D. J. **2002.** The amyloid hypothesis of Alzheimer's disease: progress and problems on the road to therapeutics. *Science*. Vol. 297. n.º 5580. p. 353-6.

Kayed, R.; Head, E.; Thompson, J. L.; McIntire, T. M.; Milton, S. C.; Cotman, C. W.; Glabe, C. G. **2003.** Common structure of soluble amyloid oligomers implies common mechanism of pathogenesis. *Science*. Vol. 300. n.º 5618. p. 486-9.

Levine, H. **2007.** Small molecule inhibitors of A beta assembly. *Amyloid-Journal of Protein Folding Disorders*. Vol. 14. n.º 3. p. 185-197.

Lorenzo, A.; Yankner, B. A. **1994.** Beta-Amyloid Neurotoxicity Requires Fibril Formation and Is Inhibited by Congo Red. *Proceedings of the National Academy of Sciences of the United States of America*. Vol. 91. n.º 25. p. 12243-12247.

Mason, J. M.; Kokkoni, N.; Stott, K.; Doig, A. J. **2003.** Design strategies for anti-amyloid agents. *Current Opinion in Structural Biology*. Vol. 13. n.º 4. p. 526-532.

Pardridge, W. M. **2003.** Blood-brain barrier drug targeting: the future of brain drug development. *Mol Interv*. Vol. 3. n.º 2. p. 90-105, 51.

Saraiva, A. M.; Cardoso, I.; Pereira, M. C.; Coelho, M. A.; Saraiva, M. J.; Mohwald, H.; Brezesinski, G. **2010.** Controlling amyloid-beta peptide(1-42) oligomerization and toxicity by fluorinated nanoparticles. *Chembiochem*. Vol. 11. n.º 13. p. 1905-13.

Sarroukh, R.; Cerf, E.; Derclaye, S.; Dufrene, Y. F.; Goormaghtigh, E.; Ruysschaert, J. M.; Raussens, V. **2011.** Transformation of amyloid beta(1-40) oligomers into fibrils is characterized by a major change in secondary structure. *Cell Mol Life Sci*. Vol. 68. n.º 8. p. 1429-38.

Torok, M.; Abid, M.; Mhadgut, S. C.; Torok, B. **2006.** Organofluorine inhibitors of amyloid fibrillogenesis. *Biochemistry*. Vol. 45. n.º 16. p. 5377-5383.

Yang, M.; Teplow, D. B. **2008.** Amyloid beta-protein monomer folding: free-energy surfaces reveal alloform-specific differences. *J Mol Biol*. Vol. 384. n.º 2. p. 450-64.

CHAPTER 2

State of the art

2.1. Introduction

AD affects more than 35 million people and it is considered the most common form of dementia worldwide. By 2050, the prevalence is estimated to quadruple (Brookmeyer, 2007). The initial symptoms of AD are practically imperceptible and characteristically involve lapses of memory for recent events (Forstl, 1999). In addition, the performance for complex tasks and ability to acquire new information can be reduced. After a couple of years the patients lose the cognitive functions and show spatial disorientation, apathy, general disinterest and difficulty in performing simple tasks such as preparing meals. Commonly an emotional control loss is observed in patients with AD, a symptom that may be accompanied by physical or verbal aggression. With the evolution of the disease, people develop motor problems and present difficulty for walking and for simple activities like dress up. Over the time, the disease causes a progressive decline of the patient life with intense memory and cognition losses, leading to the immobility of the patients that succumb to respiratory difficulties. Normally, this disorder appears among people over the age of 65 years, with an average of eight year living after the appearance of the first symptoms (Larson, 2004). The impact of AD on the health care systems is also a very pronounced problem in developed countries. Considering the increase in population aging and survival, the

economic effects caused by this disease are expected. Therefore, strategies for its early detection and treatment are an ambitious challenge in modern medicine.

Two pathophysiological hallmarks in the brain characterize this neuropathological disease: intracellular neurofibrillar tangles of hyperphosphorylated tau protein and extracellular accumulation of Aβ peptide (senile plaques) (Calhoun, 1999; Clippingdale, 2001; Hardy, 2002a). The peptide is aggregated as amyloid fibrils within the neuritic plaques and vascular deposits (Kirschner, 1986; Selkoe, 2001). Scientific evidences from genetic and animal models have established a causative role of Aβ in AD (Hardy, 2002b; Hardy, 1992). The existing treatments only attenuate the symptoms of the disease and, at the present, no therapies have been clinically proven to effectively prevent the progression of AD.

Different factors limit the development of new medicines. Short drugs do not circulate more than some instants in the blood stream, because they suffer enzymatic degradation (J.L. Fauchere, 1992). Other limiting factor is the poor ability of the drugs to cross the BBB and reach the central nervous system (CNS). Although nanotechnology is expected to have a huge impact on the development of "smart" drug delivery devices against AD, a crucial gap still needs to be filled (Brambilla, 2011). Several types of biologically active molecules are being encapsulated into nanoparticles (NPs) for their delivery to the brain. Liposomes are one of the most studied vehicles to transport drugs toward the site of action and several improvements were achieved during the last decades (Lai, 2013). The selectivity of these carriers could be improved with ligands attached at their surfaces. Monoclonal antibodies (mAb) are probably the most efficient ligands to target NPs (Liu, 2010). This improvement increases the efficiency of the treatments and decreases the undesirable side effects of the drugs.

2.2. Amyloid beta-peptide and Alzheimer's disease

Evidences support a direct association between the degree of dementia of patients that have AD and the concentration of soluble aggregates of the Aβ peptide (Clippingdale, 2001; Hardy, 2002a; Ladiwala, 2012). The Aβ peptide derives from the amyloid precursor protein (APP) by sequential activities of β- and γ-secretases (Haass, 1993; Kang, 1987; Weidemann, 1989), a process explained by a theory that was formulated 20 years ago: the cascade hypothesis (Hardy, 1992). This hypothesis has been the most influential in the AD research conducted by the academia and in the pharmaceutical industry.

2.2.1. Amyloid cascade hypothesis

Originally, when the amyloid cascade hypothesis was presented, the Aβ peptides and their aggregated forms were suggested to be responsible for initiating cellular events leading to the pathologic effects of AD. According to the first version of the amyloid cascade hypothesis, Aβ fibrils deposited in amyloid plaques were thought to cause neuronal dysfunction (Hardy, 1992; Selkoe, 1991). Recently, studies support that diffusable Aβ oligomers including protofibrils and prefibrillar aggregates, are the major toxic species during the disease development and progression (Haass, 2007; Shankar, 2007; Shankar, 2008).

The transmembrane APP is an integral membrane protein with a single membrane-spanning domain, a large extracellular glycosylated N-terminus and a shorter cytoplasmic C-terminus, that is expressed in many tissues and concentrated in the synapses of neurons. APP is produced in several different isomers ranging in size from 695 to 770 a.a.. The shorter

sequence is the most abundant form in the brain (Mattson, 1997). This protein can be processed along two main pathways: non-amyloidogenic and amyloidogenic. In the non-amyloidogenic pathway, APP is cleaved in its transmembrane region by the α-secretase, a proteolytic enzyme. This cleavage leads to the formation of a soluble APP fragment (sAPPα) and a C83 carboxy-terminal fragment. During the amyloidogenic pathway, Aβ is obtained by the cleavage of APP through the sequential actions of β- and γ-secretases. The γ-secretase cleaves the APP in the transmembrane region, produces the C-terminal end in the Aβ peptide, generating Aβ peptides ranging in length from 38 to 43 residues (Selkoe, 2007) (Figure 2.1). The most abundant isoforms are $A\beta_{(1-40)}$ and $A\beta_{(1-42)}$. The $A\beta_{(1-42)}$ is characteristically produced by cleavage that occurs in the endoplasmic reticulum, while the $A\beta_{(1-40)}$ is produced by cleavage in the trans-Golgi network (Hartmann, 1997). After its production, Aβ may aggregate into oligomers, fibrils and finally in neurotoxic amyloid plaques by an unknown mechanism. In addition, apolipoprotein E (ApoE) gene represents the major genetic risk factor for the disease (Strittmatter, 1993). The ApoE can act as a chaperone of Aβ, promoting the conformational transformation from soluble Aβ into toxic aggregates. The formation of toxic aggregates induces an inflammatory response and a situation of oxidative stress, which consequently causes the neuronal loss characteristic of AD (Sun, 2012).

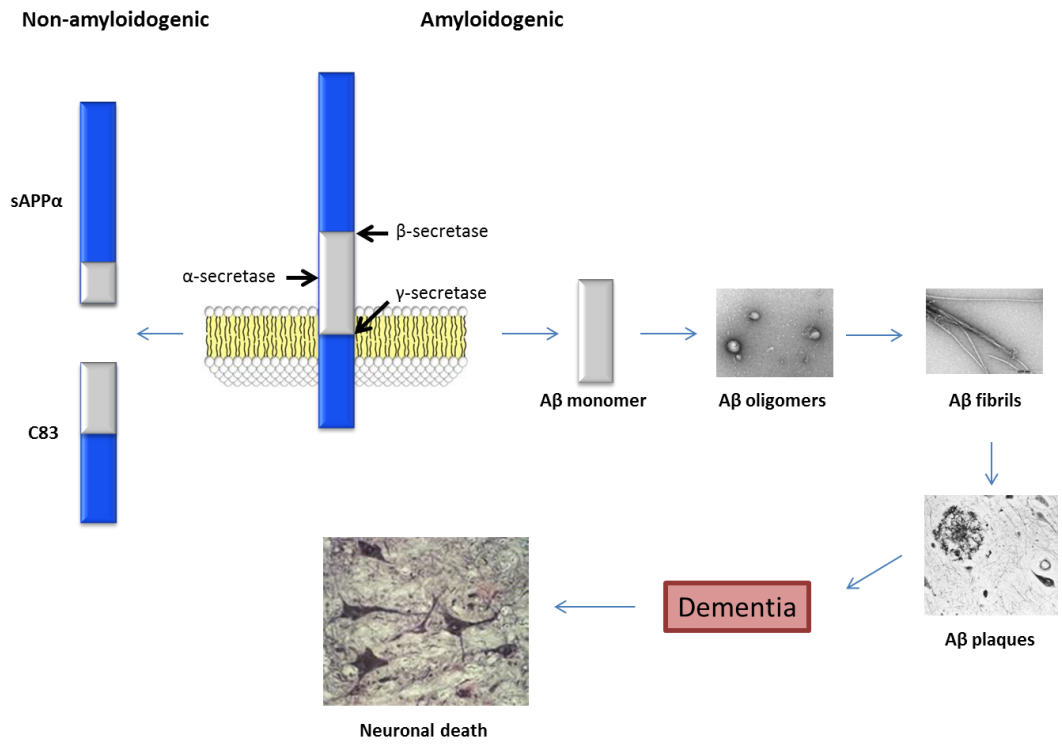

Figure 2.1 – Amyloid cascade hypothesis

2.2.2. Amyloid beta peptide

As mentioned before, Aβ is a metabolic product of an enzymatic process from a transmembranar protein, the APP. This enzymatic set of reactions has as final products, two principal sequences with a length of 40 or 42 a.a. (Kang, 1987). The sequence of 40 residues is normally produced more abundantly by cells (concentration of secreted $A\beta_{(1-42)}$ is 10-fold lower that of $A\beta_{(1-40)}$) and its aggregation kinetic rate is much lower than that of the 42 ($A\beta_{(1-40)}$ at 20 μM is stable for 8 days or more whereas $A\beta_{(1-42)}$ aggregates immediately) (Haass, 1992; Jarrett, 1993a). However, $A\beta_{(1-42)}$ is the most fibrillogenic sequence and is thus associated with disease states. The ratio $A\beta_{(1-42)}/A\beta_{(1-40)}$ has been related to the progression of AD as its increase is associated to the aggregation of $A\beta_{(1-42)}$

and consequently neurotoxicity (Haass, 2007). The aggregation process of the Aβ peptide leads to the formation of insoluble fibrils, which accumulate in senile plaques, deposits that characterize AD (Andreasen, 2002; Suh, 2002). In this state Aβ is in a β-sheet conformation. The smaller aggregated intermediates, the Aβ oligomers, are considered one of the more toxic species (Hardy, 2002a). The control of Aβ oligomerization is difficult to achieve, because the process is fast and is affected by many variables (Stine, 2003). $A\beta_{(1-40)}$ monomers inhibit the aggregation of $A\beta_{(1-42)}$/$A\beta_{(1-40)}$ mixtures (in a concentration-dependent manner), whereas $A\beta_{(1-42)}$ fibrils accelerate their fibrillogenesis (Jan, 2008; Kuperstein, 2010). The $A\beta_{(1-42)}$ also affects the aggregation of the mixture by accelerating the process. The factors that lead to the *in vivo* aggregation of amyloid peptides can be numerous and are difficult to identify. An important feature is the conformation of soluble oligomers (smaller intermediates in the aggregation process) which is common for several different amyloid-prone synthetic proteins (Kayed, 2003).

This aggregation process has a nucleation-dependent mechanism in which partially folded forms of the peptide associate to form a stable nucleus (Jahn, 2005; Merlini, 2003). This nucleus acts as a template to sequester other intermediates to add to the growing thread of aggregated peptide forming the protofibrils. The consecutive addition of partially folded intermediates to the ends of the chain leads to the formation of a highly structured and insoluble amyloid fibrils. The time course of the conversion of the peptide into fibrils typically includes three phases: lag phase, elongation phase and plateau phase. In the first phase, the lag phase, the unfolding of Aβ and the formation of oligomers occur, which include β-sheet-rich species that act as nuclei for the formation of mature fibrils. In the elongation phase, once a nucleus is formed, the fibril growth is thought to proceed by the exponentially addition of monomers or

oligomers to the growing nucleus. In the last phase, the plateau phase, the maximum fibril growth is reached (Figure 2.2).

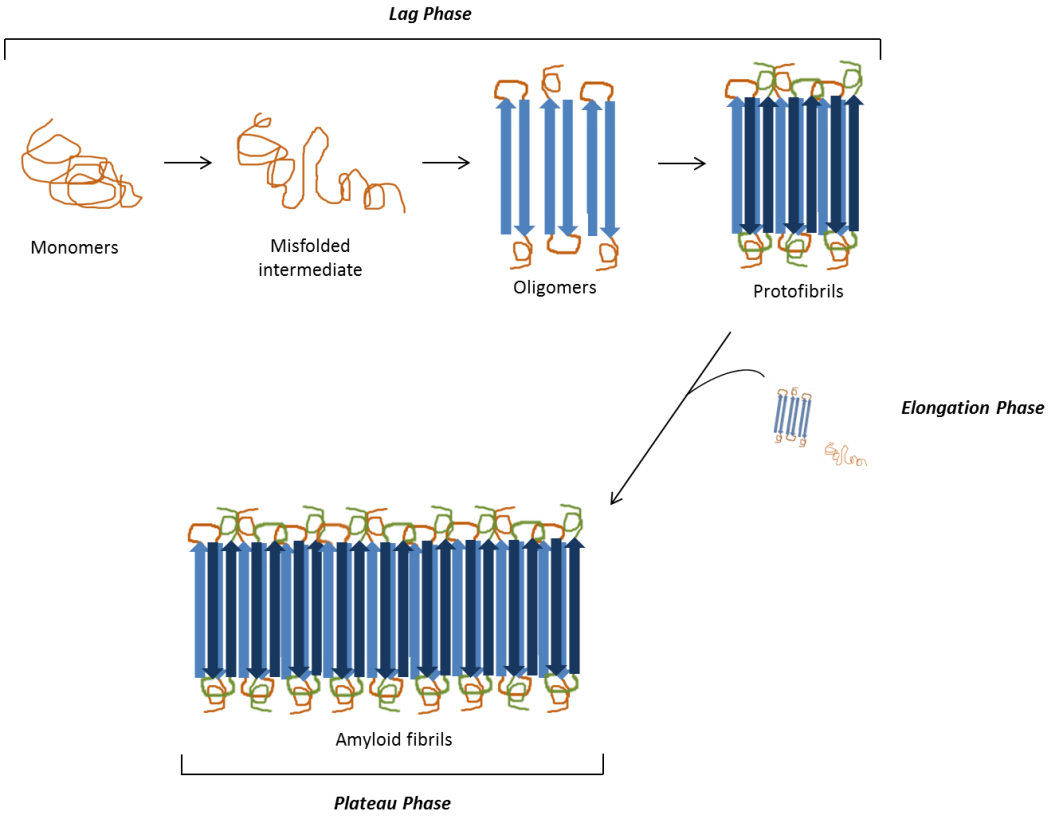

Figure 2.2 – Representation of the Aβ peptide aggregation process.

2.3. Beta-sheet breaker peptides

Peripheral treatment of AD with molecules that do not cross the BBB but have a high affinity for Aβ can reduce the level of the peptide in the brain through the sink effect (Brambilla, 2011). The inhibition of Aβ aggregation is an attractive therapeutic strategy because this is the first step in the pathogenic process of amyloidosis. Until now, several groups developed different chemical compounds that inhibit Aβ aggregation or promote the disaggregation of the already formed fibrils (Esler, 1997;

Kisilevsky, 1995; Merlini, 1995; Wood, 1996). There are several examples of molecules with these properties: β-cyclodextrin, hemin and related porphyrins, anthracycline 4'-iodo-4'-deoxydoxorubicin, hexadecyl-n-methylpiperidinium bromide, rifampicin, (-)-5,8-dihydroxy-3r-methyl-2r-(dipropylamino)-1,2,3,4-tetrahydronapthalene and melatonin (a hormone that crosses the BBB and can block Aβ fibril formation) (Mason, 2003; Pappolla, 1998; Schwarzman, 2005). Also, it was demonstrated that natural occurring inositol stereoisomers stabilized the small Aβ aggregates (McLaurin, 2000). Nevertheless, most of small molecules tested are weekly potent and poorly bioavailable, particularly to the brain.

In parallel with these traditional small molecule drugs, an attractive strategy is the use of therapeutic peptides (linear molecules with two or more a.a. residues, but less than 100) because of their high biological activity associated with low toxicity and high specificity (Funke, 2012). These therapeutic peptides have many advantages including little unspecific binding to molecular structures other than the desired target, minimization of drug-drug interactions and negligible accumulation in tissues, reducing risks of complications due to metabolic products (Sun, 2012). Today, around 70 therapeutic peptides to treat different types of diseases are on the market, 150 in clinical phases and more than 400 in the pre-clinics (Funke, 2012).

Considerable progress has already been made in discovering inhibitors of Aβ aggregation and a range of peptides, which block amyloid formation, were developed for therapeutic purposes (Findeis, 2000; Findeis, 1999; Hughes, 1996; Soto, 1998; Tjernberg, 1996). Mostly, the inhibitors are focused on the internal Aβ sequence 16-22, KLVFFAE, because this region has been reported to be primarily responsible for the self-association and aggregation of the peptide (Tjernberg, 1997; Tjernberg, 1996). The starting point of modified peptide aggregation inhibitors was the $A\beta_{(16-20)}$ (KLVFF) peptide which can bind to the full-

length Aβ and prevent the formation of fibrils (Tjernberg, 1997; Tjernberg, 1996). Based on this peptide, Soto *et al*. designed an 11 a.a. peptide, iAβ1 (RDLPFFPVPID), which binds to Aβ and inhibits Aβ aggregation *in vitro* (Soto, 1996). They designed also a shorter peptide, iAβ5 (LPFFD), that presented a similar inhibitory effect to the 11 residue sequence but improved BBB permeability due to the reduced molecular mass (Soto, 1996). LPFFD is based on one of the two hydrophobic zones of Aβ peptide responsible for the aggregation, residues 17-21 (LVFFA) (Hilbich, 1992; Jarrett, 1993b; Soto, 1996). This inhibitor has a similar degree of hydrophobicity, but has a very low propensity to adopt a β-sheet conformation due to the proline residue (Soto, 1996). In order to block the oligomerization, the LVFFA sequence was modified. The a.a. valine, which is considered a key residue for β-sheet formation, was replaced by an a.a. thermodynamically unable to fit in the β-sheet structure, the proline (P), and the a.a. alanine was replaced by aspartic acid (D) to increase the solubility (Chou, 1978; Soto, 1996; Wood, 1995). The peptide LPFFD binds to $A\beta_{(1-42)}$ and blocks the interaction between monomers and oligomers and therefore the formation of the oligomeric β-sheet conformation precursor of the fibrils. However, the peptides generally show poor bioavailability both in tissues and organs, preventing their usefulness as therapeutic agents. Short peptides usually do not circulate more than a few minutes in blood stream and therefore they cannot reach their site of action (J.L. Fauchere, 1992). To prevent the enzymatic degradation in the blood stream, Rocha et al. coupled the iAβ5 to PEG to increase their molecular weight, reduce their immunogenicity and, consequently, prolong their half-life *in vivo* (Rocha, 2009). The pegylation of $iA\beta_5$ did not affect its activity (Rocha, 2009). PEG has very low toxicity and it is known to mask the protein, reducing its degradation by proteolytic enzymes (Veronese, 2001). This is an exceptional advantage for the preparation of peptide conjugates. Other peptide sequences were developed with the

same objective of preventing the Aβ aggregation, nevertheless only very few were shown to be effective in rodent AD models or in clinical trials (Table 2.1) (Funke, 2012).

Table 2.1 - The AD therapeutic sequences that were shown to be effective in rodent AD models or in clinical studies.

Name	Sequence	Description	Ref.
iAβ11	RDLPFFPVPID	Aβ based β-sheet breaker	(Soto, 1996)
iAβ5	LPFFD		(Soto, 1998)
PPI-1019*	Metyl-LVFFL	iAβ5 derivatives to improve the pharmaceutical properties	(Findeis, 2002)
Ac-iAβ5-amid	Ac- LPFFD-amid		(Chacon, 2004; Permanne, 2002)
LPYFDa	LPYFDamid		(Datki, 2004; Juhasz, 2009; Szegedi, 2005)
NH_2-D-Trp-Aib-OH	Ac-Trp-Aib	Dipeptide β-sheet breaker	(Frydman-Marom, 2009)

*Completed phase II clinical trial

Another promising amyloid-inhibitor is the OR1, with the a.a. sequence RGKLVFFGR. This peptide was designed based on the central region of Aβ, KLVFF (residues 16-20), which as mentioned above, is part of the binding region responsible for its aggregation (Tjernberg, 1996). the cationic a.a. arginine was added at N- and C-termini of the sequence, using a glycine as a spacer, to improve the solubility of the inhibitor and prevent its self-aggregation and thus its action as a "seed" that would promote Aβ aggregation, (Austen, 2008). Also, the introduction of the glycine residues as spacers simplify the interaction between the inhibitor peptides and Aβ (Austen, 2008). The addition of the -NH_2 group at the end of the sequence OR1, RGKLVFFGR-NH_2 (named OR2), increases the inhibitor effect in the

Aβ aggregation (Tjernberg, 1997). On the other hand, OR2 presents several potential sites for proteolytic cleavage. To solve this problem a "retro-inverso" peptide that maintains the inhibitor effect and blocks the proteolytic degradation was designed (RI-OR2) (Matharu, 2010).

Additionally, a possible strategy to prevent enzymatic cleavage is to use N-methylated peptides that bind to Aβ through one hydrogen-bonding face while blocking the propagation of the hydrogen bond array of the β-sheet with the other non-hydrogen-bonding face (Gordon, 2001; Kokkoni, 2006).

2.4. The importance of fluorine in medical chemistry

Compounds that contains fluorine atoms are of exceptional interest for medical applications due to the unique properties of these atoms (Torok, 2006). The substitution of various chemical groups by fluorine has played and continues to play an important role in the development of more active, efficient and selective agents (Kirk, 2006).

As predictable from its place on the periodic table of chemical elements, fluorine possesses high electronegativity in comparison with other halogens and presents a small atomic radius among these elements (Smart, 2001). The advantages to design drugs with fluorine atom include the small size, the specific effects that enhance binding to target macromolecules and the high electronegativity. This last benefit has been used in many ways to develop enzyme inhibitors or to render molecule resistant to chemical degradation (Kirsch, 2004; Ojima, 1996; Soloshonok, 1999). Other beneficial property of the fluorine substitution is the increase of BBB permeability due to changes in the lipophilicity or amine pKa that

are of high interest in the design of CNS active drugs (Filler, 1982; Kirsch, 2004; Malamas, 2010).

Recent studies suggest that the C–F bond (van der Waals radius = 1.5 Å) is greater than the C–H bond (van der Waals radius = 1.2 Å), thus the substitution of hydrogen by fluorine is regarded as a bioisosteric way of introducing strong electron-withdrawing properties into molecules (Banks, 1994; O'Hagan, 2008). The importance of fluorine in medicinal chemistry is well recognized and the number of drugs on the market that contain fluorine are increasing (Kirk, 2006).

Over the past decade a steady stream of fluorinated drugs brought significant advances into drug development for the treatment of different diseases, for example, diseases of the CNS, various cardiovascular diseases, obesity, and it was also used as antibacterial agents as it is the case of the fluoroquinolone and antifungal like fluoroazole (Kirk, 2006; Kirsch, 2004; Ojima, 1996; Soloshonok, 1999). Fluorine has played a particularly important and historical role in the development of antipsychotic drugs, also called neuroleptics or major tranquilizers. These agents are used in the treatment of schizophrenia, mania and psychotic depression (Granger, 2005; Rowley, 2001).

Small organic molecules are known to efficiently regulate protein-protein interactions and are proposed to be good candidates to interfere with the aggregation of Aβ (Berg, 2003; Iversen, 2002). In order to inhibit the protein misfolding, compounds with fluorine atoms have been studied (Makhaeva, 2009). Adsorption studies of Aβ monomers and small oligomers on poly(tetrafluoroethylene) surfaces have shown that the fluorinated surface promotes α-helix re-formation (Giacomelli, 2003). A comparable effect was verified when Aβ was in contact with a CF3-group-containing solvents (2,2,2-trifluoroethanol, 1,1,1,3,3,3-hexafluoro-2-propanol) (Vieira, 2003). On the other hand, ethanol and 2-propanol have showed only reasonable stabilizing effects at high concentrations (75%

concentration, 26% α-helix). The fluorinated derivatives are significantly more effective as stabilizers at lower concentrations (10% concentration, 48% α-helix). Also, Torok et al, demonstrate an exceptional efficacy of a new class of organofluorine inhibitors on the inhibition of the *in vitro* self-assembly of $A\beta_{(1-40)}$ peptide (Torok, 2006). Sood and co-workers have observed that 5'-halogen substituted 3,3,3-trifluoromethyl-2-hydroxyl-(indol-3-yl)-propionic acid esters showed significant activity in the disassembly of preformed fibrils making them candidates for further drug development (Sood, 2011).

Aminoisoindoles have also been evaluated as inhibitors of the β-site amyloid precursor protein cleaving enzyme 1 (BACE1). The introduction of fluorine adjacent to the amidine moiety, besides improving the permeability properties in the brain, it resulted in *in vivo* brain reduction of $A\beta_{(1-40)}$ (Swahn, 2012). Also, novel polyhydroxylated (E)-stilbenes were synthesized with the objective of inhibiting the enzymes acetyl- and butyrylcholinesterase and one of them carrying an extra fluorine substituent presented a very stronger action when compared with other known inhibitors (Csuk, 2013).

2.5. Blood-brain barrier

The exchange of molecules between the blood and brain parenchyma is regulated by three main barriers: the BBB formed by glial cells and endothelial cells of the blood vessels in the brain; the choroid plexus epithelium, which is the border between the blood and ventricular cerebrospinal fluid; and the arachnoid epithelium, which separates the blood from the subarachnoid cerebrospinal fluid (Pedro Ramos-Cabrer, 2013). The BBB is formed by the endothelial cell layer, which constitutes the capillary, followed by a basement membrane where pericytes and astrocytic feet processes lie (Alam, 2010; Egleton, 1997). These cells are responsible for several functions like maintenance of neuronal

microenvironment, tissue homeostasis, vasotonous regulation, fibrinolysis, coagulation, blood cell activation or migration during physiological and pathological processes. The barrier also helps in the vascularisation of normal neoplastic tissues (Alam, 2010; Risau, 1995), even though the main role of the cerebral membrane is to protect the CNS from foreign substances (Huang, 2013; Pardridge, 2007). This protection is achieved due to the capillary bed of the brain, which was found to differ from peripheral capillary beds mainly in the following features: i) the intercellular spaces between adjacent capillaries are reduced by tight junctions; ii) pinocytosis is significantly decreased; iii) fenestrations and other intracellular leaks are essentially absent (Banks, 2008). The presence of the tight junctions between the endothelial cells at the BBB promotes a very high electrical resistance of around 1500–2000 $\Omega.cm^2$ in the brain (Crone, 1982) as compared to 3.33 $\Omega.cm^2$ in other body tissues (Crone, 1981). Endothelial cells also contain large concentrations of P-glycoprotein (P-gp), an adenosine triphosphate (ATP) dependent protein that actively transports a wide range of molecules out of the brain, by an efflux pump (Begley, 1996; Bernacki, 2008; Wohlfart, 2012).

Most molecules are forced to cross the BBB via the transcellular route due to the tight junction between adjacent endothelial cells. Only small lipophilic molecules, with less than 400 Da, are able to cross the BBB by simple diffusion (Figure 2.3) (Boado, 2011; Pardridge, 2002). The BBB is not a passive, anatomical lipid phase membrane, but rather a dynamic interface containing both physical and metabolic transporter components (Fricker, 2004). Different endogenous transport systems are expressed at the BBB surface and are responsible for the transport of essential hydrophilic molecules/macromolecules to the brain. Molecules such as glucose or a.a. are transported through membrane proteins (Figure 2.1). Hydrophilic essential macromolecules such as proteins are transferred by endocytosis in vesicles, which can be either specific (receptor-mediated

transcytosis) or less specific (adsorptive-mediated transcytosis) (Figure 2.3). Some large molecules such as transferrin and insulin are transported via the receptor mediated transport (RMT) which is the transport through specialized ligand-specific receptor systems expressed at the surface of the brain endothelial cells (Alam, 2010). The receptors that are more abundantly expressed by the BBB endothelial cells are the transferrin and the insulin receptors (Boado, 2007; Jefferies, 1984; Wohlfart, 2012). Adsorptive endocytosis occurs with plasmatic proteins such as albumin in which the transport is triggered by the electrostatic interactions between the positively charged proteins and negatively charged regions of the membrane surface of brain endothelial cells (Pedro Ramos-Cabrer, 2013).

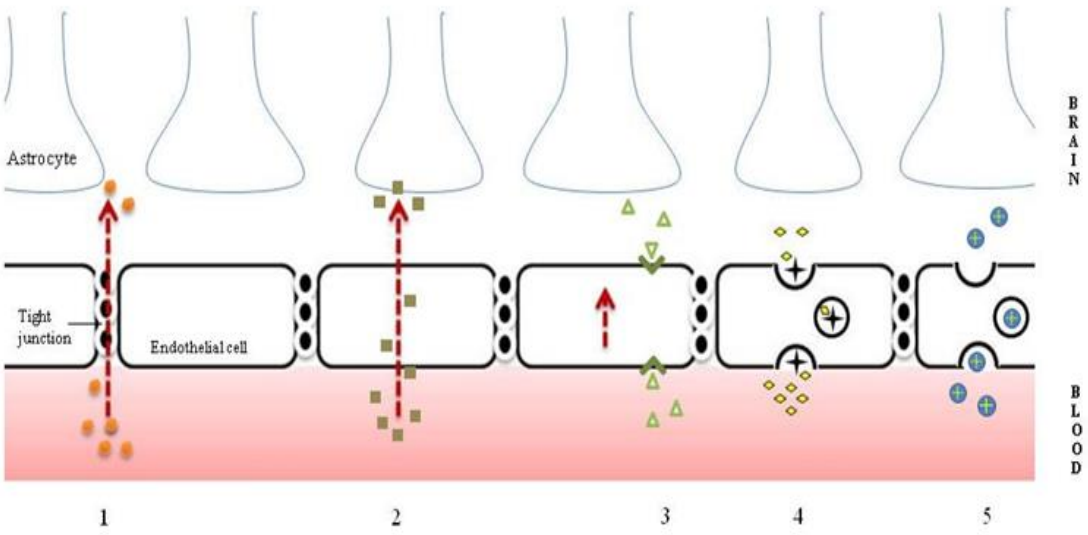

Figure 2.3 - Mechanisms of transport of substances across the BBB: 1- paracellular aqueous pathway used by water soluble agents; 2- transport of lipophilic molecules by transcellular pathway; 3-transport through membrane proteins used by glucose or a.a.; 4- receptor mediated transcytosis of macromolecules (e.g. insulin, transferrin); 5-Adsorptive transcytosis of cationized plasmatic proteins.

2.6. Drug delivery systems to cross the blood brain barrier

The therapy of CNS diseases is hampered by the low bioavailability of drugs and their rapid degradation in the blood. Colloidal systems have the potential of transporting drugs that normally would not cross the BBB to the brain by masking their physicochemical characteristics through encapsulation (Andrieux, 2009). Several NPs have been developed to protect and transport the desired molecules into the brain. NPs can be classified in either reversible or irreversible complexes. The reversible NPs are supramolecular complexes formed by noncovalent intermolecular interactions as van der Waals forces or lipophilic interactions. Liposomes are the best known example of this type of nanoparticle (Pedro Ramos-Cabrer, 2013). Non-reversible NPs (including dendrimers, nanocapsules, nanospheres, nanocages, and nanotubes) comprise molecules with strong molecular interactions like covalent or metallic bonds, which confer a high degree of stability (Alam, 2010; Pedro Ramos-Cabrer, 2013). A major problem of the nanocarriers is their low cell specificity (Banks, 2008). In addition, they need to be optimized for each specific drug to lead to its efficient and controlled delivery. For example, the molecular weight of polymers used to prepare NPs can be modulated for controlling the release mechanism: the higher the molecular weight of the polymer, the slower the *in vitro* release of the drug (Kumari, 2010; Zambaux, 1999). The loading of the drug into the core of particles can be achieved by incorporation of the molecule during the nanoparticle production (Danhier, 2012). This approach prevents agglutination of the drug with plasmatic proteins or its retention in the liver, spleen, or other organs such as the lungs. Hydrophobic NPs are rapidly opsonized and cleared by the macrophages of the mononuclear phagocytic system. Thus the surface of this type of NPs must be modified with specific molecules to increase their

circulation time in the blood (Brigger, 2002; Kumari, 2010). The nanoparticle surface needs also to be altered for the system to be able to cross the BBB and normally the modifications are based on: a) covalent attachment of PEG, b) coating with certain surfactants that should have PEG fragments in their structure and c) covalent attachment or adsorption of targeting molecules (Wohlfart, 2012).

Liposomes are one of the more studied vehicles to transport drugs to the site of action and several improvements were achieved during the last decades (Lai, 2013). The addition of PEG molecules is the more relevant progress since it allowed the increase of the stability and bioavailability of the systems (Torchilin, 1994). PEG protects the liposomes from clearance by cells of the reticulo-endothelial system. The increase of the half life time up to 90 hours in humans, due to a reduced uptake by the liver and spleen, was an important feature for the use of these systems in drug delivery (Gabizon, 2003; Papahadjopoulos, 1991; Torchilin, 1996). PEG also rendered the dose independent from the blood clearance kinetics for a wide range of drug dosages (Papahadjopoulos, 1991). Several experiments confirmed the benefits of PEG as a steric stabilizer (Blume, 1990; Klibanov, 1990; Papahadjopoulos, 1991). These carriers can be prepared synthetically at high purity and in large quantities, which has led to its acceptance for clinical applications (Schnyder, 2005). Liposomes are considered non-toxic, biocompatible and fully biodegradable carriers (Salvati, 2013; Torchilin, 2005). There are already some formulations based on liposomes that are used in clinics: Ambisome® (Gilead Sciences, Foster City, CA, USA) in which the encapsulated drug is the antifungal amphotericin B (Veerareddy and Vobalaboina 2004), Myocet® (Elan Pharmaceuticals Inc., Princeton, NJ, USA) has the anticancer agent doxorubicin (Alberts et al 2004), and Daunoxome® (Gilead Sciences), in which the incorporated drug is daunorubicin (Allen and Martin 2004). *In vivo* studies have shown that

liposomes can decrease the toxicity of several drugs leading to recent clinical trials of other formulations, which have shown promising results (Immordino, 2006).

Normally, the lipids used in liposomes are phospholipids that form a cell membrane-like phospholipid-bilayer structure. Liposomes contain a hydrophilic phase inside the core and a lipophilic phase between the bilayers and thus they can carry either hydrophilic or lipophilic molecules (Huang, 2013; Torchilin, 2005). The phospholipids can originate liposomes of various sizes like small unilamellar vesicles (SUVs) with diameters inferior of 100 nm and multilamellar vesicles (MLVs) with diameters between 100 and 1000 nm (Samad, 2007; Vyas, 2001). SUVs are preferred for an efficient and constant drug release. Besides phospholipids, cholesterol is also added to the formulations to increase the circulation time of the liposomes in the blood through the increase of their stability (Papahadjopoulos, 1991). PEGylation of liposomes enhances their hydrophilicity making these carriers non ideal brain delivery systems for crossing the BBB (Huang, 2013). However after surface modification with antibodies, they have shown promising results for the transport of drugs through the BBB.

2.7. Monoclonal antibodies

Monoclonal antibodies are being used for targeting drugs, proteins and peptides to the brain (Alam, 2010). Köhler and Milstein developed a hybridoma technique that allows to obtain large quantities of mAbs with a unique specificity, which accelerates the use of antibodies and immuno-conjugates in therapy (Kohler, 1975). Antibodies have long serum half-lives and are both hydrophilic and large molecules (approximately 150 kDa), which hinder them from entering the BBB through simple diffusion. Empirical evidence shows that intravenously injected antibodies have a

low efficiency in reaching the brain. Such antibodies do not reach high enough therapeutic concentrations in the CNS because their accumulation in the brain is shortened by an apparent efflux system (Banks, 2008; Frank, 2011). However antibodies can be used as active targeting molecules to BBB receptors, allowing the passage of drugs through this barrier by RMT (Calvo, 2001; Huang, 2013). This transport mechanism seems to be one of the more promising strategies in drug delivery to the brain due to the high incorporation capacity, reduction of side effects and circumvention of the multidrug efflux system (Bao, 2012; Calvo, 2001). Some high molecular weight molecules including insulin, insulin-like growth factor, melanotransferrin, transferrin and vasopressin have receptors at the luminal side of the endothelial cells of the BBB and are transported via RMT (Table 2.2) (Demeule, 2002; Frank, 2011). These transportation systems are saturable, which means that they have a finite capacity to bind and transport their ligands. The rate of transmembrane diffusion of molecules across the BBB is generally lower than it would be expected for a transport mediated by receptors (Banks, 2009; Frank, 2011). The transferrin receptor (TfR) is very concentrated in brain capillary endothelium, comparatively to other organs, making it a desirable target for enhanced drug delivery to the brain (Carroll, 2010). Despite the increased use of transferrin as ligand for brain targeting, its application *in vivo* is very limited (Chang, 2009; Visser, 2005). Endogenous levels of transferrin are very high, which results in a saturation of the TfR (de Boer, 2007; van Rooy, 2011).

The antibodies against the TfR are thus preferable than the P-gp. The mAb for TfR does not compete with the natural transferrin present in the blood circulation (Lee, 2000). Antibodies against the TfR (for example, OX-26 mAb) have been investigated in a number of studies (Huwyler, 1996; Kuo, 2011; Zhang, 2003). Radiolabeling and immuno-histochemical

approaches were used to study the brain penetration of OX-26 mAb (Gosk, 2004; Moos, 2001; Paris-Robidas, 2011).

Table 2.2 - Receptors at the brain endothelial cells that could be used as targets for brain drug delivery (Alam, 2010; Dehouck, 1997; Fillebeen, 1999; Wu, 1999).

Receptors	Molecules
Insulin Receptor	Insulin
Transferrin Receptor	Transferrin
Insulin-like growth factor receptors	Insulin-like growth factor 1 and 2, mannose-6-phosphate
Leptin receptor	Leptin
Fc like growth factor receptor	Immunoglobulin G
Scavenger receptor type B1	Modified lipoproteins, like acetylated low density lipoprotein (LDL)
LDL receptor	LDL
Lactoferrin receptor	Lactoferrin
Interleukin 1 receptor	Interleukin 1
Folic acid receptor	Folic acid

The studies showed that OX-26 is transported into brain capillary endothelial cells but does not penetrate into the CNS at appreciable concentrations (Couch, 2013). As OX-26 is directed against the rat TfR, other mAbs were used to target the mouse TfR, including the 8D3 (Kissel, 1998) and the RI7217 mAbs (Lesley, 1984), and are reported to associate to human TfR *in vitro*, probably due to the 86% homology between mouse and human receptors (Table 2.3) (Salvati, 2013; Wang, 2008). *In vitro* experiments performed by van Rooy *et. al.* showed that RI7217 binds significantly to human endothelial cells (hCMEC/D3) (van Rooy, 2011).

A receptor frequently found in the human brain endothelial cells is the insulin receptor (IR) and its antibody is the most potent mAb discovered until today (Alam, 2010). Kuo et *al.* used the 83-14 human mAb

to target the IR and proved that it is 10 times more efficient than the anti-transferrin mAb to target TfR (Kuo, 2013; Walus, 1996). The 83-14 mAb has a strong affinity to brain capillary and can bind with a subunit of the human IR (Prigent, 1990). As the size of the 83-14 mAb is similar to the neuroactive molecule, its transport is effective (Boado, 2007; Kuo, 2013) (Table 2.3).

Table 2.3 - mAbs specific for brain receptors and their reactivity (Alam, 2010; Boado, 2011; Boado, 2007; Boado, 2009; Chekhonin, 2005; Lee, 2000; Ng, 2000; Pardridge, 1991; Pardridge, 1995; Salvati, 2013)

Targeting mAb	Target receptor	Reactivity
Murine OX26	TfR	Rat, Human
Rat 8D3	TfR	Mouse
Murine 8314	IR	Human
Chimeric anti-TfR	TfR	Mouse
Humanized anti-IR	IR	Human
RI7217	TfR	Mouse, Human
Chimeric anti-IR	IR	Human
HYB-241	P-gp	Human
D4	gliofibrillary acidic protein	Human, Rat
Anti-E-selectin	E-selectin	Human

2.7.1. Immuno-nanocarriers

Nanosystems coupled to mAbs that can be recognized by the BBB receptors are being studied for the development of nano-drug delivery systems to treat CNS disorders (Alam, 2010). The principal reason to the worldwide acceptance of these carriers is their controlled properties and the ability of releasing the drug at the selected target site. Immuno-

targeted drug delivery systems have several advantages that include a high capacity of drug loading, the relatively few mAbs necessary to achieve high levels of drug targeting, a protection of the encapsulated drug from degradation in the biological environment and the ability to provide stimulus-sensitive compositions for controlled and enhanced release of the drug in the targeting areas (Koshkaryev, 2013). In order to meet the requirements of a "Directed Trojan horse", the antibody must bind to the brain microvascular endothelial cells, specifically to a transcytosis receptor, with sufficient affinity. After binding, the transcytosis pathway needs to be activated (Frank, 2011; Kuo, 2013; Pardridge, 1999). Therapies with the use of these immuno-targeting systems may be more efficient by directing the drug to diseased cells and reducing unnecessary delivery of excessive amounts of drugs into the bloodstream (Pedro Ramos-Cabrer, 2013).

The BBB TfR is a bidirectional transcytosis system (Zhang, 2001), and mediates the transport of the system through the endothelial barrier into the brain interstitial space. In the case of the liposomes, they fuse with the intracellular endosomal membrane subsequent to endocytosis and release the drug into the cytosol of the target cell (Figure 2.4) (Mok, 1999; Shi, 2001).

Chekhonin *et al.* tested the D4 mAb against human gliofibrillary acidic protein as a potential vector to direct immunoliposomes against embryonic rat brain astrocytes. These immunoliposomes (palmitoyl-oleyl-phosphatidylcholine, cholesterol, maleimido-4-(*p*-phenylbutyryl)-phosphatidylethanolamine and distearoylphosphatidylethanolamine-PEG_{2000}) may be useful to deliver drugs to the glial brain cells or to *loci* in the brain with a partially disintegrated BBB. The referred system cannot be applied to the treatment of neurodegenerative diseases such as Alzheimer or Parkinson, but could be used for the treatment of other brain pathologies in which the BBB integrity is altered (Chekhonin, 2005).

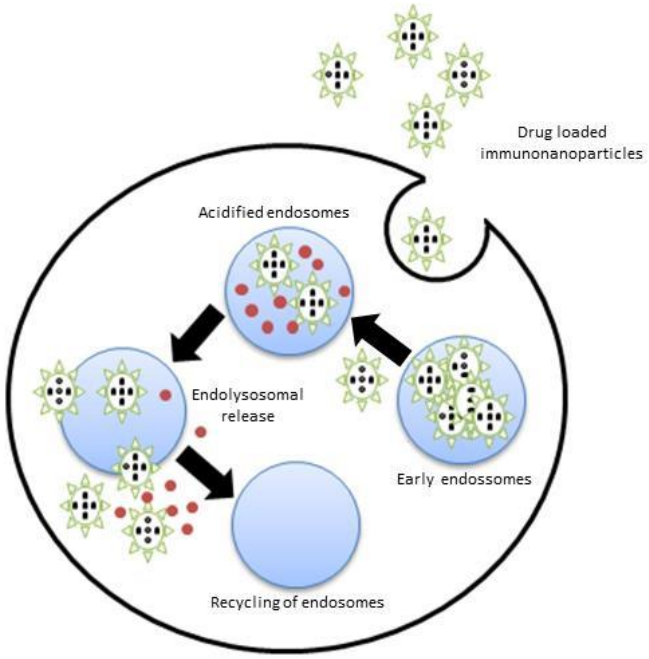

Figure 2.4 - Schematic representation of the interaction between immunoliposomes and cells. Adapted from (Acharya, 2011).

HYB-241 is a mouse antihuman P-gp mAb and was used by Ng *et al.* to target liposomes (dioleoylphosphatidylethanolamine, dioleoylphosphatidylethanolamine-PEG_{2000}, dioleoylphosphatidic acid and *N*-glutarylphosphatidylethanolamine) to the brain. This nanocarrier induces a bilayer destabilization of the BBB that results in a site-specific release of the liposome contents (Ng, 2000).

References

Acharya, S.; Sahoo, S. K. **2011.** PLGA nanoparticles containing various anticancer agents and tumour delivery by EPR effect. *Adv Drug Deliv Rev*. Vol. 63. n.º 3. p. 170-83.

Alam, M. I.; Beg, S.; Samad, A.; Baboota, S.; Kohli, K.; Ali, J.; Ahuja, A.; Akbar, M. **2010.** Strategy for effective brain drug delivery. *Eur J Pharm Sci*. Vol. 40. n.º 5. p. 385-403.

Andreasen, N.; Blennow, K. **2002.** beta-amyloid (A beta) protein in cerebrospinal fluid as a biomarker for Alzheimer's disease. *Peptides*. Vol. 23. n.º 7. p. 1205-1214.

Andrieux, K.; Couvreur, P. **2009.** Polyalkylcyanoacrylate nanoparticles for delivery of drugs across the blood-brain barrier. *Wiley Interdiscip Rev Nanomed Nanobiotechnol*. Vol. 1. n.º 5. p. 463-74.

Austen, B. M.; Paleologou, K. E.; Ali, S. A.; Qureshi, M. M.; Allsop, D.; El-Agnaf, O. M. **2008.** Designing peptide inhibitors for oligomerization and toxicity of Alzheimer's beta-amyloid peptide. *Biochemistry*. Vol. 47. n.º 7. p. 1984-92.

Banks, R. E.; Smart, B. E.; Tatlow, J. C. - Organofluorine chemistry : principles and commercial applications. New York: Plenum, 1994.

Banks, W. A. **2008.** Developing drugs that can cross the blood-brain barrier: applications to Alzheimer's disease. *BMC Neurosci*. Vol. 9 Suppl 3. p. S2.

Banks, W. A. **2009.** Characteristics of compounds that cross the blood-brain barrier. *Bmc Neurology*. Vol. 9.

Bao, H.; Jin, X.; Li, L.; Lv, F.; Liu, T. **2012.** OX26 modified hyperbranched polyglycerol-conjugated poly(lactic-co-glycolic acid) nanoparticles: synthesis, characterization and evaluation of its brain delivery ability. *J Mater Sci Mater Med*. Vol. 23. n.º 8. p. 1891-901.

Begley, D. J. **1996.** The blood-brain barrier: principles for targeting peptides and drugs to the central nervous system. *J Pharm Pharmacol*. Vol. 48. n.º 2. p. 136-46.

Berg, T. **2003.** Modulation of protein-protein interactions with small organic molecules. *Angew Chem Int Ed Engl*. Vol. 42. n.º 22. p. 2462-81.

Bernacki, J.; Dobrowolska, A.; Nierwinska, K.; Malecki, A. **2008.** Physiology and pharmacological role of the blood-brain barrier. *Pharmacol Rep*. Vol. 60. n.º 5. p. 600-22.

Blume, G.; Cevc, G. **1990.** Liposomes for the sustained drug release in vivo. *Biochim Biophys Acta*. Vol. 1029. n.º 1. p. 91-7.

Boado, R. J.; Pardridge, W. M. **2011.** The Trojan Horse Liposome Technology for Nonviral Gene Transfer across the Blood-Brain Barrier. *J Drug Deliv*. Vol. 2011. p. 296151.

Boado, R. J.; Zhang, Y.; Pardridge, W. M. **2007.** Humanization of anti-human insulin receptor antibody for drug targeting across the human blood-brain barrier. *Biotechnol Bioeng*. Vol. 96. n.º 2. p. 381-91.

Boado, R. J.; Zhang, Y.; Wang, Y.; Pardridge, W. M. **2009.** Engineering and expression of a chimeric transferrin receptor monoclonal antibody for blood-brain barrier delivery in the mouse. *Biotechnol Bioeng*. Vol. 102. n.º 4. p. 1251-8.

Brambilla, D.; Le Droumaguet, B.; Nicolas, J.; Hashemi, S. H.; Wu, L. P.; Moghimi, S. M.; Couvreur, P.; Andrieux, K. **2011.** Nanotechnologies for Alzheimer's disease: diagnosis, therapy, and safety issues. *Nanomedicine*. Vol. 7. n.º 5. p. 521-40.

Brigger, I.; Dubernet, C.; Couvreur, P. **2002.** Nanoparticles in cancer therapy and diagnosis. *Adv Drug Deliv Rev*. Vol. 54. n.º 5. p. 631-51.

Brookmeyer, R.; Johnson, E.; Ziegler-Graham, K.; Arrighi, H. M. **2007.** Forecasting the global burden of Alzheimer's disease. *Alzheimers Dement*. Vol. 3. n.º 3. p. 186-91.

Calhoun, M. E.; Burgermeister, P.; Phinney, A. L.; Stalder, M.; Tolnay, M.; Wiederhold, K. H.; Abramowski, D.; Sturchler-Pierrat, C.; Sommer, B.; Staufenbiel, M.; Jucker, M. **1999.** Neuronal overexpression of mutant amyloid precursor protein results in prominent deposition of cerebrovascular amyloid. *Proc Natl Acad Sci U S A*. Vol. 96. n.º 24. p. 14088-93.

Calvo, P.; Gouritin, B.; Chacun, H.; Desmaele, D.; D'Angelo, J.; Noel, J. P.; Georgin, D.; Fattal, E.; Andreux, J. P.; Couvreur, P. **2001.** Long-circulating PEGylated polycyanoacrylate nanoparticles as new drug carrier for brain delivery. *Pharm Res*. Vol. 18. n.º 8. p. 1157-66.

Carroll, R. T.; Bhatia, D.; Geldenhuys, W.; Bhatia, R.; Miladore, N.; Bishayee, A.; Sutariya, V. **2010.** Brain-targeted delivery of Tempol-loaded nanoparticles for neurological disorders. *J Drug Target*. Vol. 18. n.º 9. p. 665-74.

Chacon, M. A.; Barria, M. I.; Soto, C.; Inestrosa, N. C. **2004.** Beta-sheet breaker peptide prevents Abeta-induced spatial memory impairments with partial reduction of amyloid deposits. *Mol Psychiatry*. Vol. 9. n.º 10. p. 953-61.

Chang, J.; Jallouli, Y.; Kroubi, M.; Yuan, X. B.; Feng, W.; Kang, C. S.; Pu, P. Y.; Betbeder, D. **2009.** Characterization of endocytosis of transferrin-coated PLGA nanoparticles by the blood-brain barrier. *Int J Pharm*. Vol. 379. n.º 2. p. 285-92.

Chekhonin, V. P.; Zhirkov, Y. A.; Gurina, O. I.; Ryabukhin, I. A.; Lebedev, S. V.; Kashparov, I. A.; Dmitriyeva, T. B. **2005.** PEGylated immunoliposomes directed against brain astrocytes. *Drug Deliv*. Vol. 12. n.º 1. p. 1-6.

Chou, P. Y.; Fasman, G. D. **1978.** Empirical predictions of protein conformation. *Annu Rev Biochem*. Vol. 47. p. 251-76.

Clippingdale, A. B.; Wade, J. D.; Barrow, C. J. **2001.** The amyloid-beta peptide and its role in Alzheimer's disease. *J Pept Sci*. Vol. 7. n.º 5. p. 227-49.

Couch, J. A.; Yu, Y. J.; Zhang, Y.; Tarrant, J. M.; Fuji, R. N.; Meilandt, W. J.; Solanoy, H.; Tong, R. K.; Hoyte, K.; Luk, W.; Lu, Y.; Gadkar, K.; Prabhu, S.; Ordonia, B. A.; Nguyen, Q.; Lin, Y.; Lin, Z.; Balazs, M.; Scearce-Levie, K.; Ernst, J. A.; Dennis, M. S.; Watts, R. J. **2013.** Addressing safety liabilities of TfR bispecific antibodies that cross the blood-brain barrier. *Sci Transl Med*. Vol. 5. n.º 183. p. 183ra57, 1-12.

Crone, C.; Christensen, O. **1981.** Electrical resistance of a capillary endothelium. *J Gen Physiol*. Vol. 77. n.º 4. p. 349-71.

Crone, C.; Olesen, S. P. **1982.** Electrical resistance of brain microvascular endothelium. *Brain Res*. Vol. 241. n.º 1. p. 49-55.

Csuk, R.; Albert, S.; Kluge, R.; Strohl, D. **2013.** Resveratrol derived butyrylcholinesterase inhibitors. *Arch Pharm (Weinheim)*. Vol. 346. n.º 7. p. 499-503.

Danhier, F.; Ansorena, E.; Silva, J. M.; Coco, R.; Le Breton, A.; Preat, V. **2012.** PLGA-based nanoparticles: an overview of biomedical applications. *J Control Release*. Vol. 161. n.º 2. p. 505-22.

Datki, Z.; Papp, R.; Zadori, D.; Soos, K.; Fulop, L.; Juhasz, A.; Laskay, G.; Hetenyi, C.; Mihalik, E.; Zarandi, M.; Penke, B. **2004.** In vitro model of neurotoxicity of Abeta 1-42 and neuroprotection by a pentapeptide: irreversible events during the first hour. *Neurobiol Dis*. Vol. 17. n.º 3. p. 507-15.

de Boer, A. G.; Gaillard, P. J. **2007.** Drug targeting to the brain. *Annu Rev Pharmacol Toxicol*. Vol. 47. p. 323-55.

Dehouck, B.; Fenart, L.; Dehouck, M. P.; Pierce, A.; Torpier, G.; Cecchelli, R. **1997.** A new function for the LDL receptor: transcytosis of LDL across the blood-brain barrier. *J Cell Biol*. Vol. 138. n.º 4. p. 877-89.

Demeule, M.; Poirier, J.; Jodoin, J.; Bertrand, Y.; Desrosiers, R. R.; Dagenais, C.; Nguyen, T.; Lanthier, J.; Gabathuler, R.; Kennard, M.; Jefferies, W. A.; Karkan, D.; Tsai, S.; Fenart, L.; Cecchelli, R.; Beliveau, R. **2002.** High transcytosis of melanotransferrin (P97) across the blood-brain barrier. *J Neurochem*. Vol. 83. n.º 4. p. 924-33.

Egleton, R. D.; Davis, T. P. **1997.** Bioavailability and transport of peptides and peptide drugs into the brain. *Peptides*. Vol. 18. n.º 9. p. 1431-9.

Esler, W. P.; Stimson, E. R.; Ghilardi, J. R.; Felix, A. M.; Lu, Y. A.; Vinters, H. V.; Mantyh, P. W.; Maggio, J. E. **1997.** A beta deposition inhibitor screen using synthetic amyloid. *Nat Biotechnol*. Vol. 15. n.º 3. p. 258-63.

Fillebeen, C.; Descamps, L.; Dehouck, M. P.; Fenart, L.; Benaissa, M.; Spik, G.; Cecchelli, R.; Pierce, A. **1999.** Receptor-mediated transcytosis of lactoferrin through the blood-brain barrier. *J Biol Chem*. Vol. 274. n.º 11. p. 7011-7.

Filler, Robert; Kobayashi, Yoshir o; American Chemical Society.; Nihon Kagakkai. - Biomedicinal aspects of fluorine chemistry. Amsterdam ; New York, U.S.A.: Elsevier Biomedical Press ;

Findeis, M. A. **2000.** Approaches to discovery and characterization of inhibitors of amyloid beta-peptide polymerization. *Biochim Biophys Acta*. Vol. 1502. n.º 1. p. 76-84.

Findeis, M. A. **2002.** Peptide inhibitors of beta amyloid aggregation. *Curr Top Med Chem*. Vol. 2. n.º 4. p. 417-23.

Findeis, M. A.; Musso, G. M.; Arico-Muendel, C. C.; Benjamin, H. W.; Hundal, A. M.; Lee, J. J.; Chin, J.; Kelley, M.; Wakefield, J.; Hayward, N. J.; Molineaux, S. M. **1999.** Modified-peptide inhibitors of amyloid beta-peptide polymerization. *Biochemistry*. Vol. 38. n.º 21. p. 6791-800.

Forstl, H.; Kurz, A. **1999.** Clinical features of Alzheimer's disease. *Eur Arch Psychiatry Clin Neurosci*. Vol. 249. n.º 6. p. 288-90.

Frank, R. T.; Aboody, K. S.; Najbauer, J. **2011.** Strategies for enhancing antibody delivery to the brain. *Biochim Biophys Acta*. Vol. 1816. n.º 2. p. 191-8.

Fricker, G.; Miller, D. S. **2004.** Modulation of drug transporters at the blood-brain barrier. *Pharmacology*. Vol. 70. n.º 4. p. 169-76.

Frydman-Marom, A.; Rechter, M.; Shefler, I.; Bram, Y.; Shalev, D. E.; Gazit, E. **2009.** Cognitive-performance recovery of Alzheimer's disease model mice by modulation of early soluble amyloidal assemblies. *Angew Chem Int Ed Engl*. Vol. 48. n.º 11. p. 1981-6.

Funke, S. A.; Willbold, D. **2012.** Peptides for therapy and diagnosis of Alzheimer's disease. *Curr Pharm Des*. Vol. 18. n.º 6. p. 755-67.

Gabizon, A.; Shmeeda, H.; Barenholz, Y. **2003.** Pharmacokinetics of pegylated liposomal Doxorubicin: review of animal and human studies. *Clin Pharmacokinet*. Vol. 42. n.º 5. p. 419-36.

Giacomelli, C. E.; Norde, W. **2003.** Influence of hydrophobic Teflon particles on the structure of amyloid beta-peptide. *Biomacromolecules*. Vol. 4. n.º 6. p. 1719-26.

Gordon, D. J.; Sciarretta, K. L.; Meredith, S. C. **2001.** Inhibition of beta-amyloid(40) fibrillogenesis and disassembly of beta-amyloid(40) fibrils by short beta-amyloid congeners containing N-methyl amino acids at alternate residues. *Biochemistry*. Vol. 40. n.º 28. p. 8237-45.

Granger, B.; Albu, S. **2005.** The haloperidol story. *Ann Clin Psychiatry*. Vol. 17. n.º 3. p. 137-40.

Haass, C.; Schlossmacher, M. G.; Hung, A. Y.; Vigopelfrey, C.; Mellon, A.; Ostaszewski, B. L.; Lieberburg, I.; Koo, E. H.; Schenk, D.; Teplow, D. B.; Selkoe, D. J. **1992.** Amyloid Beta-Peptide Is Produced by Cultured-Cells during Normal Metabolism. *Nature*. Vol. 359. n.º 6393. p. 322-325.

Haass, C.; Selkoe, D. J. **1993.** Cellular processing of beta-amyloid precursor protein and the genesis of amyloid beta-peptide. *Cell*. Vol. 75. n.º 6. p. 1039-42.

Haass, C.; Selkoe, D. J. **2007.** Soluble protein oligomers in neurodegeneration: lessons from the Alzheimer's amyloid beta-peptide. *Nat Rev Mol Cell Biol*. Vol. 8. n.º 2. p. 101-12.

Hardy, J. A.; Higgins, G. A. **1992.** Alzheimer's disease: the amyloid cascade hypothesis. *Science*. Vol. 256. n.º 5054. p. 184-5.

Hardy, J.; Selkoe, D. J. **2002a.** The amyloid hypothesis of Alzheimer's disease: progress and problems on the road to therapeutics. *Science*. Vol. 297. n.º 5580. p. 353-6.

Hardy, J.; Selkoe, D. J. **2002b.** Medicine - The amyloid hypothesis of Alzheimer's disease: Progress and problems on the road to therapeutics. *Science*. Vol. 297. n.º 5580. p. 353-356.

Hartmann, T.; Bieger, S. C.; Bruhl, B.; Tienari, P. J.; Ida, N.; Allsop, D.; Roberts, G. W.; Masters, C. L.; Dotti, C. G.; Unsicker, K.; Beyreuther, K. **1997.** Distinct sites of intracellular production for Alzheimer's disease A beta40/42 amyloid peptides. *Nat Med*. Vol. 3. n.º 9. p. 1016-20.

Hilbich, C.; Kisters-Woike, B.; Reed, J.; Masters, C. L.; Beyreuther, K. **1992.** Substitutions of hydrophobic amino acids reduce the amyloidogenicity of Alzheimer's disease beta A4 peptides. *J Mol Biol*. Vol. 228. n.º 2. p. 460-73.

Huang, F. Y.; Chen, W. J.; Lee, W. Y.; Lo, S. T.; Lee, T. W.; Lo, J. M. **2013.** In vitro and in vivo evaluation of lactoferrin-conjugated liposomes as a novel carrier to improve the brain delivery. *Int J Mol Sci*. Vol. 14. n.º 2. p. 2862-74.

Hughes, S. R.; Goyal, S.; Sun, J. E.; Gonzalez-DeWhitt, P.; Fortes, M. A.; Riedel, N. G.; Sahasrabudhe, S. R. **1996.** Two-hybrid system as a model to study the interaction of beta-amyloid peptide monomers. *Proc Natl Acad Sci U S A*. Vol. 93. n.º 5. p. 2065-70.

Immordino, M. L.; Dosio, F.; Cattel, L. **2006.** Stealth liposomes: review of the basic science, rationale, and clinical applications, existing and potential. *Int J Nanomedicine*. Vol. 1. n.º 3. p. 297-315.

Iversen, L. **2002.** Amyloid diseases: small drugs lead the attack. *Nature*. Vol. 417. n.º 6886. p. 231-3.

J.L. Fauchere, C. Thurieau. **1992.** Evaluation of the Stability of Peptides and Pseudopeptides as a Tool in Peptide Drug Design. *Advances in Drug Research*. Vol. 23. p. 127-159.

Jahn, T. R.; Radford, S. E. **2005.** The Yin and Yang of protein folding. *FEBS J*. Vol. 272. n.º 23. p. 5962-70.

Jan, A.; Gokce, O.; Luthi-Carter, R.; Lashuel, H. A. **2008.** The ratio of monomeric to aggregated forms of Abeta40 and Abeta42 is an important determinant of amyloid-beta aggregation, fibrillogenesis, and toxicity. *J Biol Chem*. Vol. 283. n.º 42. p. 28176-89.

Jarrett, J. T.; Berger, E. P.; Lansbury, P. T. **1993a.** The Carboxy Terminus of the Beta-Amyloid Protein Is Critical for the Seeding of Amyloid Formation - Implications for the Pathogenesis of Alzheimers-Disease. *Biochemistry*. Vol. 32. n.º 18. p. 4693-4697.

Jarrett, J. T.; Berger, E. P.; Lansbury, P. T., Jr. **1993b.** The carboxy terminus of the beta amyloid protein is critical for the seeding of amyloid formation: implications for the pathogenesis of Alzheimer's disease. *Biochemistry*. Vol. 32. n.º 18. p. 4693-7.

Jefferies, W. A.; Brandon, M. R.; Hunt, S. V.; Williams, A. F.; Gatter, K. C.; Mason, D. Y. **1984.** Transferrin receptor on endothelium of brain capillaries. *Nature*. Vol. 312. n.º 5990. p. 162-3.

Juhasz, G.; Marki, A.; Vass, G.; Fulop, L.; Budai, D.; Penke, B.; Falkay, G.; Szegedi, V. **2009.** An intraperitoneally administered pentapeptide protects against Abeta (1-42) induced neuronal excitation in vivo. *J Alzheimers Dis*. Vol. 16. n.º 1. p. 189-96.

Kang, J.; Lemaire, H. G.; Unterbeck, A.; Salbaum, J. M.; Masters, C. L.; Grzeschik, K. H.; Multhaup, G.; Beyreuther, K.; Mullerhill, B. **1987.** The Precursor of Alzheimers-Disease Amyloid-A4 Protein Resembles a Cell-Surface Receptor. *Nature*. Vol. 325. n.º 6106. p. 733-736.

Kayed, R.; Head, E.; Thompson, J. L.; McIntire, T. M.; Milton, S. C.; Cotman, C. W.; Glabe, C. G. **2003.** Common structure of soluble amyloid oligomers implies common mechanism of pathogenesis. *Science*. Vol. 300. n.º 5618. p. 486-9.

Kirk, K. L. **2006.** Fluorine in medicinal chemistry: Recent therapeutic applications of fluorinated small molecules. *Journal of Fluorine Chemistry*. Vol. 127. n.º 8. p. 1013-1029.

Kirsch, Peer - Modern fluoroorganic chemistry : synthesis, reactivity, applications. Weinheim: Wiley-VCH, 2004.

Kirschner, D. A.; Abraham, C.; Selkoe, D. J. **1986.** X-Ray-Diffraction from Intraneuronal Paired Helical Filaments and Extraneuronal Amyloid Fibers in Alzheimer-Disease Indicates Cross-Beta Conformation. *Proceedings of the National Academy of Sciences of the United States of America*. Vol. 83. n.º 2. p. 503-507.

Kisilevsky, R.; Lemieux, L. J.; Fraser, P. E.; Kong, X.; Hultin, P. G.; Szarek, W. A. **1995.** Arresting amyloidosis in vivo using small-molecule anionic sulphonates or sulphates: implications for Alzheimer's disease. *Nat Med*. Vol. 1. n.º 2. p. 143-8.

Kissel, K.; Hamm, S.; Schulz, M.; Vecchi, A.; Garlanda, C.; Engelhardt, B. **1998.** Immunohistochemical localization of the murine transferrin receptor (TfR) on blood-tissue barriers using a novel anti-TfR monoclonal antibody. *Histochem Cell Biol*. Vol. 110. n.º 1. p. 63-72.

Klibanov, A. L.; Maruyama, K.; Torchilin, V. P.; Huang, L. **1990.** Amphipathic polyethyleneglycols effectively prolong the circulation time of liposomes. *FEBS Lett*. Vol. 268. n.º 1. p. 235-7.

Kohler, G.; Milstein, C. **1975.** Continuous cultures of fused cells secreting antibody of predefined specificity. *Nature*. Vol. 256. n.º 5517. p. 495-7.

Kokkoni, N.; Stott, K.; Amijee, H.; Mason, J. M.; Doig, A. J. **2006.** N-Methylated peptide inhibitors of beta-amyloid aggregation and toxicity. Optimization of the inhibitor structure. *Biochemistry*. Vol. 45. n.º 32. p. 9906-18.

Koshkaryev, A.; Sawant, R.; Deshpande, M.; Torchilin, V. **2013.** Immunoconjugates and long circulating systems: origins, current state of the art and future directions. *Adv Drug Deliv Rev*. Vol. 65. n.º 1. p. 24-35.

Kumari, A.; Yadav, S. K.; Yadav, S. C. **2010.** Biodegradable polymeric nanoparticles based drug delivery systems. *Colloids Surf B Biointerfaces*. Vol. 75. n.º 1. p. 1-18.

Kuo, Y. C.; Ko, H. F. **2013.** Targeting delivery of saquinavir to the brain using 83-14 monoclonal antibody-grafted solid lipid nanoparticles. *Biomaterials*. Vol. 34. n.º 20. p. 4818-30.

Kuperstein, I.; Broersen, K.; Benilova, I.; Rozenski, J.; Jonckheere, W.; Debulpaep, M.; Vandersteen, A.; Segers-Nolten, I.; Van Der Werf, K.; Subramaniam, V.; Braeken, D.; Callewaert, G.; Bartic, C.; D'Hooge, R.; Martins, I. C.; Rousseau, F.; Schymkowitz, J.; De Strooper, B. **2010.** Neurotoxicity of Alzheimer's disease Abeta peptides is induced by small changes in the Abeta42 to Abeta40 ratio. *EMBO J*. Vol. 29. n.º 19. p. 3408-20.

Ladiwala, A. R.; Litt, J.; Kane, R. S.; Aucoin, D. S.; Smith, S. O.; Ranjan, S.; Davis, J.; Van Nostrand, W. E.; Tessier, P. M. **2012.** Conformational differences between two amyloid beta oligomers of similar size and dissimilar toxicity. *J Biol Chem*. Vol. 287. n.º 29. p. 24765-73.

Lai, F.; Fadda, A. M.; Sinico, C. **2013.** Liposomes for brain delivery. *Expert Opin Drug Deliv*. Vol. 10. n.º 7. p. 1003-22.

Larson, E. B.; Shadlen, M. F.; Wang, L.; McCormick, W. C.; Bowen, J. D.; Teri, L.; Kukull, W. A. **2004.** Survival after initial diagnosis of Alzheimer disease. *Annals of Internal Medicine*. Vol. 140. n.º 7. p. 501-509.

Lee, H. J.; Engelhardt, B.; Lesley, J.; Bickel, U.; Pardridge, W. M. **2000.** Targeting rat anti-mouse transferrin receptor monoclonal antibodies through blood-brain barrier in mouse. *J Pharmacol Exp Ther*. Vol. 292. n.º 3. p. 1048-52.

Lesley, J.; Hyman, R.; Schulte, R.; Trotter, J. **1984.** Expression of transferrin receptor on murine hematopoietic progenitors. *Cell Immunol*. Vol. 83. n.º 1. p. 14-25.

Liu, H. F.; Ma, J.; Winter, C.; Bayer, R. **2010.** Recovery and purification process development for monoclonal antibody production. *MAbs*. Vol. 2. n.º 5. p. 480-99.

Makhaeva, G. F.; Aksinenko, A. Y.; Sokolov, V. B.; Serebryakova, O. G.; Richardson, R. J. **2009.** Synthesis of organophosphates with fluorine-containing leaving groups as serine esterase inhibitors with potential for Alzheimer disease therapeutics. *Bioorg Med Chem Lett*. Vol. 19. n.º 19. p. 5528-30.

Malamas, M. S.; Robichaud, A.; Erdei, J.; Quagliato, D.; Solvibile, W.; Zhou, P.; Morris, K.; Turner, J.; Wagner, E.; Fan, K.; Olland, A.; Jacobsen, S.; Reinhart, P.; Riddell, D.; Pangalos, M. **2010.** Design and synthesis of aminohydantoins as potent and selective human beta-secretase (BACE1) inhibitors with enhanced brain permeability. *Bioorg Med Chem Lett*. Vol. 20. n.º 22. p. 6597-605.

Mason, J. M.; Kokkoni, N.; Stott, K.; Doig, A. J. **2003.** Design strategies for anti-amyloid agents. *Current Opinion in Structural Biology*. Vol. 13. n.º 4. p. 526-532.

Matharu, B.; El-Agnaf, O.; Razvi, A.; Austen, B. M. **2010.** Development of retro-inverso peptides as anti-aggregation drugs for beta-amyloid in Alzheimer's disease. *Peptides*. Vol. 31. n.º 10. p. 1866-72.

Mattson, M. P. **1997.** Cellular actions of beta-amyloid precursor protein and its soluble and fibrillogenic derivatives. *Physiol Rev*. Vol. 77. n.º 4. p. 1081-132.

McLaurin, J.; Golomb, R.; Jurewicz, A.; Antel, J. P.; Fraser, P. E. **2000.** Inositol stereoisomers stabilize an oligomeric aggregate of Alzheimer amyloid beta peptide and inhibit abeta -induced toxicity. *J Biol Chem*. Vol. 275. n.º 24. p. 18495-502.

Merlini, G.; Ascari, E.; Amboldi, N.; Bellotti, V.; Arbustini, E.; Perfetti, V.; Ferrari, M.; Zorzoli, I.; Marinone, M. G.; Garini, P.; et al. **1995.** Interaction of the anthracycline 4'-iodo-4'-deoxydoxorubicin with amyloid fibrils: inhibition of amyloidogenesis. *Proc Natl Acad Sci U S A*. Vol. 92. n.º 7. p. 2959-63.

Merlini, G.; Bellotti, V. **2003.** Molecular mechanisms of amyloidosis. *N Engl J Med*. Vol. 349. n.º 6. p. 583-96.

Mok, K. W.; Lam, A. M.; Cullis, P. R. **1999.** Stabilized plasmid-lipid particles: factors influencing plasmid entrapment and transfection properties. *Biochim Biophys Acta*. Vol. 1419. n.º 2. p. 137-50.

Ng, K.; Zhao, L.; Liu, Y.; Mahapatro, M. **2000.** The effects of polyethyleneglycol (PEG)-derived lipid on the activity of target-sensitive immunoliposome. *Int J Pharm*. Vol. 193. n.º 2. p. 157-66.

O'Hagan, D. **2008.** Understanding organofluorine chemistry. An introduction to the C-F bond. *Chem Soc Rev*. Vol. 37. n.º 2. p. 308-19.

Ojima, Iwao; McCarthy, James R.; Welch, John T.; American Chemical Society. Division of Fluorine Chemistry.; American Chemical Society. Division of Medicinal Chemistry. - Biomedical frontiers of fluorine chemistry. Washington, DC: American Chemical Society, 1996.

Papahadjopoulos, D.; Allen, T. M.; Gabizon, A.; Mayhew, E.; Matthay, K.; Huang, S. K.; Lee, K. D.; Woodle, M. C.; Lasic, D. D.; Redemann, C.; et al. **1991.** Sterically stabilized liposomes: improvements in pharmacokinetics and antitumor therapeutic efficacy. *Proc Natl Acad Sci U S A*. Vol. 88. n.º 24. p. 11460-4.

Pappolla, M.; Bozner, P.; Soto, C.; Shao, H.; Robakis, N. K.; Zagorski, M.; Frangione, B.; Ghiso, J. **1998.** Inhibition of Alzheimer beta-fibrillogenesis by melatonin. *J Biol Chem*. Vol. 273. n.º 13. p. 7185-8.

Pardridge, W. M. **1999.** Vector-mediated drug delivery to the brain. *Adv Drug Deliv Rev*. Vol. 36. n.º 2-3. p. 299-321.

Pardridge, W. M. **2002.** Drug and gene delivery to the brain: the vascular route. *Neuron*. Vol. 36. n.º 4. p. 555-8.

Pardridge, W. M. **2007.** Drug targeting to the brain. *Pharm Res*. Vol. 24. n.º 9. p. 1733-44.

Pardridge, W. M.; Buciak, J. L.; Friden, P. M. **1991.** Selective transport of an anti-transferrin receptor antibody through the blood-brain barrier in vivo. *J Pharmacol Exp Ther*. Vol. 259. n.º 1. p. 66-70.

Pardridge, W. M.; Kang, Y. S.; Buciak, J. L.; Yang, J. **1995.** Human insulin receptor monoclonal antibody undergoes high affinity binding to human brain capillaries in vitro and rapid transcytosis through the blood-brain barrier in vivo in the primate. *Pharm Res*. Vol. 12. n.º 6. p. 807-16.

Pedro Ramos-Cabrer, Francisco Campos. **2013.** Liposomes and nanotechnology in drug development: focus on neurological targets. *International Journal of Nanomedicine*. Vol. 8. p. 951-960.

Permanne, B.; Adessi, C.; Saborio, G. P.; Fraga, S.; Frossard, M. J.; Van Dorpe, J.; Dewachter, I.; Banks, W. A.; Van Leuven, F.; Soto, C. **2002.** Reduction of amyloid load and cerebral damage in a transgenic mouse model of Alzheimer's disease by treatment with a beta-sheet breaker peptide. *FASEB J*. Vol. 16. n.º 8. p. 860-2.

Prigent, S. A.; Stanley, K. K.; Siddle, K. **1990.** Identification of epitopes on the human insulin receptor reacting with rabbit polyclonal antisera and mouse monoclonal antibodies. *J Biol Chem*. Vol. 265. n.º 17. p. 9970-7.

Risau, W. **1995.** Differentiation of endothelium. *FASEB J*. Vol. 9. n.º 10. p. 926-33.

Rocha, S.; Cardoso, I.; Borner, H.; Pereira, M. C.; Saraiva, M. J.; Coelho, M. **2009.** Design and biological activity of beta-sheet breaker peptide conjugates. *Biochem Biophys Res Commun*. Vol. 380. n.º 2. p. 397-401.

Rowley, M.; Bristow, L. J.; Hutson, P. H. **2001.** Current and novel approaches to the drug treatment of schizophrenia. *J Med Chem*. Vol. 44. n.º 4. p. 477-501.

Salvati, E.; Re, F.; Sesana, S.; Cambianica, I.; Sancini, G.; Masserini, M.; Gregori, M. **2013.** Liposomes functionalized to overcome the blood-brain barrier and to target amyloid-beta peptide: the chemical design affects the permeability across an in vitro model. *Int J Nanomedicine*. Vol. 8. p. 1749-58.

Samad, A.; Sultana, Y.; Aqil, M. **2007.** Liposomal drug delivery systems: an update review. *Curr Drug Deliv*. Vol. 4. n.º 4. p. 297-305.

Schnyder, A.; Huwyler, J. **2005.** Drug transport to brain with targeted liposomes. *NeuroRx*. Vol. 2. n.º 1. p. 99-107.

Schwarzman, A. L.; Tsiper, M.; Gregori, L.; Goldgaber, D.; Frakowiak, J.; Mazur-Kolecka, B.; Taraskina, A.; Pchelina, S.; Vitek, M. P. **2005.** Selection of peptides binding to the amyloid b-protein reveals potential inhibitors of amyloid formation. *Amyloid*. Vol. 12. n.º 4. p. 199-209.

Selkoe, D. J. **1991.** The molecular pathology of Alzheimer's disease. *Neuron*. Vol. 6. n.º 4. p. 487-98.

Selkoe, D. J. **2001.** Presenilins, beta-amyloid precursor protein and the molecular basis of Alzheimer's disease. *Clinical Neuroscience Research*. Vol. 1. n.º 1-2. p. 91-103.

Selkoe, D. J.; Wolfe, M. S. **2007.** Presenilin: running with scissors in the membrane. *Cell*. Vol. 131. n.º 2. p. 215-21.

Shankar, G. M.; Bloodgood, B. L.; Townsend, M.; Walsh, D. M.; Selkoe, D. J.; Sabatini, B. L. **2007.** Natural oligomers of the Alzheimer amyloid-beta protein induce reversible synapse loss by modulating an NMDA-type glutamate receptor-dependent signaling pathway. *J Neurosci*. Vol. 27. n.º 11. p. 2866-75.

Shankar, G. M.; Li, S.; Mehta, T. H.; Garcia-Munoz, A.; Shepardson, N. E.; Smith, I.; Brett, F. M.; Farrell, M. A.; Rowan, M. J.; Lemere, C. A.; Regan, C. M.; Walsh, D. M.; Sabatini, B. L.; Selkoe, D. J. **2008.** Amyloid-beta protein dimers isolated directly from Alzheimer's brains impair synaptic plasticity and memory. *Nat Med*. Vol. 14. n.º 8. p. 837-42.

Shi, N.; Boado, R. J.; Pardridge, W. M. **2001.** Receptor-mediated gene targeting to tissues in vivo following intravenous administration of pegylated immunoliposomes. *Pharm Res*. Vol. 18. n.º 8. p. 1091-5.

Smart, B. E. **2001.** Fluorine substituent effects (on bioactivity). *Journal of Fluorine Chemistry*. Vol. 109. n.º 1. p. 3-11.

Soloshonok, V. A. - Enantiocontrolled synthesis of fluoro-organic compounds : stereochemical challenges and biomedical targets. Chichester ; New York: Wiley, 1999.

Sood, A.; Abid, M.; Sauer, C.; Hailemichael, S.; Foster, M.; Torok, B.; Torok, M. **2011.** Disassembly of preformed amyloid beta fibrils by small organofluorine molecules. *Bioorg Med Chem Lett*. Vol. 21. n.º 7. p. 2044-7.

Soto, C.; Kindy, M. S.; Baumann, M.; Frangione, B. **1996.** Inhibition of Alzheimer's amyloidosis by peptides that prevent beta-sheet conformation. *Biochem Biophys Res Commun*. Vol. 226. n.º 3. p. 672-80.

Soto, C.; Sigurdsson, E. M.; Morelli, L.; Kumar, R. A.; Castano, E. M.; Frangione, B. **1998.** Beta-sheet breaker peptides inhibit fibrillogenesis in a rat brain model of amyloidosis: implications for Alzheimer's therapy. *Nat Med*. Vol. 4. n.º 7. p. 822-6.

Stine, W. B., Jr.; Dahlgren, K. N.; Krafft, G. A.; LaDu, M. J. **2003.** In vitro characterization of conditions for amyloid-beta peptide oligomerization and fibrillogenesis. *J Biol Chem*. Vol. 278. n.º 13. p. 11612-22.

Strittmatter, W. J.; Saunders, A. M.; Schmechel, D.; Pericak-Vance, M.; Enghild, J.; Salvesen, G. S.; Roses, A. D. **1993.** Apolipoprotein E: high-avidity binding to beta-amyloid and increased frequency of type 4 allele in late-onset familial Alzheimer disease. *Proc Natl Acad Sci U S A*. Vol. 90. n.º 5. p. 1977-81.

Suh, Y. H.; Checler, F. **2002.** Amyloid precursor protein, presenilins, and alpha-synuclein: molecular pathogenesis and pharmacological applications in Alzheimer's disease. *Pharmacol Rev*. Vol. 54. n.º 3. p. 469-525.

Sun, N.; Funke, S. A.; Willbold, D. **2012.** A survey of peptides with effective therapeutic potential in Alzheimer's disease rodent models or in human clinical studies. *Mini Rev Med Chem*. Vol. 12. n.º 5. p. 388-98.

Swahn, B. M.; Kolmodin, K.; Karlstrom, S.; von Berg, S.; Soderman, P.; Holenz, J.; Berg, S.; Lindstrom, J.; Sundstrom, M.; Turek, D.; Kihlstrom, J.; Slivo, C.; Andersson, L.; Pyring, D.; Rotticci, D.; Ohberg, L.; Kers, A.; Bogar, K.; von Kieseritzky, F.; Bergh, M.; Olsson, L. L.; Janson, J.; Eketjall, S.; Georgievska, B.; Jeppsson, F.; Falting, J. **2012.** Design and synthesis of beta-site amyloid precursor protein cleaving enzyme (BACE1) inhibitors with in vivo brain reduction of beta-amyloid peptides. *J Med Chem*. Vol. 55. n.º 21. p. 9346-61.

Szegedi, V.; Fulop, L.; Farkas, T.; Rozsa, E.; Robotka, H.; Kis, Z.; Penke, Z.; Horvath, S.; Molnar, Z.; Datki, Z.; Soos, K.; Toldi, J.; Budai, D.; Zarandi, M.; Penke, B. **2005.** Pentapeptides derived from Abeta 1-42 protect neurons from the modulatory effect of Abeta fibrils--an in vitro and in vivo electrophysiological study. *Neurobiol Dis*. Vol. 18. n.º 3. p. 499-508.

Tjernberg, L. O.; Lilliehook, C.; Callaway, D. J.; Naslund, J.; Hahne, S.; Thyberg, J.; Terenius, L.; Nordstedt, C. **1997.** Controlling amyloid beta-peptide fibril formation with protease-stable ligands. *J Biol Chem*. Vol. 272. n.º 19. p. 12601-5.

Tjernberg, L. O.; Naslund, J.; Lindqvist, F.; Johansson, J.; Karlstrom, A. R.; Thyberg, J.; Terenius, L.; Nordstedt, C. **1996.** Arrest of beta-amyloid fibril formation by a pentapeptide ligand. *J Biol Chem*. Vol. 271. n.º 15. p. 8545-8.

Torchilin, V. P. **1996.** Affinity liposomes in vivo: Factors influencing target accumulation. *Journal of Molecular Recognition*. Vol. 9. n.º 5-6. p. 335-346.

Torchilin, V. P. **2005.** Recent advances with liposomes as pharmaceutical carriers. *Nat Rev Drug Discov*. Vol. 4. n.º 2. p. 145-60.

Torchilin, V. P.; Omelyanenko, V. G.; Papisov, M. I.; Bogdanov, A. A., Jr.; Trubetskoy, V. S.; Herron, J. N.; Gentry, C. A. **1994.** Poly(ethylene glycol) on the liposome surface: on the mechanism of polymer-coated liposome longevity. *Biochim Biophys Acta*. Vol. 1195. n.º 1. p. 11-20.

Torok, M.; Abid, M.; Mhadgut, S. C.; Torok, B. **2006.** Organofluorine inhibitors of amyloid fibrillogenesis. *Biochemistry*. Vol. 45. n.º 16. p. 5377-5383.

van Rooy, I.; Mastrobattista, E.; Storm, G.; Hennink, W. E.; Schiffelers, R. M. **2011.** Comparison of five different targeting ligands to enhance accumulation of liposomes into the brain. *J Control Release*. Vol. 150. n.º 1. p. 30-6.

Veronese, F. M. **2001.** Peptide and protein PEGylation: a review of problems and solutions. *Biomaterials*. Vol. 22. n.º 5. p. 405-17.

Vieira, E. P.; Hermel, H.; Mohwald, H. **2003.** Change and stabilization of the amyloid-beta(1-40) secondary structure by fluorocompounds. *Biochim Biophys Acta*. Vol. 1645. n.º 1. p. 6-14.

Visser, C. C.; Stevanovic, S.; Voorwinden, L. H.; van Bloois, L.; Gaillard, P. J.; Danhof, M.; Crommelin, D. J.; de Boer, A. G. **2005.** Targeting liposomes with protein drugs to the blood-brain barrier in vitro. *Eur J Pharm Sci*. Vol. 25. n.º 2-3. p. 299-305.

Vyas, S. P., Sihorkar V. - Advances in liposomal therapeutics. New Delhi: CBS Publishers, 2001.

Walus, L. R.; Pardridge, W. M.; Starzyk, R. M.; Friden, P. M. **1996.** Enhanced uptake of rsCD4 across the rodent and primate blood-brain barrier after conjugation to anti-transferrin receptor antibodies. *Journal of Pharmacology and Experimental Therapeutics*. Vol. 277. n.º 2. p. 1067-1075.

Wang, E.; Obeng-Adjei, N.; Ying, Q.; Meertens, L.; Dragic, T.; Davey, R. A.; Ross, S. R. **2008.** Mouse mammary tumor virus uses mouse but not human transferrin receptor 1 to reach a low pH compartment and infect cells. *Virology*. Vol. 381. n.º 2. p. 230-40.

Weidemann, A.; Konig, G.; Bunke, D.; Fischer, P.; Salbaum, J. M.; Masters, C. L.; Beyreuther, K. **1989.** Identification, biogenesis, and localization of precursors of Alzheimer's disease A4 amyloid protein. *Cell*. Vol. 57. n.º 1. p. 115-26.

Wohlfart, S.; Gelperina, S.; Kreuter, J. **2012.** Transport of drugs across the blood-brain barrier by nanoparticles. *J Control Release*. Vol. 161. n.º 2. p. 264-73.

Wood, S. J.; MacKenzie, L.; Maleeff, B.; Hurle, M. R.; Wetzel, R. **1996.** Selective inhibition of Abeta fibril formation. *J Biol Chem*. Vol. 271. n.º 8. p. 4086-92.

Wood, S. J.; Wetzel, R.; Martin, J. D.; Hurle, M. R. **1995.** Prolines and amyloidogenicity in fragments of the Alzheimer's peptide beta/A4. *Biochemistry*. Vol. 34. n.º 3. p. 724-30.

Wu, D.; Pardridge, W. M. **1999.** Blood-brain barrier transport of reduced folic acid. *Pharm Res*. Vol. 16. n.º 3. p. 415-9.

Zambaux, M. F.; Bonneaux, F.; Gref, R.; Dellacherie, E.; Vigneron, C. **1999.** Preparation and characterization of protein C-loaded PLA nanoparticles. *J Control Release*. Vol. 60. n.º 2-3. p. 179-88.

Zhang, Y.; Pardridge, W. M. **2001.** Rapid transferrin efflux from brain to blood across the blood-brain barrier. *J Neurochem*. Vol. 76. n.º 5. p. 1597-600.

Chapter 3

Interaction of Aβ peptide with charged and nonionic surfactants

3.1. Introduction

Evidences support a direct association between the degree of dementia of patients that have AD and the concentration of soluble aggregates of the Aβ peptide (Clippingdale, 2001; Hardy, 2002; Ladiwala, 2012). The aggregation process of the Aβ peptide leads to the formation of insoluble fibrils, which accumulate in senile plaques, deposits that characterize AD (Andreasen, 2002; Suh, 2002). The more abundant sequences of the peptide have 40 (~90%), $A\beta_{(1-40)}$, and 42 (~10%), $A\beta_{(1-42)}$, amino acids (Citron, 1996). The peptide with 42 amino acids is more toxic and it is the major component of the neuritic plaques found in AD (Evin, 2002; Roher, 1993). The smaller aggregated intermediates, the Aβ oligomers, are considered the more toxic species (Hardy, 2002). The control and study of Aβ oligomerization is difficult to achieve, because the process is fast and is affected by many variables such as solvent hydrophobicity, pH, peptide concentration, temperature, ionic strength, and interactions with metal ions (Stine, 2003). The studies of Aβ interaction with different surfactant molecules and micelles are important to better understand the aggregation process of the Aβ peptide.

It has been demonstrated that the surfactant sodium dodecyl sulfate (SDS) is able to induce, at specific conditions, a non-fibrillar state of the peptide (Rangachari, 2007; Tew, 2008). Like other particles or molecules, the use of surfactants could provide a standard procedure for obtaining oligomeric assemblies of Aβ and for getting new insights into the oligomerization process (Ghavami, 2012). The concentration of the surfactant in solution determines its effect on Aβ aggregation (Cao, 2007; Coles, 1998; Marcinowski, 1998; Rangachari, 2007; Rangachari, 2006; Rocha, 2012a; Sabate, 2005; Shao, 1999; Wahlstrom, 2008). The interaction mechanism between surfactants and Aβ may well be generalized as it has been suggested for the case of globular proteins (Otzen, 2011; Otzen, 2010). There is already an indication of identical impacts of charged surfactants on the secondary structure of $A\beta_{(1-40)}$ and other short peptides (Cao, 2007; Rocha, 2012a; Rocha, 2008; Sabate, 2005; Wahlstrom, 2008). Also, both nonionic and zwitterionic surfactants have similar outcomes on the aggregation of $A\beta_{(1-40)}$ (Friedman, 2011).

This chapter relates to the interactions between different charged surfactants (CTAC - cetyltrimethylammonium chloride and SDS - sodium dodecyl sulphate) and a nonionic surfactant (OG - octyl β-D-glucopyranoside) with $A\beta_{(1-42)}$. The ionic surfactants were selected in order to have micelles with approximately the same shape. The nonionic surfactant was chosen because of its purity when compared with other nonionic surfactants.

To characterize their interaction mechanism and to define common alternate aggregation pathways different studies were performed. The studies were done using different concentrations of the surfactants, below and above their critical micelle concentration (CMC) and by characterizing the ultra-structure of the aggregates, their binding to thioflavin T (ThT) and their secondary structure.

3.2. Materials and methods

3.2.1. Amyloid-beta peptides

$A\beta_{(1-40)}$ peptide (purity 96%, molecular weight (MW) 4329.90) was purchased from GenicBio Limited and $A\beta_{(1-42)}$ peptide (purity > 95%, MW 4514.14) was purchased from Selleck Chemicals (Figure 3.1). The aggregation state and the structure of the peptide are highly dependent on the sample batch (Soto, 1995). To improve peptide solubility and disaggregate pre-formed agglomerates, the peptide was first dissolved in HFIP (1,1,1,3,3,3-hexafluoro-2-propanol, ≥ 99.8%, Sigma-Aldrich) (to disrupt intermolecular H-bonds) at 1 mg/mL concentration (Nilsson, 2004; Rocha, 2009; Sabate, 2005). HFIP was evaporated with nitrogen flow and under vacuum. The peptide film with the Aβ in a monomeric structure was dissolved in DMSO (dimethyl sulfoxide for molecular biology, ≥ 99.9%, MW 78.13, Sigma-Aldrich) at 9 mg/mL concentration.

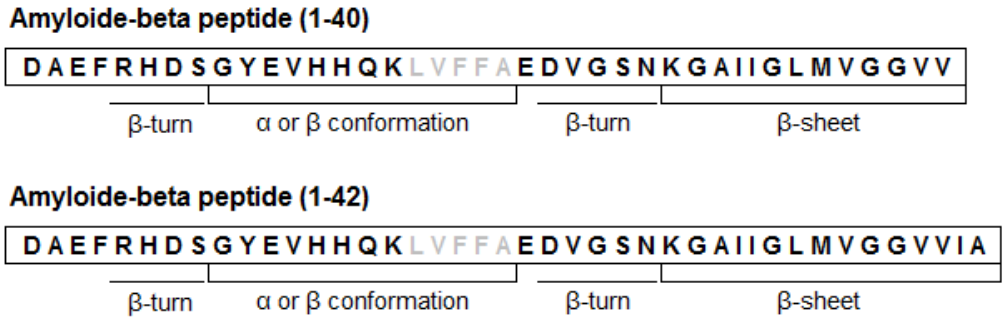

Figure 3.1 – Amino acids of the two Aβ peptides used in this study and their secondary structure prediction. The central hydrophobic cluster is represented in grey.

3.2.2. Surfactant solutions

All surfactants were purchased from Sigma-Aldrich. Stock solutions were prepared by dissolving CTAC (cetyltrimethylammonium chloride, 25 wt.% sol. in water, MW 320.01), OG (octyl β-D-glucopyranoside, ≥ 98%, MW 292.37) or SDS (sodium dodecyl sulphate, ≥98.5%, MW 288.38) (Table 3.1) in Hepes buffer 10 mM, pH 7.4 (HEPES hemisodium salt, ≥ 99%, Sigma-Aldrich) or phosphate buffered saline (PBS), pH 7.4 (PBS, 10 mM phosphate buffer, 2.7 mM potassium chloride and 137 mM sodium chloride, Sigma-Aldrich). The buffers were prepared previously with ultrapure water purified with Milli-Q equipment with the specific resistance of 18.2 MΩ·cm.

Table 3.1 – Chemical structure of the surfactants used in the interaction studies with Aβ.

Name	Charge	Structure
SDS	Anionic	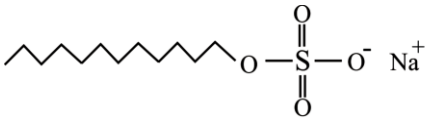
CTAC	Cationic	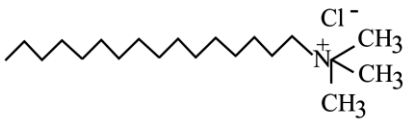
OG	Nonionic	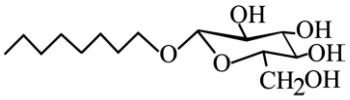

3.2.3. Critical micelle concentration measurements

Amphiphiles have two different parts that have different affinity for solvents. The part of the molecule that has an affinity for polar solutions, such as water, is called hydrophilic. The other part of the molecule, which has an affinity for non-polar solvents, such as hydrocarbons, is named hydrophobic (Butt, 2006). These molecules are called amphiphilic or amphiphiles. An amphiphilic molecule can positioning itself at the air-water interface with the polar part in contact with water and the non-polar part facing the air above the surface. Another possible arrangement occurs when the amphiphiles are present in high quantities and form aggregates in which the hydrophobic portions are oriented within the core and the hydrophilic portions are exposed to the aqueous solvent. Such aggregates are called micelles (Figure 3.2). At low concentrations, the arrangement on the surface is favored. As the surface becomes crowded with surfactant some molecules will arrange into micelles. When the surface becomes completely loaded with surfactant and any further additions must be arranged as micelles, this concentration is called the CMC (Barnes, 2011).

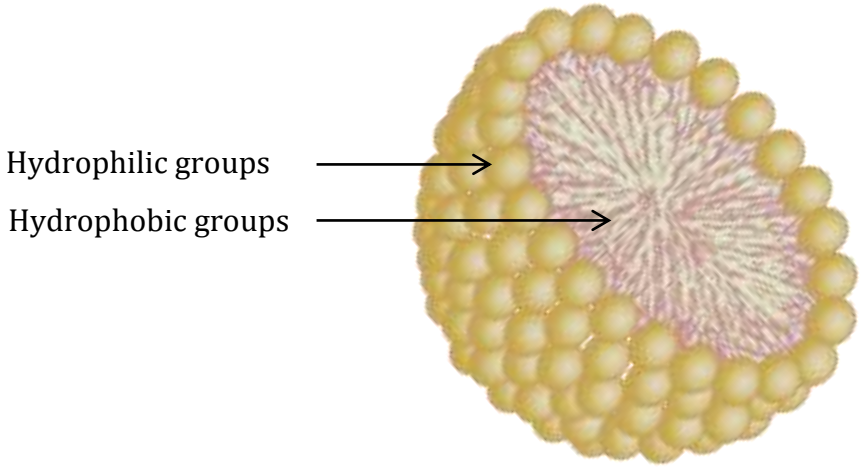

Figure 3.2 – Schematic representation of one micelle.

The CMC of surfactants was measured at room temperature in the absence and presence of the Aβ peptide (with a constant concentration of 46 μM) by two techniques: surface tension (OG and CTAC) and conductivity (SDS) measurements. The surface tension method was carried out by the hanging drop method using an optical contact angle system (OCA 15 plus). Below the CMC, the trend of the surface tension versus the logarithm of the concentration can be described by the Langmuir-Szyszkowski equation (von Szyszkowski, 1908). Above the CMC, the surface tension is almost constant, thus this range can be fitted linearly. The CMC corresponds to the value at the intersection of both curves (Arlt, 2010). Conductivity was measured using a Crison GLP 31 conductivimeter. Below and above the CMC the trend of the conductivity versus the concentration can be described by two linear equations. The intersection of this linear fit corresponds to the CMC (Azum, 2008).

3.2.4. Fluorescence measurements and Thioflavin T binding assay

When atoms, molecules, ions and complexes are exposed to light of certain wavelength, they undergo a transition from the energetically ground state to the excited state. When the molecules return to its ground state they release the previously absorbed energy by radiation or in other words, the molecules emit photons.

The light emitted from an excited singlet state or between states of the same spin state is called fluorescence. The fluorescence lifetime is very short and founded usually in the nanosecond range. The processes that occur between the absorption of light and its emission are represented in the Jablonski diagram (Figure 3.3).

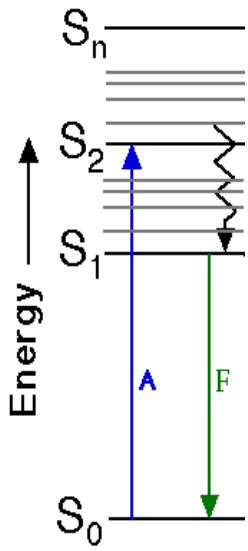

Figure 3.3 - Jablonski Diagram.

In this diagram S_0, S_1, S_2 are the singlet ground, first and second electronic states, respectively. In each of the states of energy, the fluorescent substance can have different vibrational energy levels. The

lifetime of a fluorophore is the average time since the excitation until the return to the ground state. Few molecules in condensed phases have internal conversion. It is a quickly relaxation to the lowest vibrational level of S_1 and this occurs within 10^{-12} s or less. On the other hand, the fluorescence lifetime is approximated 10^{-8} s and the internal conversion is complete before the emission (Lakowicz, 1988).

ThT is a classic amyloid dye that is commonly used to probe Aβ fibril formation because of its strong fluorescence emission upon binding to amyloid fibril structures (Nilsson, 2004). It is assumed that the intensity of fluorescence is proportional to the quantity of amyloid fibrils (Jameson, 2012).

For ThT assays, a ThT stock solution was prepared by adding 8 mg of ThT to 10 mL of either Hepes or PBS buffers (Nilsson, 2004). This solution was filtered through a 0.2 μm syringe filter and diluted (1 mL of ThT stock solution in 50 mL of buffer) before each measurement (ThT working solution). An aliquot of 20 μL of each sample was mixed with 1 mL of ThT working solution, stirred for 1 min, and the fluorescence intensity was measured using a Perkin Elmer LS 50B (Waltham, Massachusetts, USA) fluorescence spectrometer, averaging over 60 s. Upon binding to amyloid fibrils, the ThT has an excitation maximum at 450 nm and enhanced emission at 482 nm. The spectra were subtracted to the controls (ThT working solution and surfactants). For kinetic studies, the samples containing Aβ and CTAC (0.50 mM and 1.40 mM) or SDS (4.00 mM and 14.00 mM) in PBS buffer were diluted and added to ThT working solution immediately after preparation leading to the following final concentrations: 12.50 μM of Aβ peptide, 62.50 μM and 0.175 mM of CTAC; 0.50 mM and 1.75 mM of SDS. The samples were placed on a 96-well plate (Nunclon Delta Surface) and the fluorescence intensity was measured using a Biotek Synergy (Winooski, Vermont, USA) 2 fluorescence spectrometer after stirring 30 s at 37 °C every 15 min during 2 days. The

measurements were performed with a 420/50 nm excitation filter and a 485/20 nm emission filter.

3.2.5. Transmission electron microscopy

Transmission electron microscopy (TEM) gives real space images, including the surface and the internal structures of materials, tissues and cells.

In TEM technique, an electron beam is transmitted through the sample under observation (Figure 3.4). The applied intensity depends on the thickness of the sample and the concentration of atoms in that sample. This technique is used for contrasting a thin specimen with an optically opaque fluid.

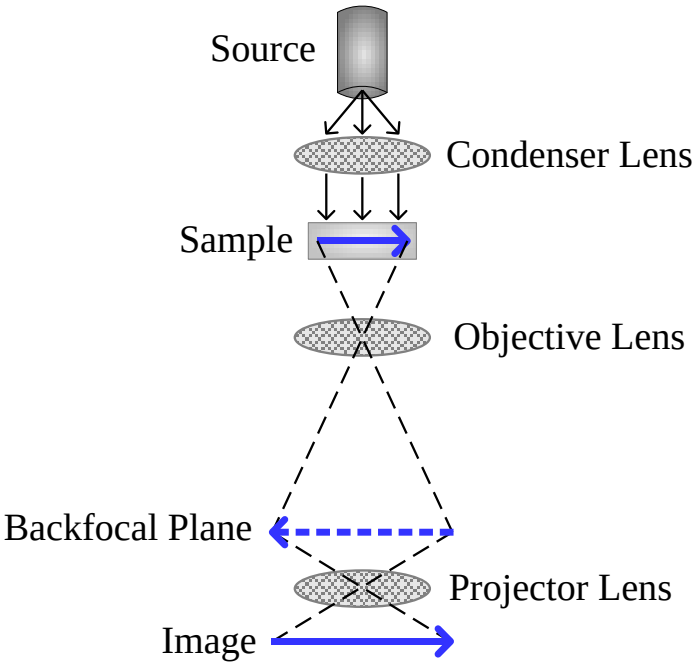

Figure 3.4 - Diagram in the area of the objective lens of an electron microscope. Adapted from (Cahn, 1996; Hiemenz, 1997).

For the ultra-structural studies of the Aβ peptide (100 μM) in the absence and presence of the different surfactants at different concentrations, 5 μL of each sample was placed on carbon-formvar coated 200-400 mesh spacing grids (Agar Scientific) and let to adsorb for five minutes. The negative staining was performed with 2% filtered aqueous solution of uranyl acetate for 45 seconds. After removing the excess of the negative staining solution and drying the grids, the samples were visualized using a Jeol JEM 1400 electron microscope at 80 kV.

3.2.6. Fourier-Transform Infrared

The Fourier-Transform Infrared (FTIR) spectroscopy studies the interaction of infrared radiation with the matter, being capable of analysing a wide variety of materials: organic or inorganic, solid, liquid or gaseous.

FTIR spectroscopy instrumentation is constituted generally by a Michelson interferometer and a computer. The interferometer comprises a source of radiation, a beam splitter, a fixed mirror, a moving mirror and the detector (Figure 3.5). The laser produces a unique frequency of red light which follows the same trajectory of the infrared radiation. There are many types of detectors, but the most used are the deuterated triglycine sulfate detector (DTGS) and the mercury cadmium telluride detector (MCT). A computer performs the conversion of the interferogram into the representation in the frequency domain, using the Fourier transform.

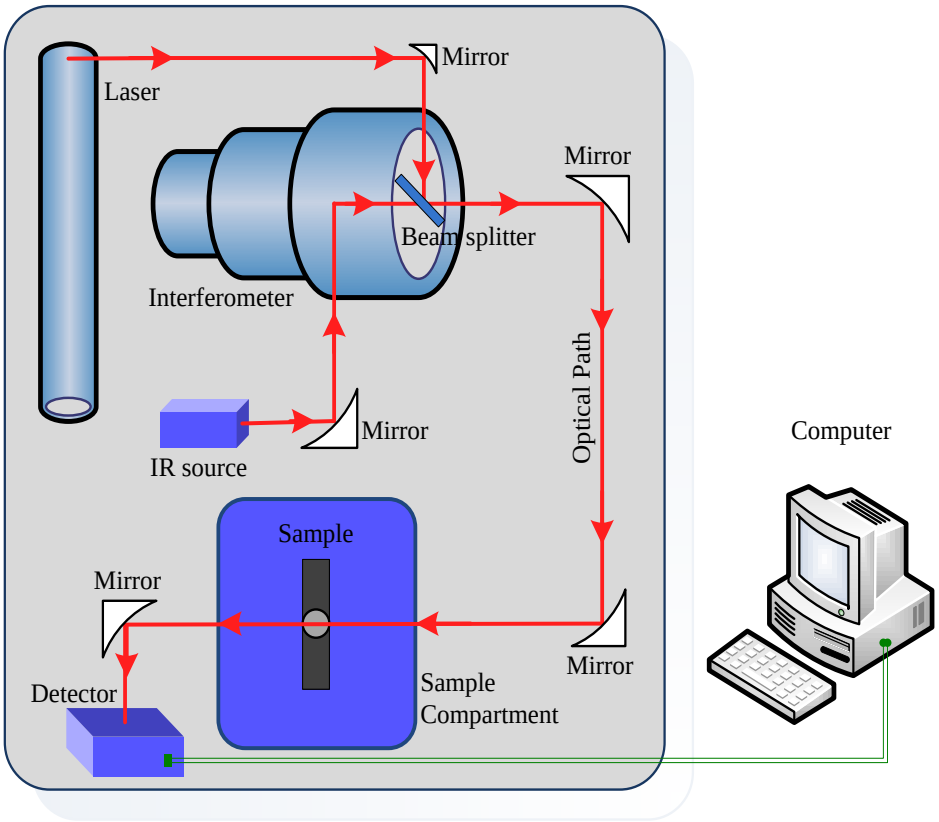

Figure 3.5 - Schematic representation of a FTIR equipment. Adapted from (Silva, 2007).

This technique is useful for the identification of different chemical bonds in molecules, as each specific chemical bond absorbs incident light at a specific wavelength. FTIR measures the frequency of the vibrations of chemical bonds between atoms when excitation occurs. The absorption frequencies of radiation depend on the functional groups present and the configuration of the atoms in the molecule. When a given bond absorbs radiation, it will become excited, and consequently the frequency of its molecular vibration will increase. The infrared vibrational spectrum of a molecule consists of a sequence of bands, each of which results from a transition between pairs of vibrational levels related to the ground electronic state.

FTIR Spectroscopy has qualitative and quantitative applications. Its qualitative applications rely on the fact that pure compounds possess a very characteristic FTIR spectrum. Therefore, an unknown material can be identified by comparing its FTIR spectrum to spectra of known compounds. The technique is also used to identify functional groups of a sample and to control the quality of a specific material by comparison with a standard material. Besides the qualitative information, this method also gives quantitative information. All quantitative applications of FTIR Spectroscopy lay on the Lambert-Beer law (the intensity of the transmitted radiation is inversely proportional to the concentration of the sample).

Attenuated total reflectance (ATR) accessories are especially useful for obtaining infrared spectra of difficult samples that cannot be readily examined by the normal transmission method. They are suitable for studying thick or highly absorbing solid and liquid materials, including films, coatings, powders, threads, adhesives, polymers, and aqueous samples. ATR requires little or no sample preparation for most samples and is one of the most versatile sampling techniques.

ATR-FTIR spectra were recorded with a Bruker Alpha-P spectrophotometer. The measurements were performed using the same solutions used in the TEM experiments and the buffer spectrum was subtracted. All spectra were recorded by averaging 200 scans at a resolution of 4 cm^{-1}.

3.2.7. Theoretical kinetic model

The theoretical kinetic model created by Hellstrand et *al.* (Hellstrand, 2010), which describes protein aggregation is a tool to find the time at half completion of aggregation process, $t_{1/2}$, that was estimated by fitting sigmoidal function (Equation 3.1) to each parameter.

$$F(t) = F_0 + \frac{A}{1 + exp\left[-k\left(t - t_{1/2}\right)\right]} \quad (3.1)$$

The fitted parameters are $t_{1/2}$, the elongation rate constant, k, the amplitude, A, and the baseline before aggregation, F_0. The lag time, t_{lag}, is the interception between the time axis and the tangent with slope k from the midpoint of the fitted sigmoidal curve. By this definition, t_{lag} was calculated from the fitted parameter as described by equation 3.2.

$$t_{lag} = t_{1/2} - \frac{2}{k} \quad (3.2)$$

The kinetic data from ThT assay was fitted by the model.

3.3. Results and Discussion

3.3.1. Interaction of amyloid-beta with surfactants

The aggregation of Aβ peptides was studied in the presence of surfactants by ultra-structural analysis at a peptide concentration of 100 μM and surfactant concentrations below and above the CMC. The CMC values for the surfactants at the given buffer conditions used in the experiments were determined by surface tension and conductivity and are listed in Table 3.2. In the case of charged surfactants, the CMC decreases drastically in the presence of salts.

Table 3.2 - Properties of the surfactants that were used in this study.

Surfactant	CMC[4] in Hepes[5] (mM)	CMC in PBS[6] (mM)	Size of the micelle (nm)	Shape of the micelle
CTAC[1]	0.9 ± 0.2	0.19 ± 0.02	4.8	spherical
SDS[2]	6.9 ± 0.3	1.4 ± 0.2	4.8	spherical
OG[3]	22.4 ± 0.1	22.2 ± 0.5	R = 1.3; L = 9.6	cylinder

[1]cetyltrimethylammonium chloride;

[2]sodium dodecyl sulphate;

[3]octyl β-D-glucopyranoside;

[4]critical micelle concentration;

[5]10 mM sodium HEPES buffer, pH 7.4;

[6]phosphate buffered saline, 10 mM phosphate buffer, 2.7 mM potassium chloride and 137 mM sodium chloride, pH 7.4;

For OG, R is the radius of the cylinder, and L is its length.

Also, it was verified that charged and non-charged surfactants, in Hepes buffer, in the presence $A\beta_{(1-40)}$ monomers present different behaviors. The presence of $A\beta_{(1-40)}$ does not change the CMC of charged surfactants, the SDS maintains its CMC at 6.4 ± 0.3 mM and CTAC presents a CMC of 0.8 ± 0.2 mM. The CMC value of the nonionic amphiphile (OG), on the other hand, significantly increases from 22 to 28.2 ± 0.9 mM. This variation was statistically significant as determined by *t*-Student test ($P < 0.01$). Micelle formation is driven by the hydrophobic effect and the interactions between nonionic surfactant monomers are usually stronger than that between ionic monomers due to the lack of electrostatic repulsion of the polar heads. The increase of the OG CMC induced by $A\beta_{(1-40)}$ indicates that the surfactant–peptide interactions are favorable enough to stabilize the non-ionic monomers in aqueous solutions. In the case of the ionic surfactants, the number of sequestered monomers by the peptide is most likely too low to be detected by the techniques used to determine the CMC.

The ultra-structural analysis shows that both the cationic surfactant (CTAC) and the anionic surfactant (SDS) promote, in Hepes buffer and at concentrations below the CMC, the aggregation of $A\beta_{(1-42)}$. In these solution conditions, the surfactants lead to the formation of amyloid-like, unbranched fibrils similar to that observed for the peptide alone (Figure 3.6). These fibrils have an average diameter of 21 nm. The negative-staining agent (uranyl acetate) is estimated to increase by approximately 1 nm the size of the fibrils. The obtained values for $A\beta_{(1-42)}$ fibril size are concordant with that presented in the literature (Chen, 2005; Klement, 2007). In the case of $A\beta_{(1-42)}$ incubated with the charged surfactants at micellar concentrations (concentration above the CMC), only small aggregates are observed, indicating that they inhibit the Aβ fibrillogenesis. The aggregates were similar to that observed for the peptide in the initial state (Figure 3.6, time = 0 h). Comparable results were obtained for surfactant micellar concentrations in the presence of salt (PBS buffer).

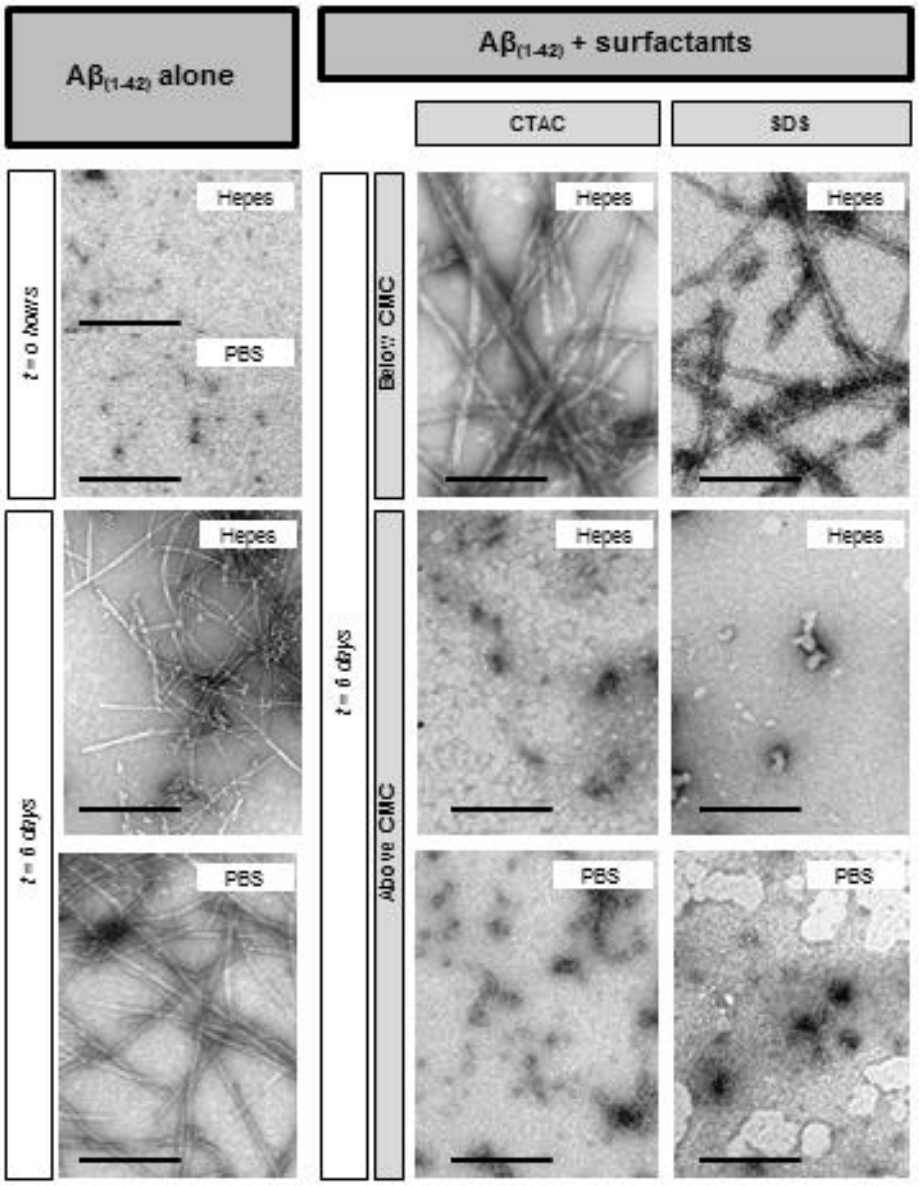

Figure 3.6 - TEM images of the effect of the surfactants CTAC and SDS on $A\beta_{(1-42)}$ aggregation. The $A\beta_{(1-42)}$ concentration was 100 μM. The samples were incubated for 6 days at 37 °C in the presence or absence of surfactants in Hepes or PBS buffer. The surfactant concentrations were below and above the CMC (CTAC 0.50 mM and 1.40 mM; SDS 4.00 mM and 14.00 mM) in Hepes buffer and above the CMC (CTAC - 1.40 mM; SDS – 14.00 mM) in PBS buffer. The scale bar corresponds to 400 nm.

A significant binding to ThT is observed for $A\beta_{(1-42)}$ incubated alone. The fluorescence intensity at 450 nm, which is the characteristic excitation maximum observed upon ThT binding, increased after 1 day incubation time at 37 °C; for the samples containing OG, the non-ionic surfactant, the fluorescence intensity of ThT was higher than that observed for Aβ alone (Figure 3.7), whereas for the mixtures of $A\beta_{(1-42)}$ and charged micelles the intensity of fluorescence was low and maintained close to that of the Aβ starting point. These results reveal that charged micelles show significant inhibition of Aβ fibril formation.

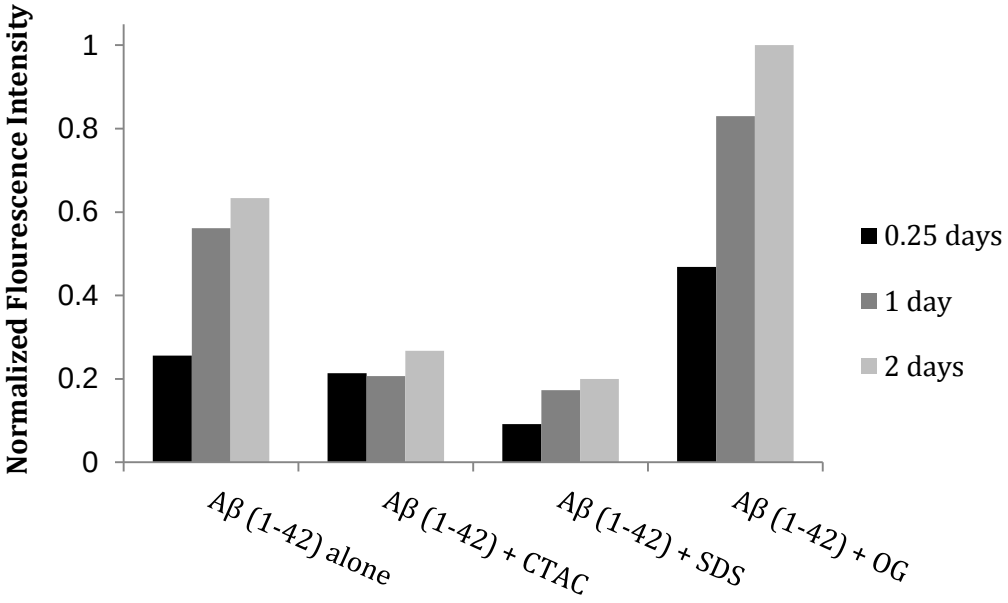

Figure 3.7 - The effect of surfactants on $A\beta_{(1-42)}$ fibril content as monitored by ThT fluorescence. The $A\beta_{(1-42)}$ concentration was 100 μM. The samples were incubated at 37 °C in the presence or absence of surfactants in 10 mM Hepes buffer, pH 7.4. All the surfactant concentrations were above the CMC (CTAC – 1.40 mM; SDS - 14.00 mM; OG – 29.80 mM).

The $A\beta_{(1-42)}$ aggregation kinetics in surfactant environment was studied for SDS and CTAC at two different concentrations close to their CMC by means of ThT fluorescence (Figure 3.8). The $A\beta_{(1-42)}$ concentration was kept at 12.5 μM, which was significantly above the critical concentration below which fibrils cannot form (0.2 μM) (Hellstrand, 2010). The lag time, t_{lag}, and the time at half completion of the aggregation process, $t_{1/2}$, were obtained by fitting a sigmoidal function to each kinetic trace according to the model presented by Hellstrand et al. (Hellstrand, 2010). Both parameters were affected by the presence of surfactants and were significantly longer for $A\beta_{(1-42)}$ incubated with SDS than for $A\beta_{(1-42)}$ alone (Figure 3.8). Also, the ThT fluorescence plateau decreased.

The increase of surfactant concentrations slowed down the fibril formation and the higher value of $t_{1/2}$ was obtained for the highest concentrations of SDS (1.75 mM). In the case of CTAC at 0.18 mM, the fluorescence intensity was below the noise level, and thus it was not possible to calculate the t_{lag} and $t_{1/2}$, suggesting a stronger inhibitory action.

The $t_{1/2}$ of the aggregation process was approximately four times higher in the case of the sample with SDS 1.75 mM when compared with the peptide alone. SDS at 0.50 mM induced an inhibitory effect of 0.37 days (approximately 9 h).

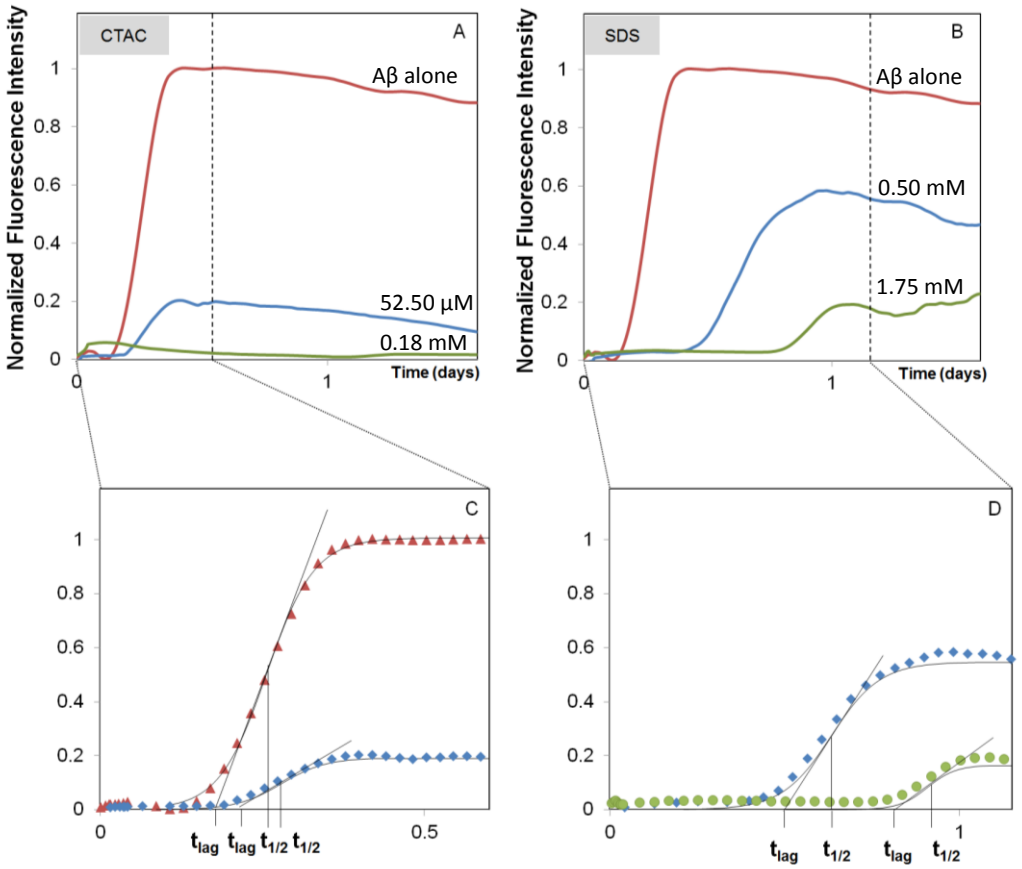

	$t_{1/2}$ (days)	t_{lag} (days)
$A\beta_{(1-42)}$ *alone*	0.26	0.18
$A\beta_{(1-42)}$ *+ 62.50 µM CTAC*	0.28	0.21
$A\beta_{(1-42)}$ *+ 0.18 mM CTAC*	-	-
$A\beta_{(1-42)}$ *+ 0.50 mM SDS*	0.63	0.49
$A\beta_{(1-42)}$ *+ 1.75 mM SDS*	0.91	0.83

Figure 3.8 – Concentration dependence of charged surfactants in $A\beta_{(1-42)}$ fibril formation in PBS. A) and B) Aggregation kinetics of $A\beta_{(1-42)}$ (100 µM) in the presence of two different surfactant concentration close to the CMC. C) and D) Fitting of equation 3.1 to $A\beta_{(1-42)}$ kinetic points, with data showed as points and the fitted curve (solid line). The values for $t_{1/2}$ were obtained by the fit and t_{lag} was achieved by the equation 3.2.

The nonionic surfactant OG promoted the $A\beta_{(1-42)}$ aggregation both at submicellar and micellar concentrations (and either in Hepes or PBS buffer) (Figure 3.9). The fibrils had a different morphology and to confirm if they were of the amyloid type, their secondary structure was analyzed by ATR-FTIR spectroscopy. The spectra of $A\beta_{(1-42)}$ in the presence of OG below and above the CMC in PBS buffer were similar to that of the $A\beta_{(1-42)}$ incubated alone (Figure 3.9). These spectra are characterized by a band in the Amide I region with a maximum intensity at 1624 cm^{-1}, which is assigned to β-sheet-rich amyloid fibrils (Cerf, 2009).

The results indicate that charged surfactant monomers interact with $A\beta_{(1-42)}$ through electrostatic interactions. This will cause the exposure of peptide hydrophobic parts that will promote hydrophobic interactions between peptide molecules, which eventually lead to aggregation (Figure 3.10). Charged micelles will also interact electrostatically with $A\beta_{(1-42)}$. In this case, however, the concentration of charged micelles is high enough for surrounding the $A\beta_{(1-42)}$ peptide molecules inducing consequently an electrostatic repulsion between the peptide-micelle structures (Figure 3.10) favoring a non-aggregated state. This study confirms the fibrillization-inhibiting effect of charged micelles.

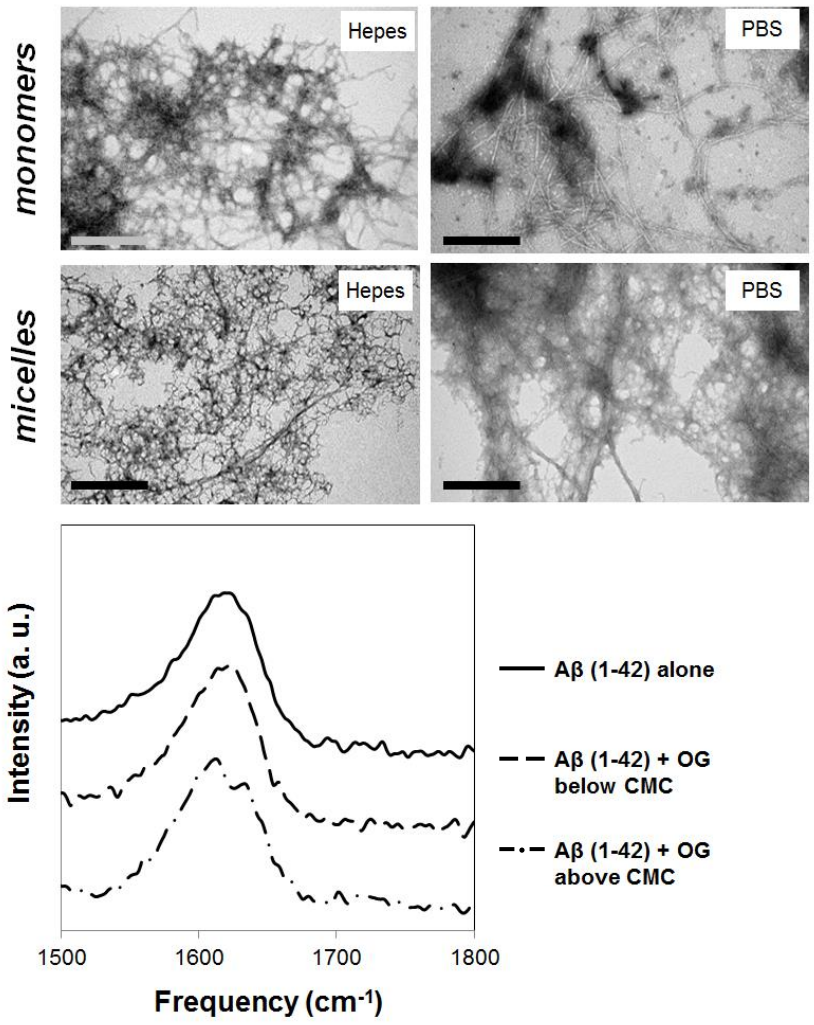

Figure 3.9 – Effect of non-charged surfactants in $A\beta_{(1-42)}$ aggregation. TEM images and FTIR spectra of the $A\beta_{(1-42)}$ in the presence of monomers and micelles of OG surfactant (respectively 10.00 mM and 29.80 mM). For TEM analysis, the samples were incubated for 2 days at 37 °C in the presence of surfactant in 10 mM Hepes buffer or 10 mM PBS buffer, pH 7.4. The scale bar corresponds to 400 nm. FTIR spectra were obtained for the peptide incubated for 2 days at 37 °C in PBS buffer, 137 mM NaCl, pH 7.4.

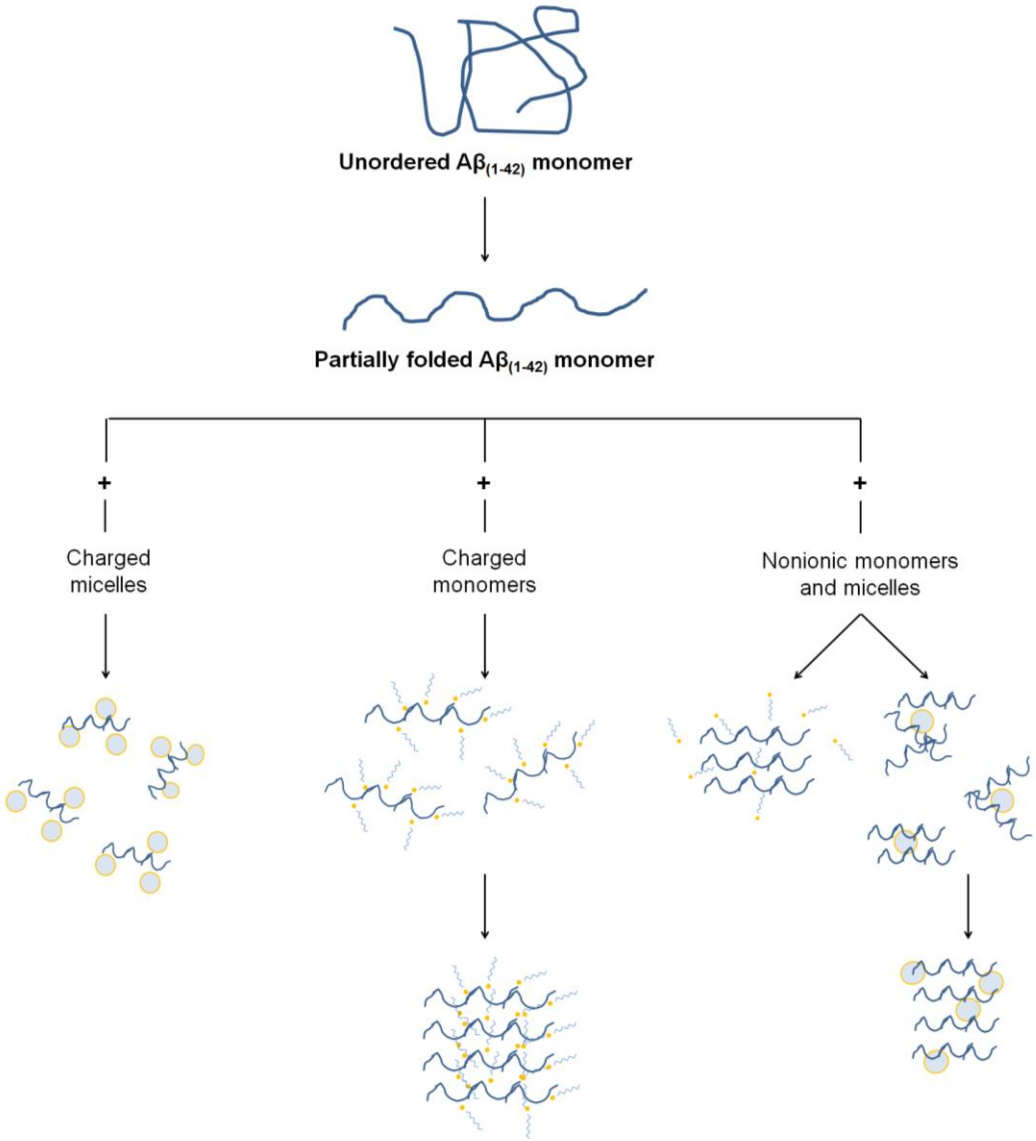

Figure 3.10 – Schematic representation of the possible mechanism for the interactions of $A\beta_{(1-42)}$ with the charged and nonionic surfactants at monomeric or micelle concentrations. Experimental data show that the peptide in the presence of charged micelles does not aggregate, whereas in the presence of monomers it aggregates. The Aβ in the presence of nonionic monomers and micelles reaches complete aggregation.

Other charged NPs were shown to have also a fibrillization-inhibiting effect (Liao, 2012; Saraiva, 2010a; Saraiva, 2010b). Liao *et al.* used bare and carboxyl conjugated gold nanoparticles (AuNPs) to inhibit the formation of fragmented fibrils and spherical oligomers. They showed that the negative surface potential of AuNPs is essential for the interactions between the peptide ($A\beta_{(1-40)}$) and the AuNPs and as a result of this interaction the peptide aggregation is inhibited (Liao, 2012). Saraiva *et al*. demonstrated that fluorinated NPs promote an increase in the α-helical content of the $A\beta_{(1-42)}$ peptide and have an anti-oligomeric effect (Saraiva, 2010a). Sulfonated and sulfated polystyrene NPs, which are negatively charged polymeric nanostructures, also affected the conformation of Aβ and induced an unordered state, delaying the peptide oligomerization (Saraiva, 2010b).

The effect of non-charged surfactants below the CMC on $A\beta_{(1-42)}$ may be explained by the presence of more hydrophobic molecules (monomers) in solution that favor hydrophobic interactions (Figure 3.10). The OG micelles in solution behave as inert bodies and act as nuclei of aggregation.

Other previous studies with $A\beta_{(1-40)}$ fragment (46 μM) in aqueous buffer, pH 7.4, suggest that the peptide shows a low content of β-sheet structures in the presence of micelles of charged surfactants, SDS and CTAC (Rocha, 2012b). On the contrary, the presence of these surfactants below the CMC induces a β-sheet conformation. The presence of OG at concentrations above the CMC leads to a β-sheet conformation as opposed to what is observed in the case of charged micelles (Rocha, 2012b). The hypothesis is that $A\beta_{(1-40)}$ interacts with uncharged OG monomers through hydrophobic interactions.

A dual effect of cationic surfactants (alkylammonium bromides) on $A\beta_{(1-40)}$ structure has also been reported, as the alkylammonium bromide surfactants favored the Aβ fibril formation at concentrations below the

CMC and delay the fibril formation at concentrations above their CMC (Sabate, 2005). Cao *et al.* found that cationic Gemini surfactant hexamethylene-1,6-bis (dodecyl dimethylammonium bromide) ($C_{12}C_6C_{12}Br_2$) micelles delay the formation of $A\beta_{(1\text{-}40)}$ fibrils. The interaction of charged and zwitterionic surfactants with the Aβ-peptide fragment (1-28) demonstrated that the promotion and stabilization of α-helix secondary structure are highly dependent on the surface charge of the micelles (Marcinowski, 1998). The aggregation kinetics of the peptide is also significantly affected by the presence of salt ions (Klement, 2007). Ions may concentrate non-specifically in the vicinity of oppositely charged peptide groups, increasing the apparent dielectric constant of water and promoting stronger electrostatic interactions between peptide–peptide molecules. Alternatively, ions may interact specifically with charged or polar chemical groups of the peptide chain (Baldwin, 1996; RiesKautt, 1997).

The aggregation mechanism of Aβ peptides is still very much debatable because studies performed under different conditions lead to different proposed mechanisms. The fast aggregation kinetics and different aggregation stages of peptide samples are obstacles for uniform and generalized studies. The use of surfactants may contribute to a better understanding of the peptide aggregation and above all may allow the study of the fibrillization process at concentrations that can easily be reproduced.

References

Andreasen, N.; Blennow, K. **2002.** beta-amyloid (A beta) protein in cerebrospinal fluid as a biomarker for Alzheimer's disease. *Peptides*. Vol. 23. n.° 7. p. 1205-1214.

Arlt, B.; Datta, S.; Sottmann, T.; Wiegand, S. **2010.** Soret effect of n-octyl beta-D-glucopyranoside (C8G1) in water around the critical micelle concentration. *J Phys Chem B*. Vol. 114. n.° 6. p. 2118-23.

Azum, N.; Naqvi, A. Z.; Akram, M.; Kabir-ud-Din. **2008.** Studies of mixed micelle formation between cationic gemini and cationic conventional surfactants. *Journal of Colloid and Interface Science*. Vol. 328. n.° 2. p. 429-435.

Baldwin, R. L. **1996.** How Hofmeister ion interactions affect protein stability. *Biophysical Journal*. Vol. 71. n.° 4. p. 2056-2063.

Barnes, Geoff; Gentle, Ian - Interfacial science : an introduction. 2nd. Oxford ; New York: Oxford University Press, 2011. 9780199571185

Butt, Hans-Jürgen; Graf, Kh; Kappl, Michael - Physics and chemistry of interfaces. 2nd., rev. and enl. Weinheim: Wiley-VCH, 2006.

Cahn, R. W.; Haasen, P. - Physical metallurgy. 4th, rev. and enhanced. Amsterdam ; New York: North-Holland, 1996.

Cao, M. W.; Han, Y. C.; Wang, J. B.; Wang, Y. L. **2007.** Modulation of fibrillogenesis of amyloid beta(1-40) peptide with cationic gemini surfactant. *Journal of Physical Chemistry B*. Vol. 111. n.° 47. p. 13436-13443.

Cerf, E.; Sarroukh, R.; Tamamizu-Kato, S.; Breydo, L.; Derclaye, S.; Dufrene, Y. F.; Narayanaswami, V.; Goormaghtigh, E.; Ruysschaert, J. M.; Raussens, V. **2009.** Antiparallel beta-sheet: a signature structure of the oligomeric amyloid beta-peptide. *Biochem J*. Vol. 421. n.° 3. p. 415-23.

Chen, Z.; Krause, G.; Reif, B. **2005.** Structure and orientation of peptide inhibitors bound to beta-amyloid fibrils. *J Mol Biol*. Vol. 354. n.° 4. p. 760-76.

Citron, M.; Diehl, T. S.; Gordon, G.; Biere, A. L.; Seubert, P.; Selkoe, D. J. **1996.** Evidence that the 42- and 40-amino acid forms of amyloid beta protein are generated from the beta-amyloid precursor protein by different protease activities. *Proceedings of the National Academy of Sciences of the United States of America*. Vol. 93. n.° 23. p. 13170-13175.

Clippingdale, A. B.; Wade, J. D.; Barrow, C. J. **2001.** The amyloid-beta peptide and its role in Alzheimer's disease. *J Pept Sci*. Vol. 7. n.° 5. p. 227-49.

Coles, M.; Bicknell, W.; Watson, A. A.; Fairlie, D. P.; Craik, D. J. **1998.** Solution structure of amyloid beta-peptide(1-40) in a water-micelle environment. Is the membrane-spanning domain where we think it is? *Biochemistry*. Vol. 37. n.° 31. p. 11064-11077.

Evin, G.; Weidemann, A. **2002.** Biogenesis and metabolism of Alzheimer's disease Abeta amyloid peptides. *Peptides*. Vol. 23. n.° 7. p. 1285-97.

Friedman, R.; Caflisch, A. **2011.** Surfactant Effects on Amyloid Aggregation Kinetics. *Journal of Molecular Biology*. Vol. 414. n.° 2. p. 303-312.

Ghavami, Mahdi; Rezaei, Meisam; Ejtehadi, Reza; Lotfi, Mina; Shokrgozar, Mohammad A.; Abd Emamy, Baharak; Raush, Jens; Mahmoudi, Morteza. **2012.** Physiological Temperature Has a Crucial Role in Amyloid Beta in the Absence and Presence of Hydrophobic and Hydrophilic Nanoparticles. *ACS Chemical Neuroscience*.

Hardy, J.; Selkoe, D. J. **2002.** The amyloid hypothesis of Alzheimer's disease: progress and problems on the road to therapeutics. *Science*. Vol. 297. n.° 5580. p. 353-6.

Hellstrand, E.; Boland, B.; Walsh, D. M.; Linse, S. **2010.** Amyloid beta-protein aggregation produces highly reproducible kinetic data and

occurs by a two-phase process. *ACS Chem Neurosci*. Vol. 1. n.° 1. p. 13-8.

Hiemenz, Paul C.; Rajagopalan, Raj - Principles of colloid and surface chemistry. 3rd. New York: Marcel Dekker, 1997.

Jameson, L. P.; Smith, N. W.; Dzyuba, S. V. **2012.** Dye-binding assays for evaluation of the effects of small molecule inhibitors on amyloid (abeta) self-assembly. *ACS Chem Neurosci*. Vol. 3. n.° 11. p. 807-19.

Klement, K.; Wieligmann, K.; Meinhardt, J.; Hortschansky, P.; Richter, W.; Fandrich, M. **2007.** Effect of different salt ions on the propensity of aggregation and on the structure of Alzheimer's abeta(1-40) amyloid fibrils. *J Mol Biol*. Vol. 373. n.° 5. p. 1321-33.

Ladiwala, A. R. A.; Litt, J.; Kane, R. S.; Aucoin, D. S.; Smith, S. O.; Ranjan, S.; Davis, J.; Van Nostrand, W. E.; Tessier, P. M. **2012.** Conformational Differences between Two Amyloid beta Oligomers of Similar Size and Dissimilar Toxicity. *Journal of Biological Chemistry*. Vol. 287. n.° 29. p. 24765-24773.

Lakowicz, J. R. **1988.** Principles of frequency-domain fluorescence spectroscopy and applications to cell membranes. *Subcell Biochem*. Vol. 13. p. 89-126.

Liao, Y. H.; Chang, Y. J.; Yoshiike, Y.; Chang, Y. C.; Chen, Y. R. **2012.** Negatively charged gold nanoparticles inhibit Alzheimer's amyloid-beta fibrillization, induce fibril dissociation, and mitigate neurotoxicity. *Small*. Vol. 8. n.° 23. p. 3631-9.

Marcinowski, K. J.; Shao, H.; Clancy, E. L.; Zagorski, M. G. **1998.** Solution structure model of residues 1-28 of the amyloid beta peptide when bound to micelles. *Journal of the American Chemical Society*. Vol. 120. n.° 43. p. 11082-11091.

Nilsson, M. R. **2004.** Techniques to study amyloid fibril formation in vitro. *Methods*. Vol. 34. n.° 1. p. 151-60.

Otzen, D. **2011.** Protein-surfactant interactions: A tale of many states. *Biochimica Et Biophysica Acta-Proteins and Proteomics*. Vol. 1814. n.° 5. p. 562-591.

Otzen, D. E. **2010.** Amyloid Formation in Surfactants and Alcohols: Membrane Mimetics or Structural Switchers? *Current Protein & Peptide Science*. Vol. 11. n.° 5. p. 355-371.

Rangachari, V.; Moore, B. D.; Reed, D. K.; Sonoda, L. K.; Bridges, A. W.; Conboy, E.; Hartigan, D.; Rosenberry, T. L. **2007.** Amyloid-beta(1-42) rapidly forms protofibrils and oligomers by distinct pathways in low concentrations of sodium dodecylsulfate. *Biochemistry*. Vol. 46. n.° 43. p. 12451-62.

Rangachari, V.; Reed, D. K.; Moore, B. D.; Rosenberry, T. L. **2006.** Secondary structure and interfacial aggregation of amyloid-beta(1-40) on sodium dodecyl sulfate micelles. *Biochemistry*. Vol. 45. n.° 28. p. 8639-8648.

RiesKautt, M.; Ducruix, A. **1997.** Inferences drawn from physicochemical studies of crystallogenesis and precrystalline state. *Macromolecular Crystallography, Pt A*. Vol. 276. p. 23-59.

Rocha, S.; Cardoso, I.; Borner, H.; Pereira, M. C.; Saraiva, M. J.; Coelho, M. **2009.** Design and biological activity of beta-sheet breaker peptide conjugates. *Biochemical and Biophysical Research Communications*. Vol. 380. n.° 2. p. 397-401.

Rocha, S.; Loureiro, J. A.; Brezesinski, G.; Pereira Mdo, C. **2012a.** Peptide-surfactant interactions: consequences for the amyloid-beta structure. *Biochemical and Biophysical Research Communications*. Vol. 420. n.° 1. p. 136-40.

Rocha, S.; Loureiro, J. A.; Brezesinski, G.; Pereira Mdo, C. **2012b.** Peptide-surfactant interactions: consequences for the amyloid-beta structure. *Biochem Biophys Res Commun*. Vol. 420. n.° 1. p. 136-40.

Rocha, S.; Lucio, M.; Pereira, M. C.; Reis, S.; Brezesinski, G. **2008.** The conformation of fusogenic B18 peptide in surfactant solutions. *Journal of Peptide Science*. Vol. 14. n.° 4. p. 436-441.

Roher, A. E.; Lowenson, J. D.; Clarke, S.; Wolkow, C.; Wang, R.; Cotter, R. J.; Reardon, I. M.; Zurcherneely, H. A.; Heinrikson, R. L.; Ball, M. J.; Greenberg, B. D. **1993.** Structural Alterations in the Peptide Backbone of Beta-Amyloid Core Protein May Account for Its Deposition and Stability in Alzheimers-Disease. *Journal of Biological Chemistry*. Vol. 268. n.° 5. p. 3072-3083.

Sabate, R.; Estelrich, J. **2005.** Stimulatory and inhibitory effects of alkyl bromide surfactants on beta-amyloid fibrillogenesis. *Langmuir*. Vol. 21. n.° 15. p. 6944-9.

Saraiva, A. M.; Cardoso, I.; Pereira, M. C.; Coelho, M. A.; Saraiva, M. J.; Mohwald, H.; Brezesinski, G. **2010a.** Controlling amyloid-beta peptide(1-42) oligomerization and toxicity by fluorinated nanoparticles. *Chembiochem*. Vol. 11. n.° 13. p. 1905-13.

Saraiva, A. M.; Cardoso, I.; Saraiva, M. J.; Tauer, K.; Pereira, M. C.; Coelho, M. A.; Mohwald, H.; Brezesinski, G. **2010b.** Randomization of amyloid-beta-peptide(1-42) conformation by sulfonated and sulfated nanoparticles reduces aggregation and cytotoxicity. *Macromol Biosci*. Vol. 10. n.° 10. p. 1152-63.

Shao, H. Y.; Jao, S. C.; Ma, K.; Zagorski, M. G. **1999.** Solution structures of micelle-bound amyloid beta-(1-40) and beta-(1-42) peptides of Alzheimer's disease. *Journal of Molecular Biology*. Vol. 285. n.° 2. p. 755-773.

Silva, H. M. A. R. - Espectroscopia no infravermelho por transformada de Fourier (FTIR). LNEC. 2007. 9789724921228

Soto, C.; Castano, E. M.; Kumar, R. A.; Beavis, R. C.; Frangione, B. **1995.** Fibrillogenesis of synthetic amyloid-beta peptides is dependent on their initial secondary structure. *Neuroscience Letters*. Vol. 200. n.° 2. p. 105-8.

Stine, W. B., Jr.; Dahlgren, K. N.; Krafft, G. A.; LaDu, M. J. **2003.** In vitro characterization of conditions for amyloid-beta peptide oligomerization and fibrillogenesis. *J Biol Chem*. Vol. 278. n.° 13. p. 11612-22.

Suh, Y. H.; Checler, F. **2002.** Amyloid precursor protein, presenilins, and alpha-synuclein: molecular pathogenesis and pharmacological applications in Alzheimer's disease. *Pharmacol Rev*. Vol. 54. n.° 3. p. 469-525.

Tew, D. J.; Bottomley, S. P.; Smith, D. P.; Ciccotosto, G. D.; Babon, J.; Hinds, M. G.; Masters, C. L.; Cappai, R.; Barnham, K. J. **2008.** Stabilization of neurotoxic soluble beta-sheet-rich conformations of the Alzheimer's disease amyloid-beta peptide. *Biophysical Journal*. Vol. 94. n.° 7. p. 2752-2766.

von Szyszkowski, B. **1908.** Experimental studies on the capillary characteristics of watery solutions of fatty acids. *Zeitschrift Fur Physikalische Chemie--Stochiometrie Und Verwandtschaftslehre*. Vol. 64. n.° 4. p. 385-414.

Wahlstrom, A.; Hugonin, L.; Peralvarez-Marin, A.; Jarvet, J.; Graslund, A. **2008.** Secondary structure conversions of Alzheimer's A beta(1-40) peptide induced by membrane-mimicking detergents. *Febs Journal*. Vol. 275. n.° 20. p. 5117-5128.

CHAPTER 4

Effect of fluorinated peptides on Aβ assembly

4.1. Introduction

Increasing evidences suggest that soluble Aβ oligomers might be critical for the onset of AD (Gong, 2003; Kayed, 2003; Klein, 2001; Shankar, 2007; Shankar, 2008). In the view of this hypothesis, a possible strategy to treat the disease is to inhibit the early stages of Aβ aggregation (Hardy, 2002). The two hydrophobic cores of Aβ peptide, the residues 17-21 and 30-42, have been associated to its aggregation process (Hilbich, 1992; Jarrett, 1993). Based on the 17-21 hydrophobic residues, LVFFA, of Aβ Soto *et al.* designed a peptide that binds to the full length Aβ and prevents its aggregation (Soto, 1996). This inhibitor has a similar degree of hydrophobicity, but has a very low propensity to adopt a β-sheet conformation due to the presence of a proline residue. Valine, that it is considered a key residue for the β-sheet formation, was replaced by proline, an amino acid thermodynamically unable to fit in the β-sheet structure (Chou, 1978; Soto, 1996; Wood, 1995). The peptide LPFFD, referred to as $iA\beta_5$, binds to Aβ and blocks the interaction between Aβ molecules, inhibiting the formation of the oligomeric β-sheet conformation, which is the precursor of the fibrils. Certain fluorinated compounds have also been proposed as inhibitors of Aβ aggregation

(Adamski-Werner, 2004; Torok, 2006; Vieira, 2003). Fluorinated solvents such as hexafluoroisopropanol induce an α-helix structure in Aβ peptide. A similar effect is observed when Aβ interacts with poly(tetrafluoroethylene) surfaces or fluorinated nanoparticles (Giacomelli, 2005; Rocha, 2008; Saraiva, 2010). Since the hydrogenated analogues of the NPs were not able to prevent the amyloid fibril formation, it has been postulated that fluorine atoms play an important role on the inhibition of Aβ aggregation. Thus, peptides containing fluorinated amino acids were synthetized and their influence on Aβ oligomerization was studied. The fluorinated peptides are also based on the hydrophobic central residues of $A\beta_{(1-42)}$ 17-21 (LVFFA) and on the $iA\beta_5$ beta-sheet breaker peptide. The fluorinated sequences were covalently linked to PEG to increase their solubility (Figure 4.1). The coupling $iA\beta_5$ to PEG does not compromise its affinity to Aβ or the $iA\beta_5$ beta-sheet breaker activity (Rocha, 2009). PEG has additionally very low toxicity and is known to reduce protein degradation by proteolytic enzymes (Veronese, 2001). The use of non-natural residues such as fluorinated amino acids is also known to efficiently improve the stability of peptides or proteins against enzymatic degradation (Buer, 2012). The conjugates of fluorinated peptide-PEG were characterized by matrix-assisted laser desorption/ionization mass spectrometry. The kinetics of the $A\beta_{(1-42)}$ aggregation, in the presence and in the absence of the conjugates, was evaluated by the ThT assay and the data were fitted using the crystallization-like model recently described by Crespo *et. al.* (Crespo, 2012). The ultrastructure characterization of the Aβ aggregates was performed by transmission electron microscopy.

4.2. Material and Methods

4.2.1. Synthesis of conjugates of fluorinated peptides and polyethylene glycol

The conjugates were prepared by the solid-phase supported strategy. Direct synthesis of the conjugate was performed applying a resin comprising a cleavable PEG spacer. Automated stepwise amino acid attachment was applied, following standard Fmoc-protocols. TentaGel PEG Attached Peptide resin (loading: 0.24 mmol/g; PDI = 1.06 [GPC (THF, calibrated against linear PEG standards, PSS, Germany)] was purchased from Rapp, Polymere GmbH. Fmoc amino acids derivatives (Fmoc-phenylalanine OH, Fmoc-leucine OH, Fmoc-aspartic acid OH, Fmoc-valine OH, Fmoc-4;4;4-trifluoro-DL-valine, Fmoc-3;4;5-trifluoro-L-phenylalanine and Fmoc-trans-4-Fluoro-L-proline) were used as purchased from AnaSpec. The sequences of the fluorinated peptides are shown in Figure 4.1. After the synthesis, the conjugates were dissolved in distilled water with 1% guanidinium hydrochloride and the pH was adjusted to 7 with sodium hydroxide 1 M. The samples were dialyzed against ultrapure water using a regenerate cellulose membrane (MWCO 1000 Da) for 4 days followed by lyophilization.

Conjugates

Leu-FluoroPro-Phe-Phe-Asp-PEG (**LP$_f$FFD-PEG)**

Leu-Val-FluoroPhe-Phe-Asp-PEG (**LVF$_f$FD-PEG)**

Leu-FluoroVal-Phe-Phe-Asp-PEG (**LV$_f$FFD-PEG)**

Fluorinated amino acids

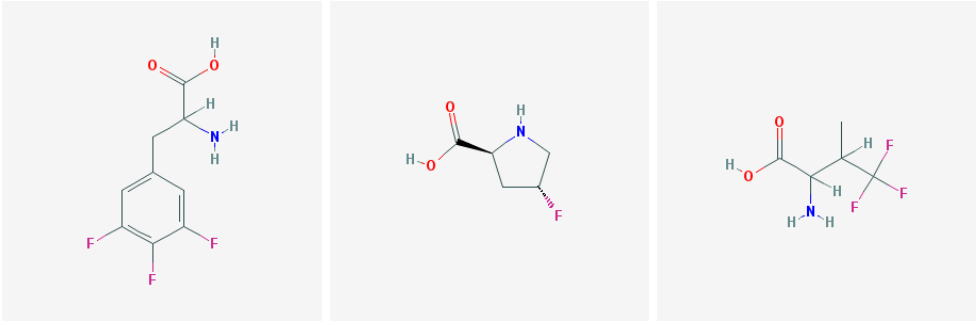

3,4,5 – trifluorophenylalanine 4-fluoroproline 4,4,4-Trifluorovaline

Figure 4.1 - Sequences of the fluorinated peptides conjugated to PEG used in this study. The chemical structure of the fluorinated amino acids is also shown (source: PubChem of the National Center for Biotechnology Information)

4.2.2. Stock solutions of amyloid-beta peptide

Aβ$_{(1-42)}$ (amyloid-β peptide 1-42, purity > 95.22%, MW 4514.14, Selleck Chemicals) was prepared as is described in the Chapter 3, Section 3.1.1.

4.2.3. Matrix-assisted laser desorption/ionization mass spectrometry

The ionization technique called Matrix-assisted laser desorption/ionization (MALDI), allows the evaluation of biomolecules, such as peptides and large organic molecules. When conventional ionization methods are used, these molecules tend to be fragile and fragment. MALDI is used in mass spectrometry procedures. MALDI is a two-step process. In the first one, the matrix material deeply absorbs the ultraviolet (UV) laser beam, which starts desorption of the upper layer (~1 μm). In the second step, the molecules are protonated or deprotonated. The most common type of mass spectrometer used with MALDI is the TOF (time-of-flight mass spectrometer), primarily because its wide mass range. In addition the combination of MALDI and TOF is suitable due the individual "shots" by the pulsed laser instead of operating continuously. MALDI-TOF instrument is capable of reflecting ions using an electric field, which double the ion path and increasing the resolution.

MALDI-TOF measurements were performed in a Voyager-DE STR BioSpectrometry Workstation MALDI-TOF mass spectrometer (Perceptive Biosystems, Inc., Framingham, MA, USA) at an acceleration voltage of 20 kV. The fluorinated peptide-PEG conjugates were dissolved in 0.1% TFA in acetonitrile–water (1:1, v/v) at a concentration of 0.1 mg/mL. One microliter of the analyte solution was mixed with l μL of alpha-cyano-4-hydroxycinnamic acid matrix solution consisting of 10 mg of matrix dissolved in 1 mL of 0.1% trifluoroacetic acid (TFA) in acetonitrile–water (1:1, v/v). From the resulting mixture, 1 μL was applied to the sample plate. Samples were air-dried at room temperature (RT) (25 °C). Each spectrum is a mean of 250 laser shots.

4.2.4. Thioflavin T binding assay

For kinetic studies, $A\beta_{(1-42)}$ peptide (12.5 μM) was incubated at 37 °C in 96 well plates (Nunclon Delta Surface) with the fluorinated peptide-PEG conjugates (250 μM) in the presence of ThT (0.7 mg/mL) in PBS buffer. ThT solution was filtered using 0.2 μm syringe filter before adding to the Aβ samples. The fibrils conjugated with ThT have the excitation maximum at 450 nm and enhanced emission at 482 nm (LeVine, 1993). The fluorescence intensity was measured every 30 minutes during 24 hours using a Biotek Synergy 2 fluorescence spectrometer with the excitation filter 420/50 nm and the emission filter 485/20 nm.

4.2.5. Theoretical Crystallization-Like Model

The Crystallization-Like Model (CLM) is a generic two-parameter model that describes protein aggregation kinetics by a sequence of nucleation and growth steps. The CLM is represented by the following equation, in which α represents the normalized fraction of amyloid protein converted into fibrils (Equation 4.1).

$$\alpha = 1 - \frac{1}{k_b[\exp(k_a t) - 1] + 1} \tag{4.1}$$

and k_a and k_b are the growth and the nucleation-to-growth rate constants. The two parameters are related with the time required to reach half of the total fibril conversion (t_{50}) and with the aggregation rate (v_{50}) given the slope of the α(t) curve at that instant.

4.2.6. Transmission electron microscopy

For ultra-structural studies, $A\beta_{(1-42)}$ peptide (100 μM) was incubated at 37 °C with each of the fluorinated peptide-PEG conjugates (2 mM) in PBS buffer (10 mM, pH 7.4), for 48 hours. An aliquot of each sample (5 μL) was placed on carbon-formvar coated 200-400 mesh spacing grids and let to adsorb for five minutes. The negative staining was performed with 2% filtered aqueous solution of uranyl acetate for 45 seconds. The grids were visualized using a Jeol JEM 1400 electron microscope at 80 kV.

4.2.7. Toxicity assay

Porcine brain capillary endothelial cells (PBCECs) were incubated in Plating-Medium - Earls Medium 199 supplemented with L-Glutamine (0.7 mM), penicillin/streptomycin (1%), gentamicin (1%) and new-born calf serum, (all the compounds were purchased at Biochrom) - in a 96 well plate (Corning) previously coated with Collagen G (Biochrom). After 48 hours incubation at 37 °C, the culture medium was replaced. Normally, apparent confluence of the monolayers was reached after 4 days (approximately 6-8 $x10^4$ cells per well). At day 4 the medium was replaced by a solution of KRB (Krebs Ringer buffer) composed by NaCl (sodium chloride p. A., Mw 58.44, AppliChem), KCl (potassium chloride, Mw 74.56, AppliChem), H_2KO_4P (potassium dihydrogen phosphate p.A., Mw 136.09, AppliChem), HEPES (hepes puffedran ≥ 99.5%, p.A., Mw 238.31, ROTH), D-Glucose (D(+)-glucose anhydrous for biochemistry, Mw 180.16, MERCK), $MgCl_2.6H_2O$ (magnesium chloride hexahydrate p.A., Mw 203.30, AppliChem) and $CaCl_2.2H_2O$ (calcium chloride dehydrate p.A., Mw 147.02, AppliChem) and fluorinated peptide-PEG conjugate at different concentrations..

The peptide was incubated with the cells for 2 hours at 37 °C. Cells without peptides and lysed cells with 1% Triton were used as, respectively, negative and positive controls. After removal of the peptide suspension by aspiration, the cells were incubated with Alamar Blue reagent 40:1 (water:Alamar Blue – v/v). Fluorescence was detected with a Fluoroskan Ascent (Labsystems) (excitation – 530 nm; emission – 590 nm).

4.3. Results

4.3.1. Fluorinated peptide-PEG conjugates

The fluorinated sequences conjugated to PEG were analysed by MALDI-TOF-MS. The spectrum of L**P$_f$**FFD-PEG is depicted as representative of the results acquired for the conjugates and shows the typical distribution of the polymer PEG with the characteristic repeat unit of 44.1 ± 0.5 Da, which could be assigned to the ethylene oxide (EO) monomer of the PEG (Figure 4.2). The experimentally found signal at m/z 3694.8, for example, can be assigned to [M+K] = 3692.3 Da by assuming a $M_{[EO]}$ of 44.05 Da, n = 68 units, a mass of the peptide of $M_{[peptide]}$ = 655.8 Da, a mass of the polymer end groups (1 H = 1 Da) and the mass of a potassium counter ion ($M_{[counter\ ion]}$ = 39.1).

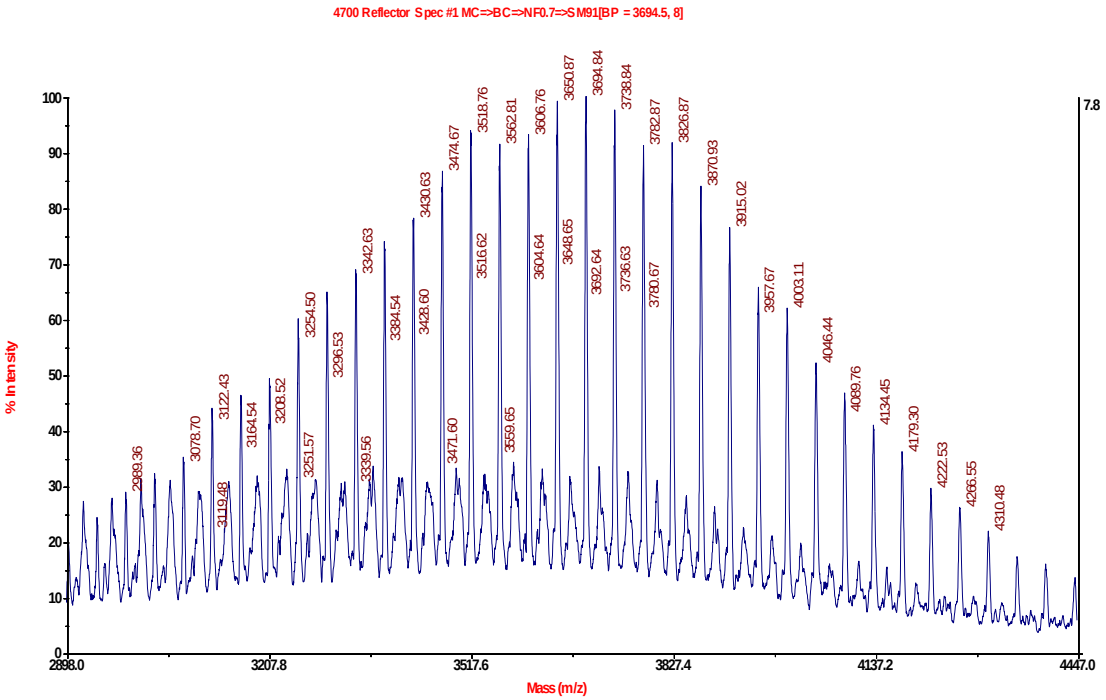

Figure 4.2 - MALDI-TOF-MS of LP$_f$FFD-PEG conjugate.

4.3.2. Impact of the peptide-PEG conjugates on Aβ$_{(1-42)}$ fibrillization

The aggregation kinetics of Aβ$_{(1-42)}$ incubated at 37 °C with L**P$_f$**FFD-PEG, LV**F$_f$**FD-PEG and L**V$_f$**FFD-PEG was evaluated by ThT binding assay (Figure 4.3). The molar ratio of Aβ$_{(1-42)}$ and conjugates was 1:20. At 15 minutes incubation time, the ThT fluorescence intensity is low for all samples, which indicates low content of amyloid fibrils. After two hours, a large increase in the fluorescence intensity is observed for Aβ$_{(1-42)}$ alone and for Aβ$_{(1-42)}$:L**P$_f$**FFD-PEG samples, reaching the maximum at 4 hours incubation time (the fluorescence intensities were normalized to that of Aβ$_{(1-42)}$ incubated with ThT at 37 °C for 24 hours). The fluorescence of ThT in the presence of Aβ$_{(1-42)}$ and LV**F$_f$**FD-PEG showed only a moderated increase (53%) after 4 hours, whereas that of the sample Aβ$_{(1-42)}$:L**V$_f$**FFD-

PEG remained low (15%). The conjugates in the absence of $A\beta_{(1-42)}$ do not induce any change in the fluorescence signal of ThT.

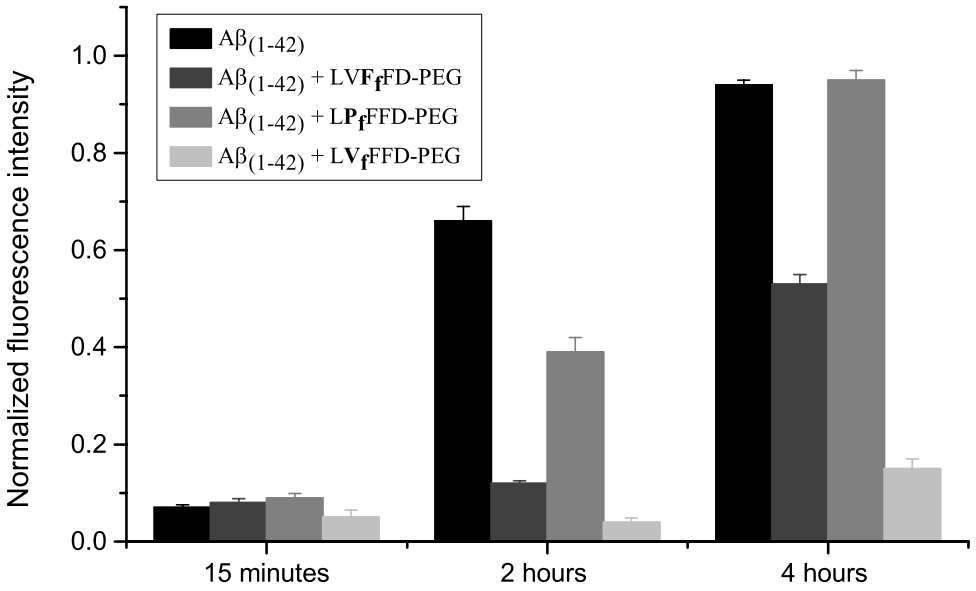

Figure 4.3 - Fluorescence intensity of ThT in $A\beta_{(1-42)}$ samples containing fluorinated peptide-PEG conjugates and incubated at 37 °C. The fluorescence signal was normalized to the maximum intensity of the sample of $A\beta_{(1-42)}$ without conjugates.

The kinetic data were fitted according to the recently proposed CLM model (Figure 4.4). The t_{50} and the v_{50} were obtained by fitting a sigmoidal function to each kinetic trace according to the CLM (Table 4.1) (Crespo, 2012). In the case of sigmoidal-type aggregation kinetics such as those represented in Figure 4.4, v_{50} is solely dictated by the growth rate constant k_a. The parameter v_{50} did not change significantly in the presence of the conjugates. A marked increase of the value of t_{50} is, however, evident for the LV**F**$_{\mathbf{f}}$FD-PEG and L**V**$_{\mathbf{f}}$FFD-PEG, which can be explained by the CLM as the result of either nucleation-prevention or solubility-change effects. The later hypothesis is discarded by the fact that the maximum fluorescence signal did not show significant variation in the presence of

conjugates (results not shown here). Therefore, the increased induction times to the inhibition of the nucleation step is ascribe as a possible consequence of the stabilization of the Aβ molecule by the conjugates. The higher value of the induction time t_{50} is obtained for the conjugate containing the fluorinated valine (L**V$_f$**FFD-PEG), suggesting a stronger inhibitory effect in this case. Inhibitors of the amyloid fibril formation may act upon the initial assembly of macromolecules forming the stable nuclei (nucleation step) or block the subsequent addition of new growth units (growth step) (Crespo, 2012). A third way of action involves the alteration of the thermodynamic solubility of the polypeptide. This alternative is more unlikely to result *in vivo* since cell and tissue media are in general buffered against non-specific interactions. For example, comparing the effect of a well-known and well accepted β-sheet breaker peptide, iAβ_5 (LPFFD) on A$\beta_{(1-42)}$ aggregation, a similar effect was obtained by the L**V$_f$**FFD-PEG conjugate (3.1 hours) (Table 4.1). At the same molar ratio and with the same A$\beta_{(1-42)}$ batch, the reduction of the aggregation time of A$\beta_{(1-42)}$ is similar for iAβ_5 and L**V$_f$**FFD-PEG. The conjugate containing fluorinated phenylalanine (LV**F$_f$**FD-PEG) induced an inhibitory effect of 1.5 hours and the L**P$_f$**FFD-PEG did not inhibit the A$\beta_{(1-42)}$ aggregation.

The A$\beta_{(1-42)}$:conjugate molar ratio of 1:5 did not significantly change the aggregation parameters of Aβ, which indicates that there is a threshold concentration for the Aβ-conjugate interaction.

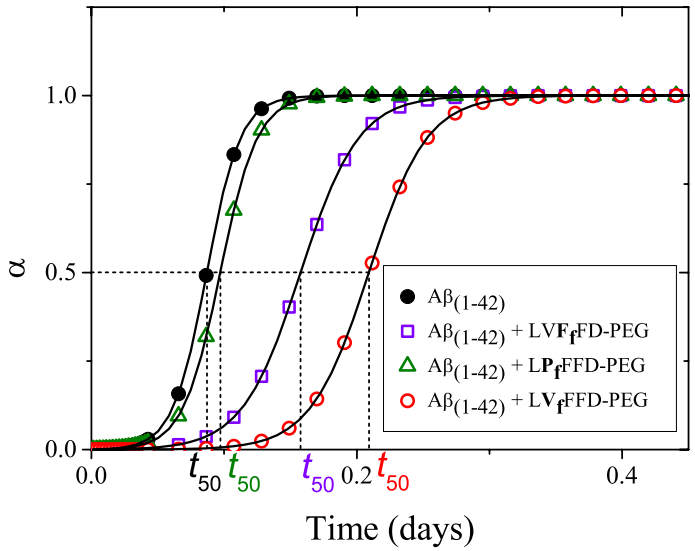

Figure 4.4 - Numerical fit of Eq. 4.1 to the normalized conversion of Aβ$_{(1-42)}$ peptide incubated in the presence of conjugates at 37 °C in PBS buffer, monitored by ThT fluorescence. The Aβ$_{(1-42)}$ concentration was keep constant at 12.5 μM and the molar ratio of Aβ$_{(1-42)}$:conjugates was 1:20. The aggregation rate (v_{50}) was obtained by fitting a sigmoidal function to each kinetic trace according to the Eq. 4.1.

Table 4.1 - Time required to reach half of the total fibril conversion (t_{50}) and delay in the aggregation of the Aβ$_{(1-42)}$ in the absence and presence of fluorinated peptide conjugates and LPFFD peptide.

	t_{50} (hours)	Delay in aggregation (hours)
Aβ$_{(1-42)}$ alone	2.1	-
Aβ$_{(1-42)}$ and L**P**$_f$FFD-PEG	2.4	0.2
Aβ$_{(1-42)}$ and LV**F**$_f$FD-PEG	3.6	1.5
Aβ$_{(1-42)}$ and LV$_f$FFD-PEG	5.2	3.1
Aβ$_{(1-42)}$ and iAβ5	5.4	3.3

This assays evidenced that two of the fluorinated peptides (LV**F$_f$**FD-PEG and L**V$_f$**FFD-PEG) are able to delay the aggregation of the A$\beta_{(1-42)}$. Hydrophobic interactions and H-bonding among side-chain groups are the two major driving forces that control protein aggregation (Petkova, 2002). A large amount of evidence indicates that there are three distinct regions within the A$\beta_{(1-42)}$ sequence that might be involved in its aggregation: the central hydrophobic cluster correspondent to the 17-21 region, the 23-28 residues and the hydrophobic C-terminus (Antzutkin, 2003; Pike, 1995; Torok, 2002). Considering that fluorine atoms increase the hydrophobicity of the sequences, it is expected that they would interact with hydrophobic regions of A$\beta_{(1-42)}$ to be segregated away from the water. This interaction might contribute to the prevention of Aβ molecules with each other, inhibiting thus their aggregation. The PEG molecules linked to the fluorinated peptides can also contribute to the interaction of the conjugates with A$\beta_{(1-42)}$. Previously Rocha *et al.* have showed that the pegylation of a beta-sheet breaker peptide did not significantly change its binding to A$\beta_{(1-42)}$ (Rocha, 2009). PEG is described to bind to proteins such as albumin and lysozyme even in solution with an ionic strength similar to the physiological conditions (Wu, 2013). In the case of the fluorinated peptide-PEG conjugates, their effect on A$\beta_{(1-42)}$ cannot be simply explained by the PEG-Aβ interaction since the three conjugates show different outcomes.

TEM analysis shows that A$\beta_{(1-42)}$ incubation at 37 °C for 48 hours resulted in amyloid-like, unbranched fibrils (Figure 4.5). A$\beta_{(1-42)}$ also forms fibrils in the presence of the conjugates (or iAβ_5), although the samples containing LV**F$_f$**FD-PEG and L**V$_f$**FFD-PEG show also small aggregates. This analysis demonstrates that the bioconjugates and the beta-sheet breaker iAβ5 only delay the A$\beta_{(1-42)}$ fibrillogenesis.

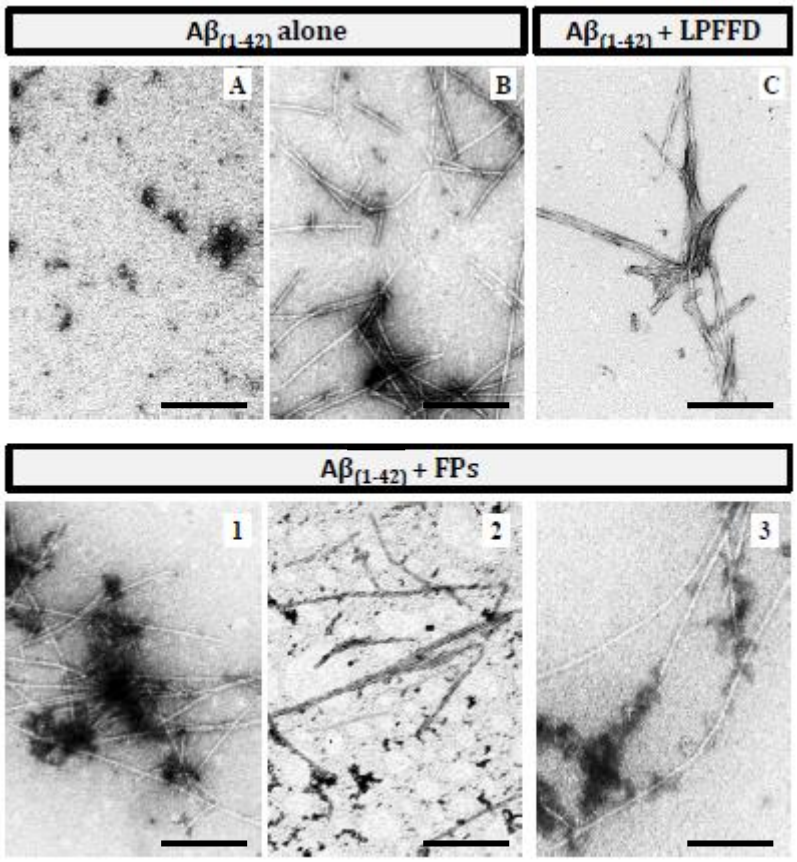

Figure 4.5 - TEM images of the $A\beta_{(1-42)}$ in the absence and presence of fluorinated peptide conjugates and LPFFD peptide. $A\beta_{(1-42)}$ was incubated at 37 °C in the presence of the conjugates (molar ratio 1:20) in 10 mM PBS buffer, pH 7.4. A) $A\beta_{(1-42)}$ alone at 0 hours incubation, B) $A\beta_{(1-42)}$ alone at 48 hours incubation, C) $A\beta_{(1-42)}$ in the presence of LPFFD peptide at 48 hours incubation, 1) $A\beta_{(1-42)}$ in the presence of LP_fFFD-PEG at 48 hours incubation, 2) $A\beta_{(1-42)}$ in the presence of LVF_fFD-PEG at 48 hours incubation and 3) $A\beta_{(1-42)}$ in the presence of LV_fFFD-PEG at 48 hours incubation. The scale bar corresponds to 200 nm.

The fluorinated amino acids of the conjugates may play an important role in delaying the $A\beta_{(1-42)}$ aggregation by interacting with the hydrophobic residues of the Aβ and preventing its interaction with other Aβ molecules. There is also a geometric preference for the interaction between C-F bond and the side-chain amides of glutamine (E) 15 and

asparagine (N) 27 residues (Muller, 2007). Therefore, the fluorine atoms might be able to interact with the two stretches of Aβ hydrophobic residues responsible for its oligomerization (17-21 and 30–42 residues) and/or with residues in their vicinity by exploiting the same interaction as in $A\beta_{(1-42)}$ assembly. A conformational tightened state is produced by the interplay of ionic and hydrophobic groups of both peptide and the conjugates.

Ferrão-Gonzales *et al.* showed that (1-anilino-8-naphthalene sulfonate)-derived molecules inhibit Aβ aggregation due to their dual nature provided by hydrophobic regions and charged groups (Ferrao-Gonzales, 2005). Vieira *et al.* demonstrated the effectiveness of different fluorinated alcohols for the β-to-α refolding process of $A\beta_{(1-40)}$ (Vieira, 2003). The observed effect was interpreted as a result of alterations of the hydration shell of the peptides and hydrophobic effects of fluorine groups. Montserret *et al.* have shown that although the folding of amphipathic α-helical peptides in hydrophilic SDS micellar solutions is mostly driven by electrostatic interactions, when hydrophobic peptides are considered, SDS–peptide hydrophobic interactions might be sufficiently strong to induce α-helical-rich structures (Montserret, 2000). The effect of fluorinated complexes made of polyampholyte and the sodium salt of perfluorododecanoic acid on Aβ was attributed to the hydrophobic and acidic characters of the perfluorododecanoic acid (Rocha, 2008; Saraiva, 2010). Also, it is proposed that LV**F_f**FD-PEG and L**V_f**FFD-PEG have the necessary hydrophobicity and spatial geometry to allow the interaction with $A\beta_{(1-42)}$. L**P_f**FFD-PEG, with one fluorine atom in the proline residue, was not able to prevent Aβ-Aβ interactions. Proline residues are generally solvent-exposed in proteins and they are considered binding motifs in protein-protein interaction (Kay, 2000). The fluorinated proline is probably inducing a conformation on the conjugate L**P_f**FFD-PEG that prevents the exposure of its amino acids and their interaction with

residues of other peptide molecules. Comparing the L**P$_f$**FFD-PEG with the non-fluorinated analogue, one can assume that the fluorine atom increases the steric hindrance of the conjugate reducing the access to the proline residue. On the other hand the hydrophobic interactions between L**P$_f$**FFD-PEG and Aβ are probably not strong enough when compared to the Aβ-Aβ interactions. Apart from the apparently reduced interaction between Aβ and L**P$_f$**FFD-PEG, the position of fluorine atoms at the extremity of the conjugate and the fluorination of hydrophobic residues seem to favour the inhibitory effect of the sequences on Aβ amyloid fibril formation.

4.3.3. Toxicity assay

The cell toxicity of the conjugate LV**F$_f$**FD-PEG was assessed using PBCEC cultures. After two hours of incubation of the cells with the fluorinated peptide conjugate, the cells were incubated with the Alamar Blue solution at 37°C. The results demonstrate that the LV**F$_f$**FD-PEG conjugate is not toxic for PBCECs at concentrations lower than 2 mM.

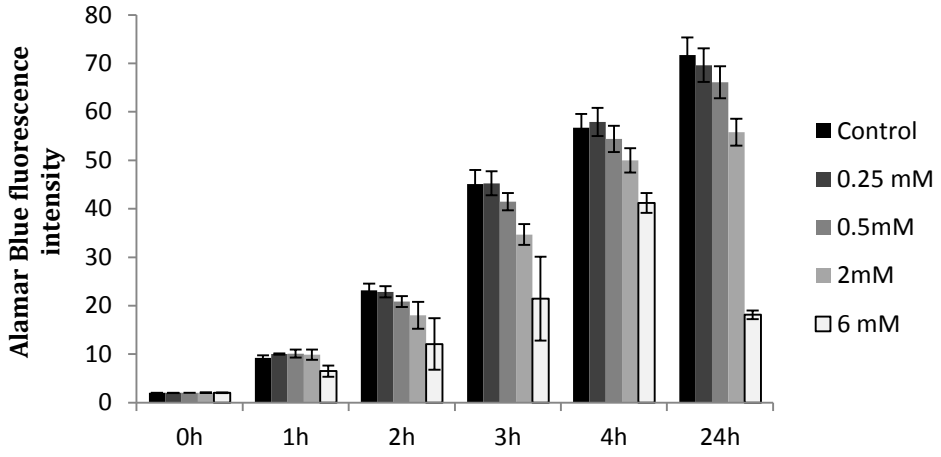

Figure 4.6 - Alamar Blue assay of PBCECs cultured with different concentrations of LVF$_f$FD-PEG conjugate monitored during 24 hours at 37°C.

This study opens up the possibility of using fluorinated peptide-PEG conjugates as inhibitors of the Aβ peptide aggregation.

References

Adamski-Werner, S. L.; Palaninathan, S. K.; Sacchettini, J. C.; Kelly, J. W. **2004.** Diflunisal analogues stabilize the native state of transthyretin. Potent inhibition of amyloidogenesis. *J Med Chem*. Vol. 47. n.° 2. p. 355-74.

Antzutkin, O. N.; Balbach, J. J.; Tycko, R. **2003.** Site-specific identification of non-beta-strand conformations in Alzheimer's beta-amyloid fibrils by solid-state NMR. *Biophys J*. Vol. 84. n.° 5. p. 3326-35.

Buer, B. C.; Marsh, E. N. G. **2012.** Fluorine: A new element in protein design. *Protein Science*. Vol. 21. n.° 4. p. 453-462.

Chou, P. Y.; Fasman, G. D. **1978.** Empirical predictions of protein conformation. *Annu Rev Biochem*. Vol. 47. p. 251-76.

Chromy, B. A.; Nowak, R. J.; Lambert, M. P.; Viola, K. L.; Chang, L.; Velasco, P. T.; Jones, B. W.; Fernandez, S. J.; Lacor, P. N.; Horowitz, P.; Finch, C. E.; Krafft, G. A.; Klein, W. L. **2003.** Self-assembly of Abeta(1-42) into globular neurotoxins. *Biochemistry*. Vol. 42. n.° 44. p. 12749-60.

Crespo, R.; Rocha, F. A.; Damas, A. M.; Martins, P. M. **2012.** A Generic Crystallization-like Model That Describes the Kinetics of Amyloid Fibril Formation. *Journal of Biological Chemistry*. Vol. 287. n.° 36. p. 30585-30594.

Ferrao-Gonzales, A. D.; Robbs, B. K.; Moreau, V. H.; Ferreira, A.; Juliano, L.; Valente, A. P.; Almeida, F. C. L.; Silva, J. L.; Foguel, D. **2005.** Controlling beta-amyloid oligomerization by the use of naphthalene sulfonates - Trapping low molecular weight oligomeric species. *Journal of Biological Chemistry*. Vol. 280. n.° 41. p. 34747-34754.

Giacomelli, C. E.; Norde, W. **2005.** Conformational changes of the amyloid beta-peptide (1-40) adsorbed on solid surfaces. *Macromol Biosci*. Vol. 5. n.° 5. p. 401-7.

Gong, Y.; Chang, L.; Viola, K. L.; Lacor, P. N.; Lambert, M. P.; Finch, C. E.; Krafft, G. A.; Klein, W. L. **2003.** Alzheimer's disease-affected brain: presence of oligomeric A beta ligands (ADDLs) suggests a molecular basis for reversible memory loss. *Proc Natl Acad Sci U S A*. Vol. 100. n.° 18. p. 10417-22.

Hardy, J.; Selkoe, D. J. **2002.** The amyloid hypothesis of Alzheimer's disease: progress and problems on the road to therapeutics. *Science*. Vol. 297. n.° 5580. p. 353-6.

Hilbich, C.; Kisters-Woike, B.; Reed, J.; Masters, C. L.; Beyreuther, K. **1992.** Substitutions of hydrophobic amino acids reduce the amyloidogenicity of Alzheimer's disease beta A4 peptides. *J Mol Biol*. Vol. 228. n.° 2. p. 460-73.

Jarrett, J. T.; Berger, E. P.; Lansbury, P. T., Jr. **1993.** The carboxy terminus of the beta amyloid protein is critical for the seeding of amyloid formation: implications for the pathogenesis of Alzheimer's disease. *Biochemistry*. Vol. 32. n.° 18. p. 4693-7.

Kay, B. K.; Williamson, M. P.; Sudol, P. **2000.** The importance of being proline: the interaction of proline-rich motifs in signaling proteins with their cognate domains. *Faseb Journal*. Vol. 14. n.° 2. p. 231-241.

Kayed, R.; Head, E.; Thompson, J. L.; McIntire, T. M.; Milton, S. C.; Cotman, C. W.; Glabe, C. G. **2003.** Common structure of soluble amyloid oligomers implies common mechanism of pathogenesis. *Science*. Vol. 300. n.° 5618. p. 486-9.

Klein, W. L.; Krafft, G. A.; Finch, C. E. **2001.** Targeting small Abeta oligomers: the solution to an Alzheimer's disease conundrum? *Trends Neurosci*. Vol. 24. n.° 4. p. 219-24.

LeVine, H., 3rd. **1993.** Thioflavine T interaction with synthetic Alzheimer's disease beta-amyloid peptides: detection of amyloid aggregation in solution. *Protein Sci*. Vol. 2. n.° 3. p. 404-10.

Montserret, R.; McLeish, M. J.; Bockmann, A.; Geourjon, C.; Penin, F. **2000.** Involvement of electrostatic interactions in the mechanism of peptide folding induced by sodium dodecyl sulfate binding. *Biochemistry*. Vol. 39. n.° 29. p. 8362-8373.

Muller, K.; Faeh, C.; Diederich, F. **2007.** Fluorine in pharmaceuticals: Looking beyond intuition. *Science*. Vol. 317. n.° 5846. p. 1881-1886.

Petkova, A. T.; Ishii, Y.; Balbach, J. J.; Antzutkin, O. N.; Leapman, R. D.; Delaglio, F.; Tycko, R. **2002.** A structural model for Alzheimer's beta -amyloid fibrils based on experimental constraints from solid state NMR. *Proc Natl Acad Sci U S A*. Vol. 99. n.° 26. p. 16742-7.

Pike, C. J.; Walencewicz-Wasserman, A. J.; Kosmoski, J.; Cribbs, D. H.; Glabe, C. G.; Cotman, C. W. **1995.** Structure-activity analyses of beta-amyloid peptides: contributions of the beta 25-35 region to aggregation and neurotoxicity. *J Neurochem*. Vol. 64. n.° 1. p. 253-65.

Rocha, S.; Cardoso, I.; Borner, H.; Pereira, M. C.; Saraiva, M. J.; Coelho, M. **2009.** Design and biological activity of beta-sheet breaker peptide conjugates. *Biochem Biophys Res Commun*. Vol. 380. n.° 2. p. 397-401.

Rocha, S.; Thuneman, A. F.; Pereira, M. D.; Coelho, M.; Mohwald, H.; Brezesinski, G. **2008.** Influence of fluorinated and hydrogenated nanoparticles on the structure and fibrillogenesis of amyloid beta-peptide. *Biophysical Chemistry*. Vol. 137. n.° 1. p. 35-42.

Saraiva, A. M.; Cardoso, I.; Pereira, M. C.; Coelho, M. A.; Saraiva, M. J.; Mohwald, H.; Brezesinski, G. **2010.** Controlling amyloid-beta peptide(1-42) oligomerization and toxicity by fluorinated nanoparticles. *Chembiochem*. Vol. 11. n.° 13. p. 1905-13.

Shankar, G. M.; Bloodgood, B. L.; Townsend, M.; Walsh, D. M.; Selkoe, D. J.; Sabatini, B. L. **2007.** Natural oligomers of the Alzheimer amyloid-beta protein induce reversible synapse loss by modulating an NMDA-type glutamate receptor-dependent signaling pathway. *J Neurosci*. Vol. 27. n.° 11. p. 2866-75.

Shankar, G. M.; Li, S.; Mehta, T. H.; Garcia-Munoz, A.; Shepardson, N. E.; Smith, I.; Brett, F. M.; Farrell, M. A.; Rowan, M. J.; Lemere, C. A.; Regan, C. M.; Walsh, D. M.; Sabatini, B. L.; Selkoe, D. J. **2008.** Amyloid-beta protein dimers isolated directly from Alzheimer's brains impair synaptic plasticity and memory. *Nat Med*. Vol. 14. n.° 8. p. 837-42.

Soto, C.; Kindy, M. S.; Baumann, M.; Frangione, B. **1996.** Inhibition of Alzheimer's amyloidosis by peptides that prevent beta-sheet conformation. *Biochem Biophys Res Commun*. Vol. 226. n.° 3. p. 672-80.

Torok, M.; Abid, M.; Mhadgut, S. C.; Torok, B. **2006.** Organofluorine inhibitors of amyloid fibrillogenesis. *Biochemistry*. Vol. 45. n.° 16. p. 5377-5383.

Torok, M.; Milton, S.; Kayed, R.; Wu, P.; McIntire, T.; Glabe, C. G.; Langen, R. **2002.** Structural and dynamic features of Alzheimer's Abeta peptide in amyloid fibrils studied by site-directed spin labeling. *J Biol Chem*. Vol. 277. n.° 43. p. 40810-5.

Veronese, F. M. **2001.** Peptide and protein PEGylation: a review of problems and solutions. *Biomaterials*. Vol. 22. n.° 5. p. 405-417.

Vieira, E. P.; Hermel, H.; Mohwald, H. **2003.** Change and stabilization of the amyloid-beta(1-40) secondary structure by fluorocompounds. *Biochim Biophys Acta*. Vol. 1645. n.° 1. p. 6-14.

Wood, S. J.; Wetzel, R.; Martin, J. D.; Hurle, M. R. **1995.** Prolines and amyloidogenicity in fragments of the Alzheimer's peptide beta/A4. *Biochemistry*. Vol. 34. n.° 3. p. 724-30.

Wu, J.; Wang, Z.; Lin, W. F.; Chen, S. F. **2013.** Investigation of the interaction between poly(ethylene glycol) and protein molecules using low field nuclear magnetic resonance. *Acta Biomaterialia*. Vol. 9. n.° 5. p. 6414-6420.

Chapter 5

Design of liposomes coupled to monoclonal antibodies to cross the blood-brain barrier

5.1. Introduction

Liposomes are one of the most studied vehicles to carry drugs to the site of action. A polymer PEG can be attached to the nanocarriers to reduce their immunogenicity and prolong their half-life time (Immordino, 2006). Also, they are rapidly biodegradable, i.e. over a time frame of a few days, which is one important major requirement for NPs brain delivery systems (Wohlfart, 2012). Liposomes have further documented advantages as increased drug loading capacity, versatile structural characteristics that permit easy surface functionalization, biocompatibility and reduced toxicity (Markoutsa, 2011a). In addition, to improve the selectivity of the nanoparticles, numerous ligands can be attached to their surface including mAb, which are one of the most efficient ligands to accomplish this action. TrR has been shown to be selectively enriched at the brain capillary endothelium and has been demonstrated to undergo RMT through the BBB (Cerletti, 2000). In general, *in vitro* models that allow reliable prediction of drug and/or carrier brain penetration are very useful. The PBCECs constitute a well-characterized cell line, which has

been demonstrated to mimic the basic characteristics of the BBB (Markoutsa, 2011a). Also, for *in vivo* studies, rats represent a good model.

This chapter describes the design, synthesis and the properties of functionalized liposomes with mAb for BBB endogenous receptors and mAb for Aβ peptide aggregates. The specific antibody type OX-26 was selected since it has been well described to bind cells that express the TfR such as the BBB cells (Schnyder, 2004). The mAb 19B8 for Aβ can be used to carry the immunoliposomes directly to Aβ plaque deposits.

5.2. Materials and methods

5.2.1. Liposomes

All the lipids were purchased from Avanti Polar Lipids: DSPC (1,2-distearoyl-*sn*-glycero-3-phosphocholine, MW 790.145), Chol (cholesterol ovine wool, MW 386.65), DSPE-PEG_{2000} (1,2-distearoyl-*sn*-glycero-3-phosphoethanolamine-N-[amino(polyethylene glycol)-2000] (ammonium salt), MW 2790.49), DSPE-PEG_{2000}-mal (1,2-distearoyl-*sn*-glycero-3-phosphoethanolamine-N-[maleimide(polyethylene glycol)-2000] (ammonium salt), MW 2941.61), DSPE-PEG_{2000}-biot (1,2-distearoyl-*sn*-glycero-3-phosphoethanolamine-N-[biotin(polyethylene glycol)-2000] (ammonium salt), MW 3016.78) and Liss Rhod PE (1,2-dipalmitoyl-*sn*-glycero-3-phosphoethanolamine-N-(lissamine rhodamine B sulfonyl) (ammonium salt), MW 1249.64).

The chemical structure of the phospholipids is shown in table 5.1. The pegylated phospholipids have a molecular weight of approximately 2000 Da in order to confer stability to the liposomes without significantly vary their size.

Table 5.1 - Chemical structure of the lipids used to prepared immunoliposomes

Chemical Structure	Names
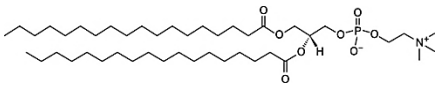	**DSPC:** 1,2-distearoyl-*sn*-glycero-3-phosphocholine
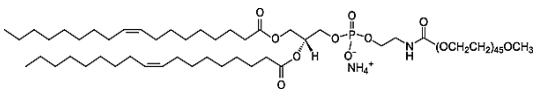	**DSPE-PEG:** 1,2-dioleoyl-*sn*-glycero-3-phosphoethanolamine-N-[methoxy(polyethylene glycol)-2000]
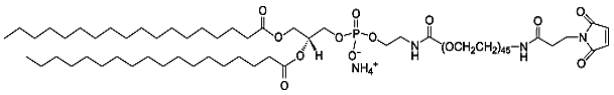	**DSPE-PEG(2000) Maleimide:** 1,2-distearoyl-*sn*-glycero-3-phosphoethanolamine-N-[maleimide(polyethylene glycol)-2000]

Chemical Structure	Names
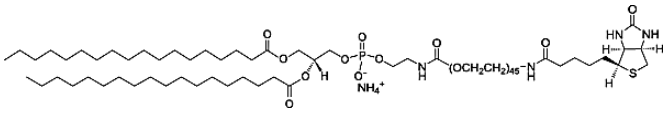	**DSPE-PEG(2000) Biotin:** 1,2-distearoyl-*sn*-glycero-3-phosphoethanolamine-N-[biotin(polyethylene glycol)-2000]
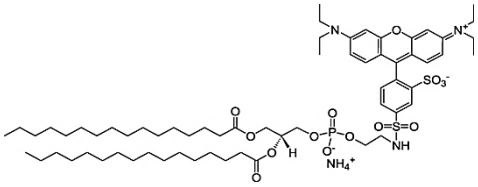	**Liss Rhod PE:** 1,2-dipalmitoyl-*sn*-glycero-3-phosphoethanolamine-N-(lissamine rhodamine B sulfonyl)
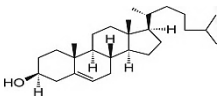	**Cholesterol**

Liposomes were prepared by the classical method of the lipid film hydration (Lasic, 1995). DSPC, Chol, DSPE-PEG_{2000}, DSPE-PEG_{2000}-mal, DSPE-PEG_{2000}-biot and Liss Rhod PE were dissolved in chloroform (Mw 119.38, Sigma-Aldrich), at the molar ratio of 52:45:3:0.015:0.015:0.01, and the solvent was evaporated to dryness with a nitrogen stream in a rotary evaporator. The resultant dried lipid film was dispersed in PBS buffer, pH

7.4 (phosphate buffered saline, 10 mM phosphate buffer, 2.7 mM potassium chloride and 137 mM sodium chloride, Sigma-Aldrich) with a final lipid concentration of 0. 8 mM and the mixture was vortexed to yield MLVs. In order to obtain LUVs, the suspension was subjected to 10 freezing/unfreezing cycles, followed by extrusion 13 times through a polycarbonate filter with a pore diameter of 200 nm, 100 nm and finally 50 nm at RT.

5.2.2. Conjugation of antibodies

The mAb for transferrin BBB receptors, OX-26 mAb, was obtained from AbD Serotec and the mAb for amyloid beta peptide, 19B8, was purchased from Abcam.

Covalent coupling methods for attaching the antibodies at the PEG terminus by using functionalized PEG with a chemically reactive end-group were applied. Two activated PEG molecules, the PEG-maleimide (thiol reactive) and a PEG-biotin (biotin–streptavidin), were used as two different antibodies were coupled to the systems. For the maleimide-mAb conjugation, the target was activated by a twenty times molar excess of Traut's reagent (2-iminothiolane hydrochloride, MW 137.73, Sigma-Aldrich). A drop of EDTA (ethylenediaminetetraacetic acid, MW 292.40, Sigma-Aldrich) 0.28 M was added to prevent metal catalyzed oxidation of sulfhydryl groups (Hermanson, 1996). To remove the unreacted EDTA/2-iminothiolane complexes, size exclusion chromatography was applied using a Sephadex column *PD-Mini Trap G25* (GE Healthcare) (Markoutsa, 2012).

The second mAb was firstly coupled to a biotin molecule using the EZ-Link micro sulfo NHS-LC-biotin (Thermo Scientific) kit. To link this mAb to the functionalized PEG-biotin, a molar ratio of 1:1 of streptavidin

(from *Streptomyces avidinii*, Sigma-Aldrich) was previously added to the liposomes.

Both antibodies were added to the liposomes at a molar ratio of 1:1 between antibodies and functionalized PEG. Each antibody was incubated at RT for 1 hour and then at 4 °C during 8 hours.

The affinity of the immunoliposomes for transferrin or Aβ was analyzed by the enzyme-linked immunosorbent assay (ELISA). The surface of a 96 well plate (flat-bottom Nunc MaxiSorp®) was coated with TfR (Abcam) and Aβ (β-Amyloid (1-42) Human, purity >95%, GenScript) during 1 hour at 37 °C. After the block with the BSA (bovine serum albumin, ~ 66 kDa) the immunoliposomes were added to each well and a period of incubation followed. After washing, the secondary antibody (Goat anti-Mouse IgG (H+L), Thermo Scientific-Pierce Antibodies), conjugated with peroxidase, reacted during 45 minutes at RT. To reveal the reaction, a citrate solution was used with citric acid (MW 210.14, Sigma-Aldrich), ABTS (2,2′-azino-bis(3-ethylbenzothiazoline-6-sulfonic acid) diammonium salt, MW 548.68, Sigma Aldrich) and H_2O_2 (hydrogen peroxide solution, MW 34.02, Sigma Aldrich). The intensity of the signal was measured by absorbance spectrometry at 405 nm using a Biotek Synergy 2 spectrometer. Liposomes without mAb were used as control.

5.2.3. Stability studies

The stability of the immunoliposomes was analyzed through the size and zeta potential variation. The size of the immunoliposomes was measured by dynamic light scattering (DLS) technique at RT. Zeta potential was also measured for the same samples by the laser doppler velocimetry method. The measurements were performed in a Malvern Zetasizer instrument.

5.2.3.1. Zeta potential

The electric potential at the shear plane is called zeta potential. The net charge density on a particle in contact with an aqueous solution gives rise to an electrical double layer, comprised of a fixed layer which includes strongly adsorbed counterions at specific sites on the surface and an outer, diffuse layer composed of counterions whose distribution is determined by a balance of electrostatic forces and random thermal motion. In the presence of an applied electric field, each particle (and strongly adsorbed ions) moves with respect to the medium. Between the two phases there is a shear plane, i.e. the hypothetical boundary between the particle with its ion atmosphere and the surrounding medium.

The zeta potential of dispersed colloidal particles can be measured by electrophoresis. The electric force causes the particle to move in relation to a stationary liquid at a constant velocity. The ratio of the velocity to the electric field E is the electrophoretic mobility, μ_E.

The mobility is converted into zeta potential, ζ, using the Smoluchowski equation 5.1:

$$\zeta = \frac{\eta \mu_E}{\varepsilon} \tag{5.1}$$

where η is the viscosity of the solution and ε is the permittivity of the solution.

5.2.3.2. Dynamic light scattering

DLS, also referred to as quasi-elastic light scattering, enables the determination of particle size and size distribution in dispersions. The method is based on the fluctuations in the intensity of light scattered by a

small volume of a solution in the microsecond time range which are directly related to the Brownian motion of the solute (Berne, 1976). Submicrometer size particles in suspension exhibit significant random motion because of collisions with the molecules of the surrounding liquid medium (Brownian motion). As a result, when light irradiates a colloidal dispersion, the phases of the scattered waves fluctuate randomly in time. The scattered light intensities from individual particles interfere with each other, and hence the net intensity of the scattered light fluctuates randomly in time. The time dependence of the intensity fluctuations, calculated from the autocorrelation function of the scattered intensity, can be related to the diffusion coefficient of the particles. For a monodisperse system, the normalized autocorrelation function, $g^{(1)}$, is an exponential decay,

$$g^{(1)}(t') = exp(-\Gamma t') \tag{5.2}$$

where t' is the decay time of the autocorrelation function, Γ is the decay constant, which is related to the diffusion coefficient D by

$$D = \frac{\Gamma}{q^2} \tag{5.3}$$

where q is the scattering wave vector, which depends on the wavelength of the light source, λ, the solvent refractive index, n, and the angle of detection, θ.

$$q = \frac{4n\pi}{\lambda} sin\frac{\theta}{2} \tag{5.4}$$

The hydrodynamic averaged intensity radius of the particles, R_H, can be calculated from the diffusion coefficient D, using the Stokes-Einstein relation

$$R_H = \frac{k_B T}{6\pi\eta D} \tag{5.5}$$

where k_B is the Boltzmann constant, T the absolute temperature and η is the viscosity of the medium. This relation is the basis of the particle size determination by dynamic light scattering, but it is valid only for monodisperse particles.

5.2.4. Uptake assays

PBCECs were incubated in Plating-Medium (Earls Medium 199 supplemented with L-Glutamine (0.7mM), penicillin/streptomycin (1%), gentamicin (1%) and new-born calf serum, all the compounds are purchased at Biochrom) in a 96 well plate (Corning) previously coated with Collagen G (Biochrom). After 48 hours incubation at 37 °C, the culture medium was replaced. Normally, apparent confluence of the monolayers was reached after 4 days (approximately 6-8 x10^4 cells per well). At day 4 the medium was replaced by a solution of KRB (composed by NaCl (sodium chloride p. A., Mw 58.44, AppliChem), KCl (potassium chloride, Mw 74.56, AppliChem), H_2KO_4P (potassium dihydrogen phosphate p.A., Mw 136.09, AppliChem), HEPES (hepes puffedran ≥ 99.5%, p.A., Mw 238.31, ROTH), D-Glucose (D(+)-glucose anhydrous for biochemistry, Mw 180.16, MERCK), $MgCl_2.6H_2O$ (magnesium chloride hexahydrate p.A., Mw 203.30, AppliChem) and $CaCl_2.2H_2O$ (calcium chloride dehydrate p.A., Mw 147.02, AppliChem)) in the presence of different liposomes concentration.

The liposomes were incubated with the cells for 2 hours. After removal of the liposome suspension by aspiration, the cells were rinsed three times with medium at 4 °C, then washed with an acid buffer pH 3 (26 mM $C_6H_2Na_3O_7.2H_2O$ (sodium citrate, Mw 294.10, Sigma), 9.2 mM

$C_6H_8O_7.H_2O$ (citric acid monohydrated, Mw 210.14, Grussing), 90.1 mM NaCl and 30 mM KCl) for 5 minutes followed by washing with KRB at 4 °C. The supernatant was discarded and the cells were lysed with a 1% triton solution for one hour at 65 °C. Fluorescence was detected with a Fluoroskan Ascent (Labsystems).

5.2.5. *in vivo* assays

Animal studies were performed with male Wistar rats (body weight 200 g). Animals were maintained under standard conditions and were allowed access to food (V1534-000 R/M-H, Ssniff, Soest, FRG) and water in agreement with animal protection standards. All animal experiments were permitted by and followed the guidelines of the local authorities (Regierungsprasidium Karlsruhe, Germany). The nanoparticles were suspended in PBS to a final concentration of 1.25 mg/mL and 0.8 mL of the solution was administered into the tail vein. After 2 h, 4 h and 6 h the animals were killed by cervical dislocation and the brains were removed and further studied after cryosection. Usually, 2 animals were used for each time point. Three animals received PBS to use as a control. Brain tissue was cut on a cryostat CM 3050 Leica, Bensheim, FRG) and the tissue slices were thaw-mounted onto surface treated glass slides (Superfrost plus, Fisher, Pittsburgh, PA, USA). Brain slices were analyzed by confocal laser scanning microscopy (CLSM) with a TCS SP5 II (Leica Microsystems, Germany).

5.2.5.1. Confocal Laser Scanning Microscopy

CLSM is a microscopy technique for obtaining high-resolution optical images of serial optical sections of the materials.

The analysis of only a single focal plane of the specimen at a time is possible because of a pinhole placed in front of the detector, which filters the reflected light that comes from the specimen. The pinhole has a rather narrow aperture, so only the light from the microscope focal plane is able to pass through it, and consequently hit the detector and be imaged. The detector images a single point at a time. The light that comes either from above or below the focal plane is physically blocked by the pinhole. This enables the in-depth analysis of thick specimens (Sheppard, 1997).

The light source consists of a laser beam, directed towards an objective which focuses this light to a single point in a given focal plane of the specimen. Two galvanometric scanners deflect the laser beam in the X and Y directions, thus enabling the line-by-line scanning of the specimen. The microscope stage is moved up and down by a computer-controlled fine-step motor, allowing the focal plane to be selected.

When the light hits the specimen, it excites fluorescence, and this radiation is collected by the objective, and directed towards the detector through a dichroic beam splitter. The intensity of that fluorescent light is directly proportional to the intensity of the resulting pixel.

The use of a laser beam as a source of light and a photomultiplier as a detector allows one to perform a point wise illumination of the specimen, and to obtain a significant output signal even if the amount of light in the final image is reduced due to the confocal filtering.

5.2.6. Peptide encapsulation

The β-sheet breaker peptide LPFFD, conjugated with a fluorophore (5-FAM-(Leu)-(Pro)-(Phe)-(Phe)-(Asp)), purity 98.9%, MW 994.04, GenScript) was encapsulated in the immunoliposomes. For an efficient peptide encapsulation, dried lipid film was hydrated with an aqueous

solution containing the peptide with molar ratios of 16:1 and 10:1 (phospholipids:peptide). To study the efficiency of encapsulation, a Sephadex column PD-Midi Trap G25 (GE Healthcare) was used to separate the encapsulated peptide from the free molecules. After this separation, liposomes were burst with water:ethanol in a 25:75 (v/v) proportion and their fluorescence was measured (Spectrofluorometer FP-6500).

The encapsulation efficiency was calculated based on equation 5.6.

$$\text{Encapsulation efficiency (\%)} = \frac{\text{Encapsulated drug (mg)}}{\text{Total drug in solution (mg)}} \text{ x } 100 \qquad (5.6)$$

5.2.7. Phase transition studies

Lipid phase transitions in biological media are correlated to discontinuities or anomalies in macroscopic physical properties such as the stability, fluidity or permeability of membranes which are closely dependent on their phase transition temperature (Mouritsen, 1995). A liposome becomes highly permeable near the gel to crystalline phase transition temperature of its membrane (Papahadjopoulos, 1973). This shape alteration induced by the phase transition was correlated with the refraction and absorption coefficients of the aqueous dispersion. In light scattering terms, the measured count rate (average number of photons detected per second) can change for any of the following reasons: alterations in the structure (i.e. refractive index) of the particle membrane, alterations in the size of the particles and alterations in the concentration of the particles (Michel, 2006).

The phase transition temperature of the liposomes was studied by the analysis of the mean count rate (Michel, 2006) with a BI-MAS DLS instrument (Brookhaven 189 Instruments, USA). The study was done in a

temperature range between (20.0 ± 0.1)°C and (70.0 ± 0.1)°C, with intervals of 1.0 ± 0.1°C and with an equilibration period of 2 minutes. At each temperature 4 runs of 2 min were performed. In order to use the photon count rate within the recommended range (250-500 kcps), liposomes were diluted, so as to have a final sample concentration of 500 μM and the liposomes loaded with peptide were prepared with a molar ratio of 16:1 (phospholipid:peptide).

5.2.8. Release studies

Drug release experiments of the peptide encapsulated into the LUVs were run using a dialysis membrane (Float-A-Lyzer G2, CE, 100 KDa, SpectrumLabs). The membranes were washed in ultrapure water for 12 hours before being used and equilibrated with buffer 1 hour before the dialysis with PBS buffer as the receiving phase. A volume of 2 mL from the immunoliposomes suspension was added to the membrane and the outside space was filled with 6 mL of buffer. The dialysis membrane was kept in continuous stirring at 200 rpm at 4 °C simulating the production of the carriers and at 37 °C simulating the physiological temperature. At different time intervals, samples were collected from the outside medium and the same volume of fresh release medium was added. The amount of released peptide was determined by fluorescence (Spectrofluorometer FP-6500). The percentage of peptide released at each time is then calculated from the Equation 5.7.

$$\text{Peptide released at time t (\%)} = \frac{[\text{peptide}]_t}{[\text{peptide}]_{total}} \times 100 \qquad (5.7)$$

where the $[peptide]_t$ is the peptide concentration at each measuring time and $[peptide]_{total}$ is the concentration of the encapsulated peptide at initial time.

5.3. Results and Discussion

5.3.1. Conjugation of antibodies

During these experiments four types of liposomes were developed. As a control, pegylated liposomes without mAb were prepared. The first study consisted in coupling just one type of mAb (OX-26) to the surface of the liposomes. To test the influence of the distance between the liposome surface and the mAb, two other systems were designed. One of them has the OX-26 linked to biotin-streptavidin, which makes it more available. The other system has the same mAb but connected to a maleimide group, which could decrease the distance between the mAb and the liposome surface, due to the different lengths of the ligands, and thus make the mAb more hidden (Figure 5.1).

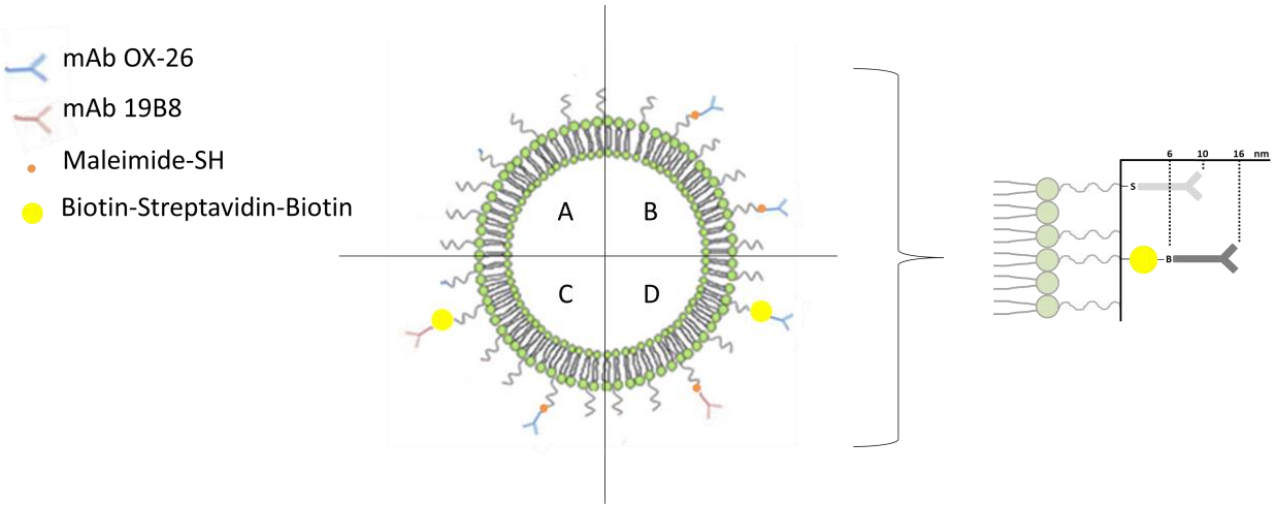

Figure 5. 1 - Schematic representation of the developed systems: A) pegylated liposomes; B) pegylated liposomes coupled with OX-26 through PEG-maleimide; C) pegylated liposomes coupled with two different mAb, OX-26 through PEG-maleimide and 19B8 through PEG-Biotin; and D) pegylated liposomes coupled with two different mAb, OX-26 through PEG-Biotin and 19B8 through PEG-maleimide.

The binding of the mAb to the nanocarriers was determined by ELISA. Significantly higher absorbance at 405 nm was observed with immunoliposomes. The control used in these assays exhibited significantly lower absorbance (0.27±0.03) when compared with the liposomes conjugated to the mAb OX-26 (0.68±0.04). Also, both pegylated liposomes coupled with two different mAb by different methods, had a positive reaction for OX-26 (0.70±0.03) and for 19B8 (0.69±0.05). Therefore, the bioactivity of the mAb used was validated by this assay: OX-26 mAb maintains its reactivity for transferrin receptor and 19B8 mAb for Aβ peptide monomers. It was also verified that 19B8 mAb has affinity for oligomers (considered to be the most toxic species of Aβ peptide).

The number of mAb conjugated on each liposome was further calculated based on the assumption that liposomes with a diameter of 100

nm contain about 100000 molecules of phospholipids (Hansen, 1995). As the prepared liposomes present a hydrodynamic diameter around 95 nm, the number of phospholipids estimated was 95000. Assuming this number, the liposomes that have just one type of antibody it will have approximately 15 OX-26 mAb molecules. In the case of the immunoliposomes containing the two mAb, they have a totally of about 30 mAb molecules (15 of the 19B8 mAb and 15 of OX-26 mAb). Interestingly, this optimal number of 30 mAb per liposome was also observed in experiments where pulmonary endothelial cells were targeted *in vivo* using mAb conjugated liposomes (Maruyama, 1995; Schnyder, 2005).

It has been proved previously that thiolation of mAb does not interfere with their binding site (Pardridge, 1995). Though maleimide group when in contact with water could be hydrolyzed, so it is essential to add the antibodies immediately after the liposome preparation.

5.3.2. Stability studies

The liposome size was determined after each step of preparation. The mean diameter and vesicle size distribution were used as an indication of sample aggregation and stability. Carriers were prepared by repeated extrusion processes through polycarbonate filter membranes with a final pore size of 50 nm. By this method, an average diameter of the liposomes was obtained with a sharp distribution of dimension (table 5.2).

For the immunoliposomes with one mAb type, the size increased of about 15 nm, which is the approximately diameter of the globular mAb (Dammer, 1996). This result also confirms an efficient conjugation. In the case of the two-mAb coated immunoliposomes, the same increase was observed with the addition of the first mAb. The second step in the preparation of this system was the addition of streptavidin that does not

change significantly the NPs size. The absence of a fluctuation in the dimension could be explained by the smaller size of streptavidin molecule comparatively to the mAb that was added first to the liposome and by its conjugation to biotin (Figure 5.1). In the last step of this procedure the second mAb causes also a rise of about 15 nm (Table 5.2).

Table 5.2 - Mean diameter, polydispersity index (PI) and zeta potential of the immunoliposomes at each step of their preparation.

Particle	*Mean diameter (nm)*	*PI*	*Zeta Potential (mV)*
Pegylated liposomes	95.2 ± 0.8	0.07 ± 0.01	0.7 ± 0.4
Pegylated liposomes with one mAb	107 ± 4	0.19 ± 0.01	-2.0 ± 0.3
Pegylated liposomes with one mAb and streptavidin	106 ± 4	0.17 ± 0.01	-2.7 ± 0.1
Pegylated liposomes with two mAb	114 ± 1	0.20 ± 0.01	-2.6 ± 0.2

In order to study the stability of the liposomes over time, their size was measured during 2 months. Over this time, there were no significant variations on these parameters, which indicate that the liposomes are stable. Changes in the size and zeta potential values means that the structures of liposomes rearrange, i.e., the structures will be different from the initial ones and the liposomes will lose their stability (Mason, 2003). It is very important to certify that the vesicles are not aggregated, since the size and stability of immunoliposomes are critical for their cell internalization. Besides, aggregation could result in a decrease of the

antibody density on the vesicles. Nonetheless, even with the highest antibody density, the vesicle diameters are <200 nm, which is the size required for targeting (Markoutsa, 2011a).

The addition of the mAb to the liposomes does not significantly affect their zeta potential. Although a smaller variation to a negative value was verified due to the negative nature of the immunoglobulins.

5.3.3. Uptake assay

Current most common method for modeling the BBB penetration includes the use of cultured endothelial cells *in vitro*. In this study the PBCECs were used to mimic the endogenous microvascular endothelial cells due to their expression of tight junctions proteins (Brown, 2007). The *in vitro* cell uptake index of liposomes was studied with 2 h incubation time at 37 °C. The relative uptake efficiency was calculated by dividing the uptake amount of NPs in contact with the cells during the 2 hours incubation, by the initial concentration of liposomes.

As shown in figure 5.2, when the amount of immunoliposomes incubated with cells increases, the vesicle uptake percentage decreases, which indicates a concentration-dependent mechanism. Control vesicle (pegylated liposomes with no antibody attached) uptake by PBCECs is substantially lower (2.7±0.2% at 160 μM and 2.3±1.6% at 60 μM) comparatively to the uptake of liposomes B (4.0±0.8% at 160 μM and 6.4±2.4% at 60 μM) and D (7.3±0.7% at 160 μM and 15.4±1.4% at 60 μM), which confirms that OX-26 increases the liposome uptake by the endothelial cells from BBB. The presence of the antibody at the liposome surface allows, its uptake by receptor-mediated transport which is more selective and efficient than the simple diffusion used by the control liposomes. This phenomenon is well observed for the concentration of 60

μM. A difference between the three types of carriers at 200 μM is not verified. These results suggest a saturation in the cells when in contact with the liposomes at higher concentrations, since a similar uptake was verified for liposomes A, B and D (3.1±0.8%, 3.9±0.6% and 4.0±1.2%, respectively).

Additionally, the liposomes D have a higher uptake than the liposomes B for the two lowest concentrations. This difference could be explained by the higher availability of OX-26 in the liposomes D, due to the presence of a streptavidin molecule that can work as a spacer in addition to its ligand function. Furthermore, it is known that an increase in the surface density of liposomes will imply a higher uptake (Markoutsa, 2011a).

In contrast with liposomes D, the uptake of liposomes C was very low (0.6±0.4% at 200 μM, 0.5±0.2% at 160 μM and 0.4±0.3% at 60 μM). The difference in the design of these liposomes is based on the different methods of conjugation used to couple the two types of antibodies. OX-26 is more available to the transferrin receptors when linked by biotin-streptavidin method. In the liposomes C the anti-transferrin receptor antibodies were bound through the thiol-maleimide conjugation. The addition of molecules of streptavidin and a second antibody to these liposomes could prevent the binding of OX-26 to its ligand and interfere with their uptake by receptor-mediated transport. Although their transport by simple diffusion is also not verified like in liposomes A. This may be explained by the negative nature of the liposomes C in contrast liposomes A are zwitterionic. A negative repulsion between the cellular membrane and liposomes C could be occurring.

These results demonstrated that immunoliposomes with the two mAb OX-26 and 19B8 can be an effective carrier for brain drug delivery, since they are internalized by BBB model cells.

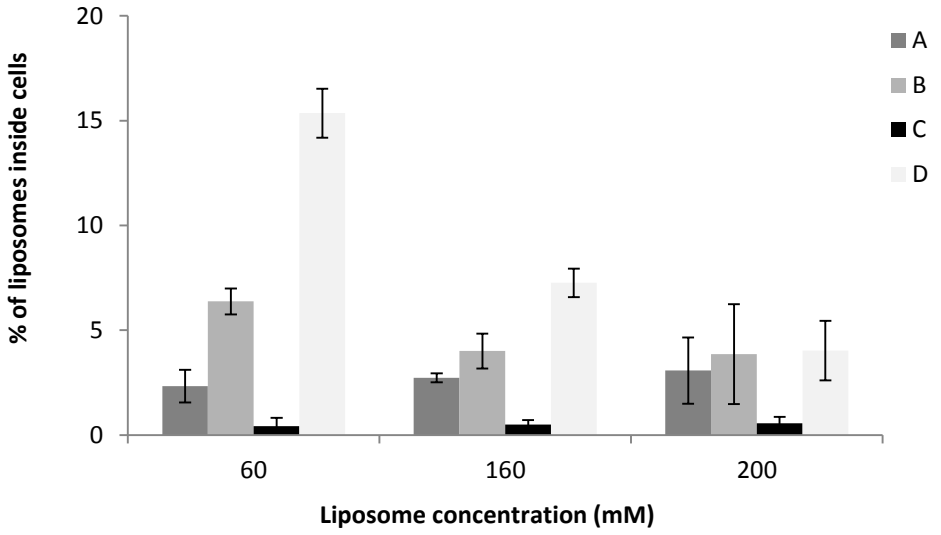

Figure 5.2 - Concentration-dependent uptake of liposomes by PBCECs. Data are the mean of three assays and respectively standard deviation. The liposomes used are: A) pegylated liposomes; B) pegylated liposomes coupled with OX-26 through PEG-maleimide; C) pegylated liposomes coupled with two different mAb, OX-26 through PEG-maleimide and 19B8 through PEG-Biotin; and D) pegylated liposomes coupled with two different mAb, OX-26 through PEG-Biotin and 19B8 through PEG-maleimide.

5.3.4. *in vivo* assays

To evaluate the capability of the liposomes to permeate the BBB, brain slices of rats treated with the immunoliposomes were observed by CLSM. Figure 5.3 shows the cryosections of the rats' brains. All of the sections were performed in the cortex of the brains. The nucleus were marked with 4',6-diamidino-2-phenylindole (DAPI). Distinct signals can be seen in the blue channel images (Figure 5.3), which coincide with the pattern of the stained nucleus of cells that can be clearly observed.

The first row shows the brain section of a rat that was treated only with PBS buffer. These sections serve as a negative control to ensure that the anesthesia and sacrifice do not leave any red fluorescing traces, which could be mistaken as fluorescing liposomes.

Further, brains of the rats injected with liposomes were also observed. The fluorescence from the rhodamine fluorophore present in the liposomes is clearly visible in all the section. The images from the brain with liposomes coupled with mAb show, however, higher fluorescence than the images of liposomes not coated with mAb. These results show higher uptake when the liposomes are coupled with mAb, and are in agreement with the results obtained in the *in vitro* assays.

The present study suggests that the circulation time that is reported herein (2 hours) is sufficiently long enough to detect BBB permeation and the concentration is maintained constant during 6 hours.

Thus, it can be concluded that the particles are located in the brain tissue confirming the resistance of the liposomes to the immune system.

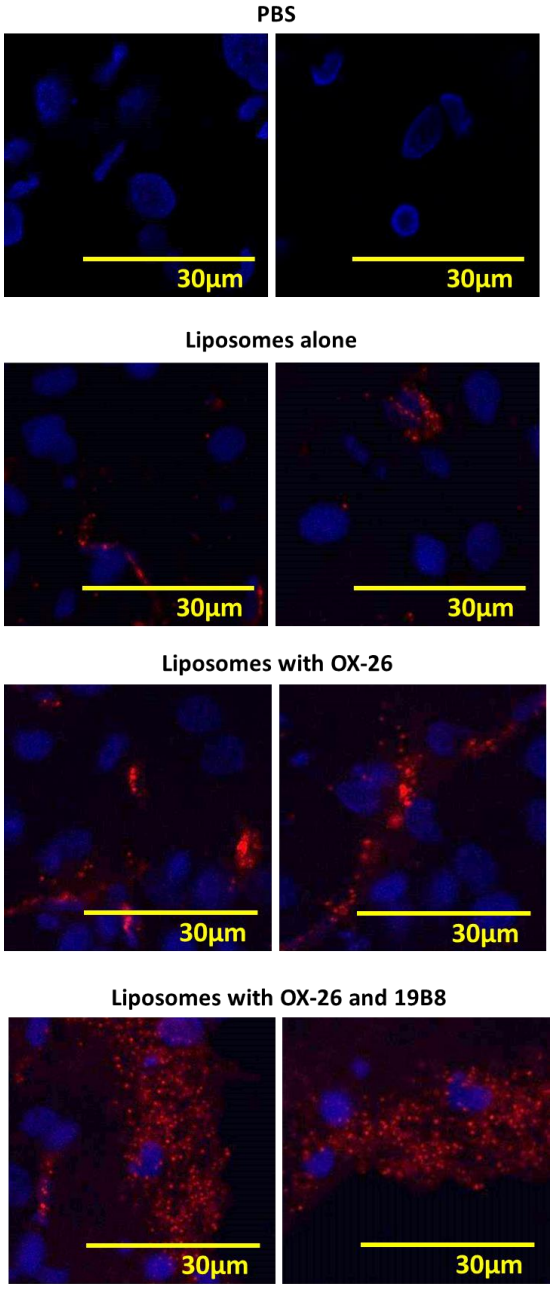

Figure 5.3 - Cryosections of the rat brains after administration of immunoliposomes. The top image shows the brain section without prior application of liposomes (only PBS buffer). Cell nucleus is labeled with DAPI. The scale bars represent 30 µm.

5.3.5. Peptide encapsulation

The peptide LPFFD binds to Aβ peptide and blocks the interaction between monomers and oligomers inhibiting the formation of fibrils. Despite this therapeutic effect, the peptide is rapidly degraded by enzymes. To circumvent this problem, the peptide was encapsulated in the liposomes described above.

The encapsulation efficiency was not significantly different between two different peptide concentrations. For a molar ratio of 16:1 (peptide:lipid; final peptide concentration of 50 μM) 93±1% of peptide was encapsulated. Similarly, the encapsulation efficiency in liposomes with a ratio of 10:1 (peptide concentration of 75 μM) was 92.5±0.1%. As these values are identical, a ratio of 16:1 was used in the follow experiments.

5.3.6. Phase transition studies

The evaluation of the main phase transition temperature (T_m) of the liposomes and the effect of the peptide loading were based on the change of the mean count rate. Discontinuity in the mean count rate, as the temperature is altered corresponds to a change in the optical properties of the material studied, arising from a transition from an initial state to another (Michel, 2006). The main phase transition and cooperativity (B) were determined, by adjusting a non-linear curve fit to the obtained sigmoidal profile, as elsewhere described (Pinheiro, 2013a; Pinheiro, 2013b).

The mean count rate dependence with temperature for the liposomes with the peptide encapsulated is shown in Figure 5.4.

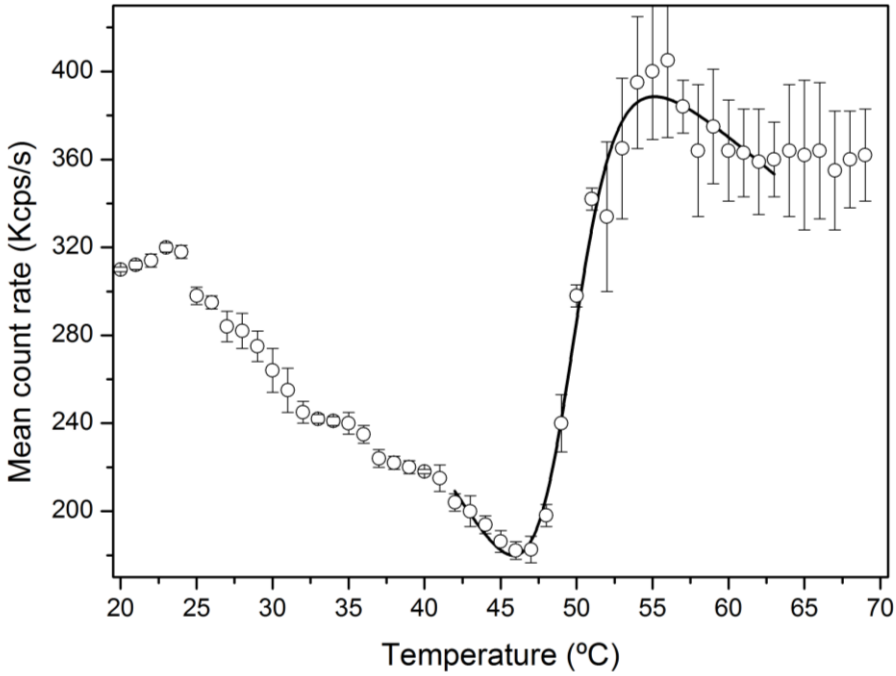

Figure 5.4 - Average count rate of liposomes loaded with the peptide (16:1) as a function of temperature. Continuous line is the best-fit curve.

In Table 5.3 the obtained values for the biophysical parameters are depicted: T_m and B of liposomes in the absence and in the presence of the peptide.

Table 5.3 - Values of main phase transition temperature (T_m) and cooperativity (B) obtained for liposomes (500 µM, pH 7.4) in the absence and in the presence of peptide (16:1).

	T_m (°C)	Cooperativity - B
Liposomes	51±1	579±99
Liposomes with peptide	49.6±0.1	1105±64

The analysis of Table 5.3 reveals that the T_m is slightly reduced by the presence of the peptide and the cooperativity (B) is increased. These two results point to a location of the peptide closer to the head group region (Grancelli, 2002).

5.3.7. Release studies

The size, solubility, composition and biodegradation of the nanoparticle matrix are the main factors that affect the release rate of a drug from nanocarriers (Kumari, 2010). Besides, a time compromise in the drug release profile is needed, since if the peptide-loaded liposomes present a too high stability, the drug liberation will not occur when the systems reach the active site, and if the drug is not well entrapped, it can lead to premature and not favorable peptide release.

The dialysis method was used to evaluate the release profile of LPFFD when free and encapsulated in liposomes. These release experiments were carried out in PBS (pH 7.4) at 4 °C and at 37 °C.

Release experiments provide a guidance to predict the possible release profile of the drug when in the designed drug carriers. The *in vitro* peptide release profile loaded in liposomes showed a regular pattern with a continuous burst release of the drug. As shown in figure 5.5, at 37 °C, in the first 12 h the 5-FAM-LPFFD was released from the carriers in a percentage of approximately 60%. After 22 h, the release of the peptide reached a percentage of cumulative release of around 80%.

In order to evaluate if the immunoliposomes preparation process influences the drug release, a study at 4 °C during 8 hours (that are the conjugation conditions) was performed. This conditions correspond to the ones necessary for an efficiently conjugation between mAb and liposomes. As seen in the figure 5.5, after 8 h under continuous agitation, about 7% of

peptide was released from the liposomes. Such results indicate that during the carriers' production the percentage of drug lost is very low which makes them a good vehicle to transport LPFFD, since its liberation is favored at 37 °C (physiological temperature).

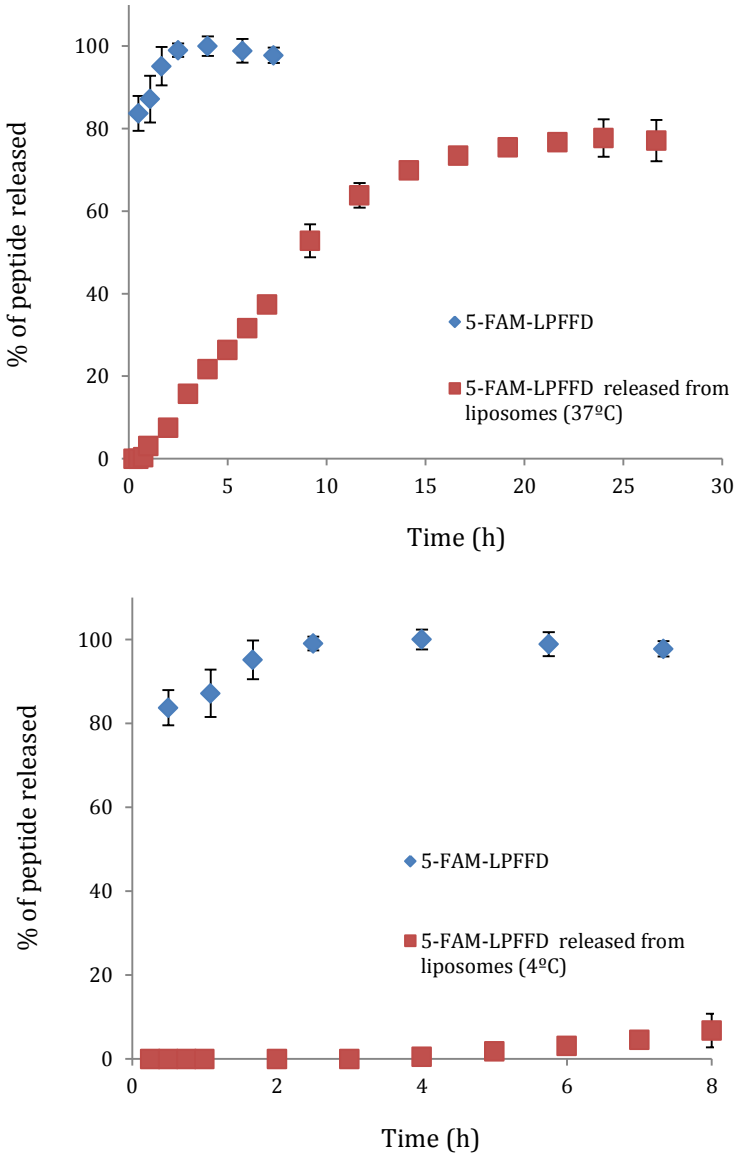

Figure 5.5 - The *in vitro* release of 5-FAM-LPFFD from liposomes under PBS buffer, pH 7.4, at 4°C and 37°C.

Zhang et *al.* showed that anionic charged immunoliposomes (composed by 1-palmitoyl-2-oleoyl-sn-glycerol-3-phosphocholine, didodecyldimethylammonium bromide, distearoylphosphatidylethanolamine-PEG_{2000}) targeted with either the OX-26 mAb or the mouse IgG2a antibody are transported intact across the BBB (Zhang, 2003). In another study, Cerletti et *al.* developed an OX-26 immunoliposome (composed of distearoylphosphatidylcholine cholesterol, distearoylphosphatidylethanolamine-PEG_{2000}) and performed *in vitro* studies using immortalized rat brain capillary endothelial RBE4 cells. Liposomes with the specific antibody were taken up by the cells, and were concentrated in distinct intracellular compartments such as endosomes or lysosomes. During prolonged incubation times, however, endosomal release of the liposomal cargo into the cytosolic compartment can be observed (Cerletti, 2000; Markoutsa, 2011b; Roux, 2005). Shi et *al.* studied the mechanisms of interaction between the BBB and liposomes coupled with OX-26 mAb. According to the authors, pegylated immunoliposomes (1-palmitoyl-2-oleoyl-*sn*-glycerol-3-phosphocholine, didodecyldimethylammonium bromide, distearoylphosphatidylethanolamine-PEG_{2000}) first undergo RMT across the BBB *in vivo,* owing to expression of the TfR at the BBB surface (Huwyler, 1998), and then undergo receptor-mediated endocytosis into neurons within the brain, owing to the expression of the TfR on the neuronal plasma membrane (Mash, 1990). The BBB TfR is a bidirectional transcytosis system (Zhang, 2001), and mediates the transport of the system through the endothelial barrier into the brain interstitial space. The phospholipids forming the liposome fuse with the intracellular endosomal membrane subsequent to endocytosis and release the drug into the cytosol of the target cell (Mok, 1999; Shi, 2001).

Also, liposomes (composed by 1-palmitoyl-2-oleoyl-sn-glycerol-3-phosphocholine, dimethyldioctadecylammonium bromide,

distearoylphosphatidylethanolamine-PEG2000) coupled to a mAb to the mouse TfR, to target the BBB and with a second mAb against the human insulin receptor, to target intracranial human U87 glioma showed promising results (Boado, 2011; Zhang, 2004).

Liposomes functionalized with two types of antibodies are promising systems for brain drug delivery because they are capable of crossing the BBB and recognize the site of action.

References

Berne, Bruce J.; Pecora, Robert - Dynamic light scattering : with applications to chemistry, biology, and physics. New York: Wiley, 1976. 0471071005.

Boado, R. J.; Pardridge, W. M. **2011.** The Trojan Horse Liposome Technology for Nonviral Gene Transfer across the Blood-Brain Barrier. *J Drug Deliv*. Vol. 2011. p. 296151.

Brown, R. C.; Morris, A. P.; O'Neil, R. G. **2007.** Tight junction protein expression and barrier properties of immortalized mouse brain microvessel endothelial cells. *Brain Res*. Vol. 1130. n.° 1. p. 17-30.

Cerletti, A.; Drewe, J.; Fricker, G.; Eberle, A. N.; Huwyler, J. **2000.** Endocytosis and transcytosis of an immunoliposome-based brain drug delivery system. *J Drug Target*. Vol. 8. n.° 6. p. 435-46.

Dammer, U.; Hegner, M.; Anselmetti, D.; Wagner, P.; Dreier, M.; Huber, W.; Guntherodt, H. J. **1996.** Specific antigen/antibody interactions measured by force microscopy. *Biophys J*. Vol. 70. n.° 5. p. 2437-41.

Grancelli, A.; Morros, A.; Cabanas, M. E.; Domenech, O.; Merino, S.; Vazquez, J. L.; Montero, M. T.; Vinas, M.; Hernandez-Borrell, J. **2002.** Interaction of 6-fluoroquinolones with dipalmitoylphosphatidylcholine monolayers and liposomes. *Langmuir*. Vol. 18. n.° 24. p. 9177-9182.

Hansen, C. B.; Kao, G. Y.; Moase, E. H.; Zalipsky, S.; Allen, T. M. **1995.** Attachment of antibodies to sterically stabilized liposomes: evaluation, comparison and optimization of coupling procedures. *Biochim Biophys Acta*. Vol. 1239. n.° 2. p. 133-44.

Hermanson, Greg T. - Bioconjugate techniques. San Diego: Academic Press, 1996.

Huwyler, J.; Pardridge, W. M. **1998.** Examination of blood-brain barrier transferrin receptor by confocal fluorescent microscopy of unfixed isolated rat brain capillaries. *J Neurochem*. Vol. 70. n.° 2. p. 883-6.

Immordino, M. L.; Dosio, F.; Cattel, L. **2006.** Stealth liposomes: review of the basic science, rationale, and clinical applications, existing and potential. *Int J Nanomedicine*. Vol. 1. n.° 3. p. 297-315.

Kumari, A.; Yadav, S. K.; Yadav, S. C. **2010.** Biodegradable polymeric nanoparticles based drug delivery systems. *Colloids Surf B Biointerfaces*. Vol. 75. n.° 1. p. 1-18.

Lasic, D. D.; Needham, D. **1995.** The ''Stealth'' liposome: A prototypical biomaterial. *Chemical Reviews*. Vol. 95. n.° 8. p. 2601-2628.

Markoutsa, E.; Pampalakis, G.; Niarakis, A.; Romero, I. A.; Weksler, B.; Couraud, P. O.; Antimisiaris, S. G. **2011a.** Uptake and permeability studies of BBB-targeting immunoliposomes using the hCMEC/D3 cell line. *Eur J Pharm Biopharm*. Vol. 77. n.° 2. p. 265-74.

Markoutsa, E.; Pampalakis, G.; Niarakis, A.; Romero, I. A.; Weksler, B.; Couraud, P. O.; Antimisiaris, S. G. **2011b.** Uptake and permeability studies of BBB-targeting immunoliposomes using the hCMEC/D3 cell line. *European Journal of Pharmaceutics and Biopharmaceutics*. Vol. 77. n.° 2. p. 265-274.

Markoutsa, E.; Papadia, K.; Clemente, C.; Flores, O.; Antimisiaris, S. G. **2012.** Anti-Abeta-MAb and dually decorated nanoliposomes: effect of Abeta1-42 peptides on interaction with hCMEC/D3 cells. *Eur J Pharm Biopharm*. Vol. 81. n.° 1. p. 49-56.

Maruyama, K.; Takizawa, T.; Yuda, T.; Kennel, S. J.; Huang, L.; Iwatsuru, M. **1995.** Targetability of novel immunoliposomes modified with amphipathic poly(ethylene glycol)s conjugated at their distal terminals to monoclonal antibodies. *Biochim Biophys Acta*. Vol. 1234. n.° 1. p. 74-80.

Mash, D. C.; Pablo, J.; Flynn, D. D.; Efange, S. M.; Weiner, W. J. **1990.** Characterization and distribution of transferrin receptors in the rat brain. *J Neurochem*. Vol. 55. n.° 6. p. 1972-9.

Mason, J. M.; Kokkoni, N.; Stott, K.; Doig, A. J. **2003.** Design strategies for anti-amyloid agents. *Curr Opin Struct Biol*. Vol. 13. n.° 4. p. 526-32.

Michel, N.; Fabiano, A. S.; Polidori, A.; Jack, R.; Pucci, B. **2006.** Determination of phase transition temperatures of lipids by light scattering. *Chem Phys Lipids*. Vol. 139. n.° 1. p. 11-9.

Mok, K. W.; Lam, A. M.; Cullis, P. R. **1999.** Stabilized plasmid-lipid particles: factors influencing plasmid entrapment and transfection properties. *Biochim Biophys Acta*. Vol. 1419. n.° 2. p. 137-50.

Mouritsen, O. G.; Jorgensen, K. **1995.** Microscale, Nanoscale and Mesoscale Heterogeneity of Lipid Bilayers and Its Influence on Macroscopic Membrane-Properties. *Molecular Membrane Biology*. Vol. 12. n.° 1. p. 15-20.

Papahadjopoulos, D.; Jacobson, K.; Nir, S.; Isac, T. **1973.** Phase transitions in phospholipid vesicles. Fluorescence polarization and permeability measurements concerning the effect of temperature and cholesterol. *Biochim Biophys Acta*. Vol. 311. n.° 3. p. 330-48.

Pardridge, W. M.; Boado, R. J.; Kang, Y. S. **1995.** Vector-mediated delivery of a polyamide ("peptide") nucleic acid analogue through the blood-brain barrier in vivo. *Proc Natl Acad Sci U S A*. Vol. 92. n.° 12. p. 5592-6.

Pinheiro, M.; Arede, M.; Giner-Casares, J. J.; Nunes, C.; Caio, J. M.; Moiteiro, C.; Lucio, M.; Camacho, L.; Reis, S. **2013a.** Effects of a novel antimycobacterial compound on the biophysical properties of a pulmonary surfactant model membrane. *Int J Pharm*. Vol. 450. n.° 1-2. p. 268-77.

Pinheiro, M.; Arede, M.; Nunes, C.; Caio, J. M.; Moiteiro, C.; Lucio, M.; Reis, S. **2013b.** Differential interactions of rifabutin with human and bacterial membranes: implication for its therapeutic and toxic effects. *J Med Chem*. Vol. 56. n.° 2. p. 417-26.

Roux, F.; Couraud, P. O. **2005.** Rat brain endothelial cell lines for the study of blood-brain barrier permeability and transport functions. *Cell Mol Neurobiol*. Vol. 25. n.° 1. p. 41-58.

Schnyder, A.; Huwyler, J. **2005.** Drug transport to brain with targeted liposomes. *NeuroRx*. Vol. 2. n.° 1. p. 99-107.

Schnyder, A.; Krahenbuhl, S.; Torok, M.; Drewe, J.; Huwyler, J. **2004.** Targeting of skeletal muscle in vitro using biotinylated immunoliposomes. *Biochem J*. Vol. 377. n.° Pt 1. p. 61-7.

Sheppard, Colin; Shotton, David; Royal Microscopical Society (Great Britain) - Confocal laser scanning microscopy. Oxford, UK BIOS Scientific Publishers ; New York, NY, USA: Springer, 1997. 0387915141

Shi, N.; Boado, R. J.; Pardridge, W. M. **2001.** Receptor-mediated gene targeting to tissues in vivo following intravenous administration of pegylated immunoliposomes. *Pharm Res*. Vol. 18. n.° 8. p. 1091-5.

Wohlfart, S.; Gelperina, S.; Kreuter, J. **2012.** Transport of drugs across the blood-brain barrier by nanoparticles. *J Control Release*. Vol. 161. n.° 2. p. 264-73.

Zhang, Y. F.; Boado, R. J.; Pardridge, W. M. **2003.** Absence of toxicity of chronic weekly intravenous gene therapy with pegylated immunoliposomes. *Pharm Res*. Vol. 20. n.° 11. p. 1779-85.

Zhang, Y.; Pardridge, W. M. **2001.** Rapid transferrin efflux from brain to blood across the blood-brain barrier. *J Neurochem*. Vol. 76. n.° 5. p. 1597-600.

Zhang, Y.; Zhang, Y. F.; Bryant, J.; Charles, A.; Boado, R. J.; Pardridge, W. M. **2004.** Intravenous RNA interference gene therapy targeting the human epidermal growth factor receptor prolongs survival in intracranial brain cancer. *Clin Cancer Res*. Vol. 10. n.° 11. p. 3667-77.

Chapter 6

Concluding remarks

The reason why Aβ peptide forms amyloid fibrils *in vivo* is still not understood. Studies *in vitro* may provide important insights into the aggregation process of the peptide. However, the fast aggregation kinetics and the different aggregation stages of peptide samples contribute to the lack of uniform and concordant results. The use of surfactants may contribute to a better understanding of the peptide aggregation and above all may allow the study of the fibril formation at conditions that can easily be reproduced.

When Aβ peptide is in solutions of negatively charged SDS micelles and positively charged CTAC micelles, only small aggregates are observed, demonstrating the inhibition of Aβ fibrillogenesis. The same results are obtained in the presence of salt ions. But if SDS concentrations are below the critical micelle concentration (CMC), the monomers promote the peptide aggregation. These results indicate that charged surfactants interact with the peptide by electrostatic interactions and induce the exposure of the peptide hydrophobic parts promoting hydrophobic interactions between the Aβ monomers. The micelles also interact with the Aβ monomers by electrostatic interactions, but they surround the peptide and consequently induce an electrostatic repulsion between the complex peptide-micelle favoring a non-aggregated state. Notably, vesicles of negatively charged surfactants have a concentration-dependence effect

on $A\beta_{(1-42)}$ structure. The increase of surfactant concentration slows down the fibril formation.

The nonionic surfactant promotes the peptide aggregation below and above the CMC in Hepes and PBS buffer solution. The presence of hydrophobic surfactant monomers in solution may favor the hydrophobic interactions. On the other hand, when the nonionic surfactant is above the CMC and micelles are present in solution they act as inert bodies that work as nuclei of aggregation.

In the second part of the work beta-sheet breaker peptides were used as model molecules to study the effect of fluorination on the Aβ aggregation. Therefore, sequences that play an important role on Aβ amyloid fibril formation were modified with fluorine atoms. The results show that fluorination of hydrophobic amino acids such as valine or phenylalanine on sequences that interfere with Aβ amyloid fibril formation induce a significant delay on the peptide aggregation. This effect is likely a result of the interaction between the fluorinated amino acids and the hydrophobic residues of Aβ, which is strong enough to prevent the contact between Aβ molecules and thus to prevent the peptide aggregation. The fluorination of other amino acids or the modification of the fluorinated sequences with hydrophilic residues at different positions will contribute to better understand the interaction between Aβ and fluorinated peptides.

A novel brain drug delivery system is also proposed to delivery drugs to brain areas affected by amyloid deposits. Liposomes were functionalized with two types of antibodies, the OX-26, a well-known blood-brain barrier targeting molecule, and the 19B8, an antibody capable of recognizing the amyloid beta peptide. To access the use of these liposomes as future drug delivery systems, stability studies were performed and the results showed that the carriers are stable for a minimum period of two months. The uptake of the liposomes by porcine

brain capillary endothelial cells was concentration dependent, and liposomes with the antibody anti-transferrin receptor OX-26 were significantly better internalized than non-functionalized systems. Moreover, the results provide evidence that biotin-streptavidin method could be preferable to link the OX-26 over the covalent coupling method in the immunoliposomes containing two different antibodies. An increase of 13% in the uptake of liposomes was observed when both antibodies are present, when compared with common pegylated liposomes. The *in vivo* assays show that the nanocarriers tested can evade the immune system cells reaching the brain in large quantities. Thus, the modified liposomes could be a promising carrier for delivering therapeutic drugs to the central nervous system (CNS). The system could provide high encapsulation efficiencies (93%) of beta-sheet breaker peptides and also showed a sustained drug release. A significantly more effective brain delivery by biodegradable liposomes will allow the drug to reach the brain at sufficient doses, leading to a significantly improvement of the treatment strategies of Alzheimer´s disease.

List of Abbreviations

A	Amplitude
Aβ	Amyloid-beta
a.a.	Amino acids
AD	Alzheimer's disease
ApoE	Apolipoprotein E
APP	Amyloid precursor protein
ATP	Adenosine triphosphate
ATR	Attenuated total reflectance
AuNPs	Gold nanoparticles
BACE1	β-site amyloid precursor protein cleaving enzyme 1
BBB	Blood-brain barrier
BSA	Bovine serum albumin
CLM	Crystallization-like model
CLSM	Confocal laser scanning microscopy
CMC	Critical micelle concentration
CNS	Central nervous system
CTAC	Cetyltrimethylammonium chloride
DLS	Dynamic light scatering
DMSO	Dimethyl sulfoxide

DTGS	Deuterated triglycine sulfate detector
EDTA	Ethylenediaminetetraacetic acid
ELISA	Enzyme-linked immunosorbent assay
F_0	Baseline before aggregation
FTIR	Fourier-transform infrared
hCMECDE	Human endothelial cells
HFIP	Hexafluoro-2-propanol
IR	Insulin receptor
κ	Elongation rate constant
KRB	Krebs ringer buffer
LDL	Low density lipoprotein
mAb	Monoclonal antibody
MALDI	Matrix-assisted laser desorption/ionization
MCT	Mercury cadmium telluride detector
MUVs	Multilamellar vesicles
MW	Molecular weight
NPs	Nanoparticles
OG	Octyl β-D-glucopyranoside
P-gp	P-glycoprotein
PBCECs	Porcine brain capillary endothelial cells
PBS	Phospate buffered saline
PEG	Poly (ethylene glycol)

PI	Polydispersity index
RMT	Receptor mediated transport
RT	Room temperature
S_0	Singlet ground electronic state
S_1	Singlet first electronic state
S_2	Singlet second electronic state
SDS	Sodium dodecyl sulfate
SUVs	Small unimellar vesicles
$t_{1/2}$	Half completion of aggregation process
t_{so}	Half of the total fibril consumerism
t_{lag}	Lag time
T_m	Main phase transition temperature
TEM	Transmission electron microscopy
TFA	Trifluoroacetic acid
TfR	Transferrin receptor
ThT	Thioflavin T
TOF	Time-of-flight mass spectrometer
Traut's reagent	2-iminothiolane hydrochloride
UV	Ultraviolet
v_{so}	Aggregation rate

List Amino Acids

A.a.	Abbreviation	Polarity	Charge (pH 7.4)
Alanine	A	nonpolar	neutral
Arginine	R	Basic polar	positive
Asparagine	N	polar	neutral
Aspartic acid	D	acidic polar	negative
Cysteine	C	nonpolar	neutral
Glutamic acid	E	acidic polar	negative
Glutamine	Q	polar	neutral
Glycine	G	nonpolar	neutral
Histidine	H	Basic polar	positive(10%) neutral(90%)
Isoleucine	I	nonpolar	neutral
Leucine	L	nonpolar	neutral
Lysine	K	Basic polar	positive
Methionine	M	nonpolar	neutral
Phenylalanine	F	nonpolar	neutral
Proline	P	nonpolar	neutral
Serine	S	polar	neutral
Threonine	T	polar	neutral
Tryptophan	W	nonpolar	neutral
Tyrosine	Y	polar	neutral
Valine	V	nonpolar	neutral

List of Figures

List of tables